Self Assembled Monolayers for Engineering of Structured Inorganic Materials in the Micrometer and Submicrometer Range

Dissertation

zur

Erlangung des Grades

„ Doktor der Naturwissenschaften ”

am Fachbereich Chemie und Pharmazie

der Johannes Gutenberg – Universität in Mainz

Marcus Bartz

geboren in Wiesbaden

Mainz 2001

Die vorliegende Arbeit wurde unter der Leitung von Herrn Prof. Dr. W. Tremel in der Zeit von April 1998 bis August 2001 am Institut für Anorganische Chemie und Analytische Chemie der Johannes Gutenberg – Universität in Mainz angefertigt.

Dekan:

1. Berichterstatter:
2. Berichterstatter:

Tag der mündlichen Prüfung: 22.11.01

Table of Contents

1. Introduction

The synthesis of organic and inorganic materials in the micrometer and submicrometer range represents a high challenge for chemistry, physics and material science in the next future. A significant market potential emerges due to the reduction of structural scale. Thereby, the "top – down" strategy displays an important access to small and smallest structures. During the next 10 years, computer chips, which today have structures in micrometer range, should incorporate transistors of 700 atoms size. [1] In doing so, an indispensable premise is to have access to applications of manufacturing - and structuring technologies up to manipulations at the atomic level for the next technical generational change. Thereby, the mainspring is the advancement from microstructures up to nanostructured materials. The development of limited structures have been examined during the past for the investigation of quantummechanical effects. [2] Another main approach for the generation of structured materials in the sub micrometer range is the aimed construction of atomic - or molecular aggregates to bigger systems (bottom up strategy). Principles of self - assembly and self - organization, organic / inorganic layers and the selective chemical and physical connection of molecular systems on functionalized substrates are predominantly used. This strategy is different compared with the lithographically oriented top down method, which is used in industry for the construction of structures in the micrometer range.

The development of new strategies to obtain structured materials was encouraged in the whole world. For example, in Germany an initiative was started from BMBF to support the development of nanotechnology. 15 Mio. Euro per year will be spent into each approach.[3] The US government invests 500 Mio. US $ for the year 2001 into similar projects.[4] Nanotechnological products provides a world market of 55 Mrd. Euro, only for the year 2001. [3]

The interest in clusters and colloids was increased in the last two decades [5] after it was recognized that these particles act as model systems for metal crystallites. Compositions of such kind play a main role in the study of heterogeneous and homogeneous catalyst processes. Colloids and metal cluster take a position between bulk materials with their special properties and molecules. For example, conductivity, magnetism begin to disappear [5] when the size of a bulk material is reduced up to the molecular range. That is based on the reduction of the quasi continuos density of state to discrete energy levels. The main interest for chemical and physical study is to approach the borderline between a bulk material and the world of extended and molecular structures. Schmid et al. had synthesized Au_{55} clusters in 1982 [6] using reduction of $(C_6H_5)_3PAuCl$ with B_2H_6. The product was characterized as $Au_{55}[P(C_6H_5)_3]_{12}Cl_6$ with a closed packed structure of 55 Au gold atoms. The cluster incorporates 4 kinds of gold atoms (I) a metallic core of 13 Au – atoms, (II) $P(C_6H_5)_3$ (II) and Cl (III) coordinated and uncoordinated free (IV) gold on the surface. Gold atoms form the closed packed structure of a cube-octaeder. The number of atoms in this type of gold cluster which are built up from increasing number of metal shells are given by the magic numbers 13, 55, 147, 309 etc. which come about because of a clustershell. The size of such metal clusters have been specified to 14.4 Å in diameter for the gold in the metal and 20.8 Å if the phosphane sphere is being included in the calculation.

Particles with a diameter of 10 nm to 1000 nm are usually called colloids. [7] However the transition in size between colloids and clusters is not sharply defined. [5] In 1861 Graham classified silver bromide particles as colloids, because they cannot move through a filter with a pore size smaller than 10 nm [8] Next to latex particles [9] and metal oxide colloids like titanium oxide [10], which have been applied technically for many years [7], the applications for small metal particles like colloids can be seen in functional units of microelectronic devices, based on quantum confined electronic properties. Gold colloids functionalized with appropriate thiols can work as templates for the structured precipitation of inorganic materials and biomaterials. [11]

Recent investigations have been done on gold salts that can be reduced in an unpolar solvent like toluene in the presence of long chain thiols. [12] The obtained aggregates perfectly bridge the world of extended solids with the world of molecules. These thiol protected gold colloids can be precipitated, redissolved sublimated crystallized etc. which permits the use of characterization techniques such as solution NMR which are not normally accessible to the study of solids. However, these colloids own an extended solid surface, which is not unlike to that of a flat gold (111) surface. In principle, IR – spectroscopic investigations of free thiol groups are difficult because of their weak appearance in IR spectra. Gold colloids can work as a high sensitive detector in this case because of their special behavior in the presence of α, ω – functionalized thiols. Using a two – phase reaction of $HAuCl_4$ with $NaBH_4$ in the presence of an alkanethiol, solutions of gold colloids can be obtained which can be handled as a simple chemical compound. [13] This represents an easy way for the synthesis of metal colloids in the range of 2 – 10 nm. Their size can be determined by surface coverage and these colloids have been found a wide range of applications.

Nanostructures on flat 2 D substrates can be fabricated using several methods [14] Micropatterning of gold substrates using the PDMS (polydimethylsiloxane) stamp technique [15] combined with self assembly methods [16], electron beam - and photolithography [17] and X-ray lithography [18] are predominant procedures for the synthesis of nanostructures on flat substrates. The soft lithography uses PDMS stamps and is a relatively new procedure compared with the other procedures mentioned above. Preparing a master structure using photolithography or micromolding techniques, a PDMS stamp can be synthesized with the original master structure. The stamp formed in that fashion can be wetted with thiol solutions. By contact printing the stamp structure on metal surfaces like gold, silver, chromium etc. the thiol is transferred to any other surface keeping the structure from the stamp. Using etching processes [19] the original micro or nanostructure can be transferred to the metal surface. Also, the surface can be bifunctionalized using multiple thiols on a single substrate.. Crystal nucleation of calcium carbonate can be controlled using surfaces functionalized with COOH and CH_3 terminated alkyl thiols. The precipitation of calcium carbonate was favored on the hydrophilic, acid terminated areas obtained on the gold substrate. The crystals were following the geometry on the structured substrates in such precision that it was possible to obtain large structured areas of inorganic material. [20]

By patterning the adsorption of mercapto hexadecane on gold using the stamp technique, and by subsequently etching the surface in a solution of cyanide, microstructures of gold can be easily produced. The region that was protected with the thiol can be not affected with the etching solution while the bare gold can be etched completely The obtained features have dimensions of 0.2 μm to several hundreds of μm. Silicon substrates can be etched using a solution of hydroxide and ethanol. Such a solution etches the (100) face 2 times faster than the (111) face of the silicon surface.

The stamp technique is also able to generate structures using electroless deposition of metal ions in solution in the presence of an reductant [21] The protected areas of the structured substrate are not infected by the deposition. Organic surfaces are normally resistant to electroless deposition. For example nickel / gold structures can be produced using this procedure. For the generation of such structure, systems like gold /thiol, thiol 1 / thiol 2 were normally used. It is also possible to obtain structures using only one thiol SAM on the surface. The structure is generated using planar islands of one metal on the surface of a second, which might not be the same as the first. Such structures can be obtained using a mask (TEM grid or photoresist pattern) during the second metal evaporation The thiol monolayer forms three different regions: two planar regions and one in between. The transition region is more active for the precipitation of $CaCO_3$ than either the two planar surfaces based on the higher disorder in the organic film their. In doing so it is possible to obtain crystals of $CaCO_3$ (as a model system) which are only precipitated in the transition region; if patterns of rectangular areas were used, the carbonate crystals were forming as rectangular lines. [22]

Alkanethiol structures with a size of 30 nm on flat gold substrates can also be produced using the atomic force microscopy (AFM) tip as a "dip – pen". The so called dip - pen lithography, in which is transferred to a paper substrate, is approximately 4000 years old and has been used extensively to transport molecules in a macroscopic scale. [23] The structure can be *written* on a gold substrate using the capillary transport of molecules from the AFM tip to the metal surface. Patterns in the submicrometer range using a few collection of molecules can be obtained. 30 nm lines can be deposited using this technique although the gold substrate was relatively rough (square roughness of 2 nm). [23]

Nevertheless the AFM tip can also work as a catalyst in the submicrometer range. Using a platinum coated AFM tip Schultz et al. [24] were able to hydrogenate terminal azide functionalized alkanethiols on flat substrates in micrometer range. The

hydrogenated areas were labeled with fluorescent latex beads can bind chemically to amino functions, to detect the positive reaction.

One of the most important analytical methods for the synthesis of structured materials in the sub micrometer range represents the scanning tunnel microscope, which was developed 1982 by Binnig et al. [25] While a metal tip is lead over a conducting surface, the metal tip is displaced due to the surface topography maintain a constant tunnel current. The changes of the tip can be displayed through voltage changes in piezzo elements holding the tip. The very high resolution is based on the strong dependence of the tunnel current between the metal tip and the surface. Resolutions at the atomic scale, better than in a scanning electron microscope, with images in 3 dimensions can be observed using a scanning tunnel microscope. The topography of these pictures is in atomic scale.

Another challenge also for industrial research is the preparation of hollow particles in micro- and submicrometer range. Such particles can be obtained from interfacial polymerization or from phase separation out of a polymer solution. Möhwald et al. [26] have developed a new way for the synthesis of hollow capsules using the stepwise assembly of oppositely charged polymer molecules. The core represents a melamine formaldehyde particle, which can be decomposed after the adsorption of the polymer films. The adsorption cycles started with the adsorption of negatively charged poly(sodium styrenesulfonate) on the positively charged melamine core. The synthesis is continued alternately up to the desired film thickness. The diameter of the obtained hollow capsules is approximately 4.0 μm. The capsules can be produced in controlled thickness with specific chemical and physical properties. In addition they represent novel structured materials in nano and micrometer range. They are permeable for small and polar molecules in contrast to lipid vesicles. Possible applications can be seen in catalytic reactions, pharmaceutic carrier systems or as micro- or nano reactors for chemical reactions. [27]

Long chain alkane thiols adsorb from dilute solution onto flat gold, silver and copper surfaces. [28] This self - assembly process forms crystalline organic thiol monolayers on the substrate in different orientations and represents an interfacial phase between the solid substrate and the liquid medium. [29] The physical properties of the surface can be changed using differently functionalized thiols. Industrial procedures favor films as small as possible because of low material costs. The ideal case is the application of a monomolecular film. The surface texture can be achieved on a maximum level. Films in qualitatively high quality can be obtained using Langmuir Blodgett techniques (LB) and self - assembly methods (SAM). The synthesis of LB mono and multilayers are described for a large number of molecules; however, this technique is limited to amphiphilic molecules. LB films are usually not stable against high temperature and in the presence of organic solvents because there is no chemical bonding to the substrate, therefore the structure of the LB layer can disappear during the transfer onto the substrate. Also, the transfer itself is related to a comparatively high effort if large surfaces are to be adsorbed. In advantage, the adjustment of a thermodynamical equilibrium after short times and the fast repair of defects in the LB film have opened many applications to this technique. For example, LB monolayers can be used as templating agents for the crystallization of biominerals such a $CaCO_3$. Mann and coworkers [30] have been established the template directed nucleation of Calcium carbonate using a large number of different amphiphiles. With the exception of aliphatic alcohols, which inhibit the nucleation, the crystals of $CaCO_3$ nucleate at the monolayer / solution interface in crystallographic orientation in order to the used monolayer.

For the controlled precipitation of calcium carbonate in its three important phases calcite, aragonite and vaterite, the self - assembly process of functionalized alkane thiols on gold substrates is a powerful tool to investigate the relationship between functionality of the SAM and the phases obtained after the crystallization. [31] The gold - coated glass slides functionalized with different alkane thiols represents a large - scale model for a biomembrane on which precipitation takes place in nature. The surface properties can be tuned using thiols with different chain length and

headgroup. By changing the shape of the adsorbed molecules different types of lattices can be generated. For example, long chain hydroxyl terminated, fluorinated alkanethiols and simple alkanethiols form hexagonal lattices. Thiols like COOH or anthracene - terminated alkanethiols form rectangular lattices. [32] The change in the crystalline structure of the monolayers induces different amounts of the $CaCO_3$ polymorphs in the templated growth of calcium carbonate because of a template effect, i.e. geometrical similarities between the carbonate plane and the monolayer lattices. [31] The faces induce the crystal habit corresponding directly with the most energetically stable atomic planes in the lattice. They normally have low Miller indices, so they appear as the Bravais lattice and the crystal shape is a macroscopic replica of the unit cell.

The growing of complex forms of inorganic materials such a calcium carbonate or silica in living systems is not fully understood and explained. [33] In recent years fundamental approaches have been done to understand the system of modifications in the habit of crystals. [33] Next to the possibility that differently functionalized and structured surfaces induce varying morphologies, the crystal shape can be modified by the addition of additives. Small molecular additives having molecular structure of variable conformation interact with charge, stereochemical and structural processes on inorganic crystal surfaces. α,ω- dicarbonic acids are efficient for the stabilization of crystal lattices, which are parallel to the $[1\bar{1}0]$ surface. However, complex structures in inorganic materials are growing in the presence of an organic matrix. The synthesis of biomineral structures represents a compromise between the force field of the inorganic crystallization and the biologic organization. The simplest method for the synthesis of typical membrane vesicles is the preparation of microemulsions. Within the emulsion capsules the precipitation of the inorganic material can be observed to form structures in variable diameter and surface texture. An other strategy for the synthesis of spherical inorganic materials represents the use of a temporary stable foam which can be removed after precipitation. [33] Structures in the micrometer range from amorphous silica can be obtained using a polycondenzation of tetraethoxy silane (TEOS). The structure obtained from a oil

– frozen emulsion. The reaction proceeds slowly at the oil water interface. The obtained hydrophilic silica species moves into the water layer in which the condensation takes place. [34]

3 D structured calcium carbonate can be obtained using thiol functionalized gold nanoparticles. The use of these gold colloids instead of a flat gold surface has permitted to obtain novel crystal aggregate geometries through templated crystallization. By coating the gold colloids surface with mercaptophenol an extremely hydrophilic surface can be obtained that leads to the formation of gold colloids, which are water soluble at high pH. Crystallization experiments carried out using these kind of gold colloids lead to the formation of precipitates in a spherical shape. The so called "pearls" have a diameter of approximately 200 μm. The rhombohedra of calcite are arranged spherically around a central point.[35]

The synthesis of nanorods and nanotubes was to be exploited using several techniques [36] CdS nanorods can be obtained using a monosurfactant system under atmospheric benchtop condition. The shapes of the nanocrystals has been developed using thermal decomposition of a single – source precursor. Temperature and precursor concentration provided the control of various architectures. [36] Silica nanotubes can be produced using a simple sol – gel technique. TEOS was decomposed in the presence of a small amount of tartaric acid. [37] While ammonium salt of tartaric acid is obtained from ethanolic solution [38] in nanometer sized fibers, silica precipitated around this precursor to form hollow tubes with approximately 500 nm hollow size.

1.1. References

[1] L. Siegel, *Salt Lake Tribune* **1995,** Oct., 19

[2] M. F. Crommie, C.P. Lutz, D. M. Eigler, *Science* **1993**, 262, 218

[3] For more datails see : http:\\www.bmbf.de

[4] P. Moriaty, *Rep. Prog. Phys.* **2001**, 64, 297

[5] G. Schmid, *Chem. Rev.* **1992**, 92, 1709

[6] G. Schmid, R. Peil, R. Boese, F. Bandermann, S. Meyer, G. H. M. Calis, J. W. A. van der Velden, *Chem Ber.* **1981**, 114, 3634

[7] J. Prost, F. Rondelez, *Nature* **1991**, 350, *Suppl. Mater.*, 11

[8] T. Graham, *Phil. Trans. R. Soc.* **1861,** 151, 183,

[9] J. W. Vanderhoff, J. van de Hul, J. macromolec. Sci. Chem. ***1973,*** A7 679

[10] G. Will, J. Sotomayor, S. Nagaraja Rao, D. Fitzmaurice, *J. Mater. Chem.,* **1999**, 9, 2297

[11] J. Küther, R. Seshadri, G. Nelles, H. J. Butt, W. Knoll, W. Tremel, *Adv. Mater.* **1998**, 10, 5

[12] M. Brust, J. Fink, D. Bethell, D. J. Schiffrin, C. Kiely, *J. Chem. Soc. Chem. Commun.* **1995**, 1955

[13] M. Brust, M. Walker, D. Bethell, D. J. Schiffrin, R. Whyman, *J. Chem Soc. Chem. Commun.* **1994,** 801

[14] Y. Xia, J. A. Rogers, K. E. Paul, G. M. Whitesides, *Chem Rev.* **1999**, 99, 1823

[15] W. T. S. Huck, A. D. Stroock, G. M. Whitesides, *Angew. Chem. Int. Ed. Engl.* **2000**, 39, 1058

[16] G. M. Whitesides, *Sci. Am.* **1995,** 273, 146

[17] J. M. Gibbson, *Phys. Today* **1997**, 56

[18] D.L. White, J. E. Bjorkholm, L. Eichner, R. R. Freeman, T. E. Jewel, W. M. Mansfield, A. A. MacDowell, L. H. Szeto, D. W. Taylor, D. M. Tennant, W. K. Waskiewicz, D. L. Windt, O. R. H. Wood, *Solid State Technol.* **1991**, 37

[19] Y. Xia, X.-M. Zhao, E. Kim, G. M. Whitesides, *Chem Mater.* **1995**, 7, 2332

[20] J. Aizenberg, A. J. Black, G. M. Whitesides, *Nature* **1999,** 398, 495

[21] S. Nakahara, Y. Okinaka, *Annu. Rev. Mater. Sci.* **1991**, 21, 93

[22] J. Aizenber, A. J. Black, G. M. Whitesides, *Nature* **1998,** 394, 868

[23] R. D. Piner, J. Zhu, F. Xu, S. Hong, C. A. Mirkin, *Sciene* **1999**, 283, 661

[24] W. T. Müller, D. L. Klein, T. Lee, J. Clarke, P. L. McEuen, P. G. Schultz, *Science* **1995**, 268, 272

[25] G. Binnig, H. Rohrer, CH. Gerber, E. Weibel, *Phys. Rev. Lett.* **1982**, 49, 57

[26] E. Donath, G. B. Sukorukov, F. Caruso, S. A. Davis, H. Möhwald, *Angew. Chem.* **1998,** 110, 2324

[27] F. Caruso, *Chem Eur. J.* **2000**, 6, 413

[28] A. Ulman, *Chem. Rev.* ***1996,*** 96, 1533

[29] R. G. Nuzzo, D. L. Allara, *J. Am. Chem. Soc.* **1983**, 105, 4481

[30] B. R. Heywood, S. Mann, *Adv. Mater.* **1994**, 6, 9

[31] J. Küther, R. Seshadri, W. Knoll, W. Tremel, J*: Mater: Chem.* **1998,** 8, 64**1**

[32] G. Nelles, H. Schönherr, M. Jascke, H. Wolf, M. Schaub, J. Küther, W. Tremel, E. Bamberg, H. Ringsdorf, H.-J. Butt, *Langmuir* **1998**, 14, 808

[33] S. Mann, Angew. Chem. Int. ed. Engl. **2000**, 39, 3392

[34] S. D, Sims, J. D. Heywod, S, Mann, *Adv. Mater.* **1998**, 10 151

[35] J. Küther, R. Seshadri, W. Tremel, *Angew. Chem. Int Ed. Engl.* **1998**, 37, 3044

[36] Y. Jun, S. Lee, N. Kang, J. Cheon, *J. Am. Chem. Soc.* **2001**, 123, 5150

[37] H. Nakamura, Y. Matsui, *J. Am. Chem. Soc.* **1995,** 117, 2651

[38] S.F. Miyaji, S. A. Davis, J. P. H. Charmant, S. Mann, *Chem Mater.* **1999**, 11, 3021

2.2 – Dimensional Structured Inorganic Materials

2.1. Stabilization of Aragonite on Polyaromatic Amide – Surfaces obtained by Step-Polymerization: Effect of Film Thickness

2.1.1. Introduction

Aragonite, one of the three important calcium carbonate polymorphs, is formed on self assembled monolayers under ambient conditions using polyaromatic amide surfaces with film thickness between 5 and 400 nm as nucleation templates. The parameters that could be controlled were (I) the polyaramide chain length, (II) the ω-substituent at the polymer, (III) the connection to the gold surface using different amino thiols and (IV) the crystallization temperature. Here, it is presented for the first time, the control of the thickness of a polyaramide monolayer during its preparation using a step polymerization technique.

The attempt to understand mineralization processes of inorganic materials in nature has been challenging an increasing number of researchers in the last decades [1] In living systems more than 5 dozen of different species of biominerals are known to exist. Calcium carbonates, - phosphates, silica and iron oxides belong to the most important representatives, which are highly optimized with a well organized structure and morphology [2] in biogenic systems. Although biomineralization processes in nature occurred for millions of years, the specific steps and mechanisms of structuring and ordering are still dissembled and not accessible for synthetic applications. In general, this is based on a large number of single steps which are engaged in biomeralization processes, and which range from the control of ion concentration, control of additives [3] , formation of phases, involvement of matri-

ces, up to the limitation of the crystallization space [4] As a consequence, the high level of complexity can increase in every higher organization step because of every change at a lower level may influence the following one. At the laboratory level, the biogenic precipitation with well defined structures and morphologies can be mimicked with organic – inorganic interfaces, accessible by Langmuir blodgett techniques, [5] protein coated substrates, [6] polymer dispersions, [7] micellar media [8] and self – assembled – monolayers (SAMs). [9] Our previous work has focused on the templated growth of $CaCO_3$ in all three common polymorphic modifications (calcite, vaterite and aragonite). [10] We have used alkylthiols, $X – (CH_2)_n$-SH (n= 2 - 16, X = OH, COOH, CH_3, Aryl etc.), self assembled on gold substrates. The properties of the resulting monolayer can be adapted using different chain length and different headgroups of the thiols. This permits a control of the polymorphic forms of the precipitated $CaCO_3$. For example, long chain alkyl thiols with non polar or slightly polar (CH_3, OH) headgroups form crystalline 2 D lattices with a hexagonal packing structure on the surface. In contrast, a long chain alkylthiol with a large polyaromatic headgroup permits the formation of a centered rectangular structure. Monoclinic structures are formed when a long chain alkylthiol with a carbonic acid headgroup is used. Vaterite and calcite are the dominating fractions obtained after deposition of $CaCO_3$. On the other hand, when short chain alkylthiols are used, the resulting surfaces are not well structured. This leads to a preferred formation of aragonite. Our studies have established that such modifications of the surface structure do indeed control the morphology and the crystal habit of the precipitated $CaCO_3$. [10] Aragonite is stabilized when polar, non well ordered and rough surfaces are used. Furthermore, higher temperatures also favor the formation of aragonite. [11] In a previous study we have used dithiol / gold colloid multilayers which form templating surfaces with higher thickness and roughness. These surfaces were able to induce the formation of aragonite at high and low temperatures as well. [12]

In the present study we have exploited the controlled polymerization of polyaramides **T 1** assembled on flat gold surfaces using terephthaloyl chloride and p - phenylendiamine as monomer units. Two different aminothiols (cysteamine and 4 - mercaptoaniline) were used to connect the polymer to the surface. In the first set of experiments oligomers with different chain length (short chain n = 2; long chain n = 8 –10) and different headgroups obtained by using functionalized aminophenyl derivatives were synthesized corresponding to the desired functionality on the surface. The connection to the gold surface was carried out with one of the aminothiols mentioned above. In the second part of the experiment the polymerization were done directly on the gold surface.

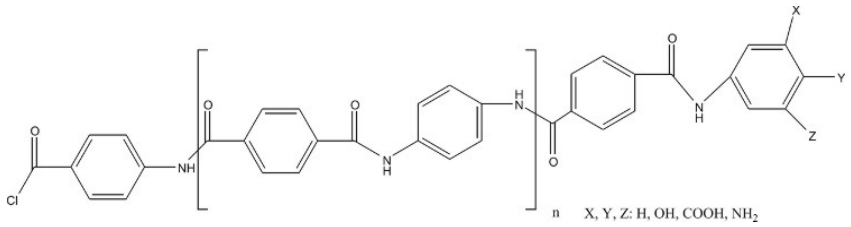

T 1

Thereby we exploited the special nature of this polymerization. Gold slides were functionalized with one of the aminothiols mentioned above and were dipped successively in solutions of both types of monomers (acid and amine). The resulting thickness of the film can be controlled exactly through the number of dipping cycles; an automatted dipping machine ensured the uniformness of each cycle (Figure 2.1.1). The experiment was carried out in such a way that the surfaces were terminated with an amino group using p - phenylendiamine as last monomer unit. The assembly of the polymer as well as the polymerization on the surface were followed by plasmon resonance spectroscopy, and the formation of polymer surfaces using the pre-synthesized oligomers.

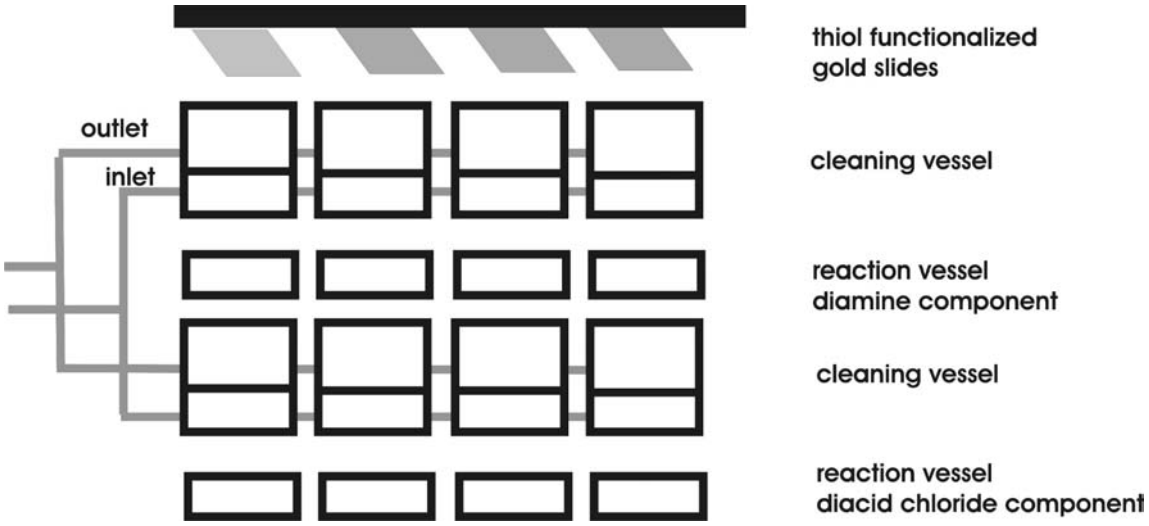

Figure 2.1.1 Scheme of the automatic dipping machine. 8 thiol functionalized gold slides can be fixed at the dip holder. They were dipped into the first reaction mixture (acid component) (a), washed (b), dipped into the second reaction mixture (diamine component) (c) and finally washed again (d). Fresh cleaning solvent was pumped through the vessels during the whole reaction period.

Reflectance FTIR spectroscopy was used to characterize the SAMs. Contact angle measurements gave insight into the stiffness of the polymer chains. The precipitation of $CaCO_3$ was carried out using a standard setup [10] . The formation of crystals was followed by scanning electron microscopy and PXRD in grazing incidence geometry; with the crystals being transferred from the substrates to Scotch™ tape. To improve the quantification, we have refined the acquired powder x-ray profiles.

2.1.2. Results and discussion

2.1.2.1. Surface growth and characterization

Polymers synthesized on the gold surfaces were characterized by surface plasmon resonance spectroscopy, IR reflectance spectroscopy and atomic force microscopy measurements. Figure 2.1.2 displays plasmon resonance spectra collected against ethanol after polymerization using the dipping method with mercaptoaniline (PH X; X = 10, 20, 40, 80 cycles PH: Mercaptoaniline anchored polymer) as connecting agent. (see Scheme T1, n= 10, 20, 40, 80; Y = NH_2; X,Z = H). The spectra were taken from different glass slides after finishing the corresponding number of cycles.

The shifts of the plasmon curves correspond to angular changes of 1,03 ° (Blank – PH 10), 0,233 ° (PH 10 – PH 20), 0,53 ° (PH 20 – PH 40) and 0,325 ° (PH 40 – PH 80) and could be fitted using the Fresnel formula. Assuming that the refractive indices of the thiol and polyaramide are not too different from those of the bulk material (n = 1.4899) the thicknesses of the SAMs were found to be 13,8 nm in case of a polymer after 10 cycles, 21,3 nm after 20 cycles, 30,7 nm after 40 cycles and at least 471,7 nm after 80 cycles.

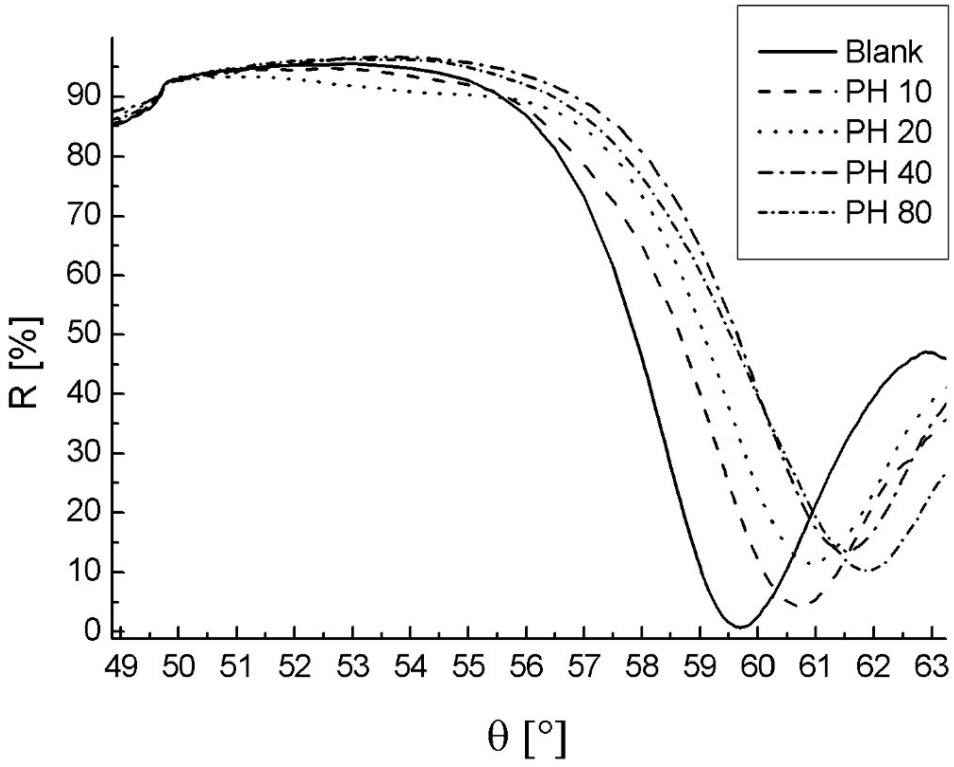

Figure 2.1.2 Typical plasmon resonance spectra of a clean gold (blank) surface and of mercaptoaniline functionalized gold surfaces after polymerization directly from the surface after 10 (PH 10), 20 (PH 20), 40 (PH 40), 80 (PH 80) cycles.

By repeating the same experiment using cysteamine as anchor group, film thickness of about 7,7 nm (10 cycles), 11,4 nm (20 cycles), 14,9 nm (40 cycles) and 14,8 nm (80 cycles) were obtained.

Figure 2.2.3 displays the results of the resulting polymer films after several cycles. Polymer chains connected with mercaptoaniline lead to an increasing thickness in contrast to polymers connected with cysteamine as anchor group. We assume that the use of mercaptoaniline leads to correspondingly stiffer polymer chains.

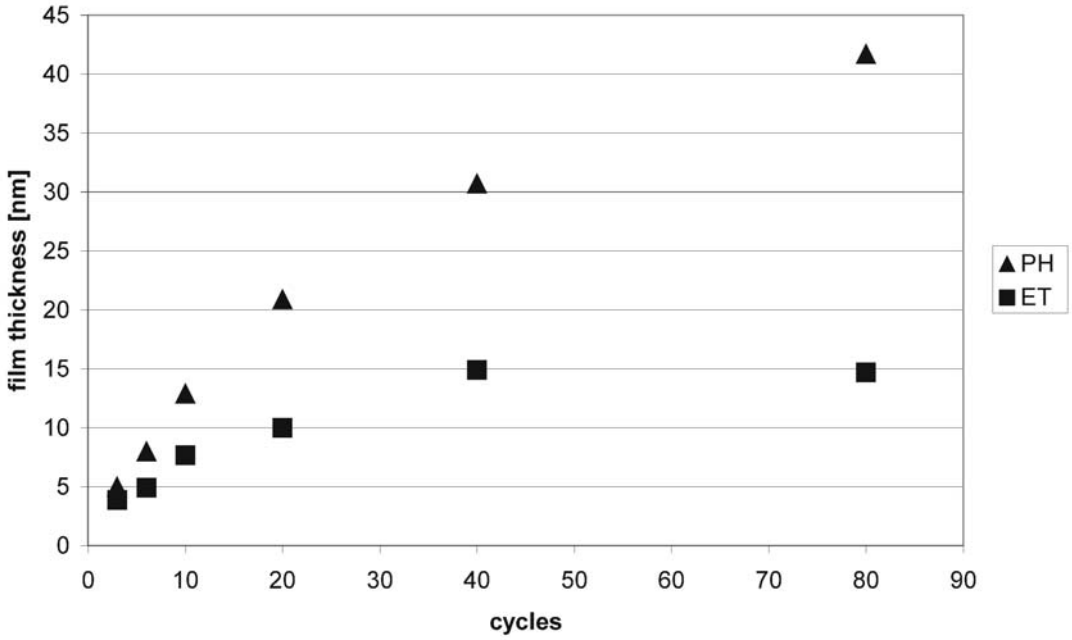

Figure 2.1.3 Film thickness obtained from polymer surfaces after different reaction cycles. Mercaptoaniline functionalized surfaces ▲ are more reactive and form longer polymer chains. Cysteamine functionalized ■ surfaces become inactive after about 40 cycles. The obtained thickness corresponds to polymer chains at 10 cycles when mercaptoaniline is used.

The headgroup is oriented towards the solution for a longer time; the surface is more active for polymerization for more cycle numbers which - in turn - leads to a higher film thickness. In contrast the use of cysteamine anchor groups leads to polymers with decreasing stiffness. The reactive headgroups seem to be embedded into the polymer film to a higher extent. Thus, the adsorption of new monomer units is hindered. Making use of the fact that stiff surfaces have do not differ in advancing and receiving contact angles we have measured a difference in both contact angles of about 8.2 ° for a long chain and about 27 ° for a short chain polymer sample. These findings indicate that the molecules forming a short chain polymer

surface are more flexible. Their orientation can be changed easily during the contact angle measurements, which leads to a relatively large difference in the observed contact angles. The effect of roughness plays a minor role, here.

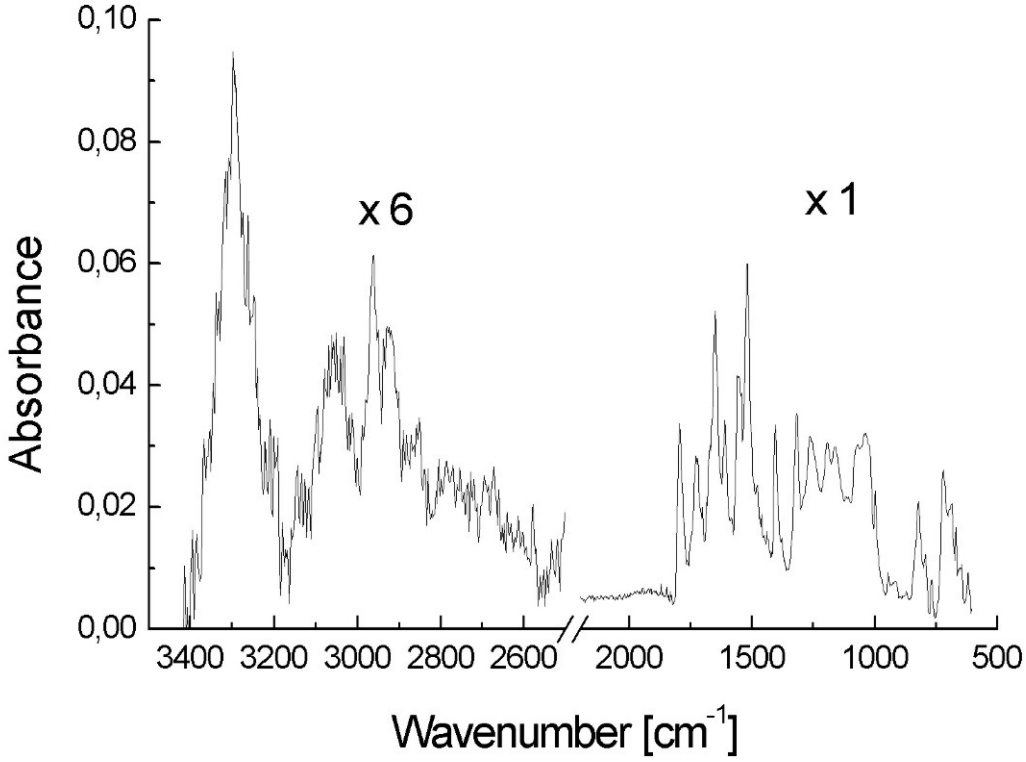

Figure 2.1.4 Typical surface reflectance FTIR measurement of a polymer surface obtained after reaction with cysteamine functionalized gold surfaces after 80 cycles.

Figure 2.1.4 displays an IR measurement taken in specular reflectance after 80 cycles. The recorded spectrum is consistent with one of a free polymer sample and has an absorption peak at 3100 cm^{-1} for the aromatic functionality. Peaks at 2900 cm^{-1} are corresponding to the CH_2 functionality of the cysteamine. The NH_2 func-

tionality has an absorption peak at 3300 cm $^{-1}$. Clear reflectance FT IR spectra can be obtained only from surfaces polymerized after 80 cycles.

The panels of Figure 2.1.5 display tapping mode AFM images of polymer functionalized gold substrates. Figure 2.1.5 a) and b) display the topography of surfaces obtained after polymerization after 10 and 80 cycles using mercaptoaniline as anchor group. The difference between fast terminated polymer chains and long chain areas correspond to the appearance of dark areas in larger scale and number (Figure 2.1.5 b) compared to the surface obtained in Figure 2.1.5 a). Figure 2.1.5 c) and d) display panels obtained after polymerization of 10 and 80 cycles using cysteamine as anchor group. Comparing the two surfaces from polymerization of 80 cycles with cysteamine and 10 cycles using mercaptoaniline as anchor group, which have approximately the same film thickness, the topography of figure 2.1.5 d) seems to be the same compared with the surface displayed in figure 2.1.5 a). Correspondingly, the surface with the smallest roughness is displayed in Figure 2.1.5 c).

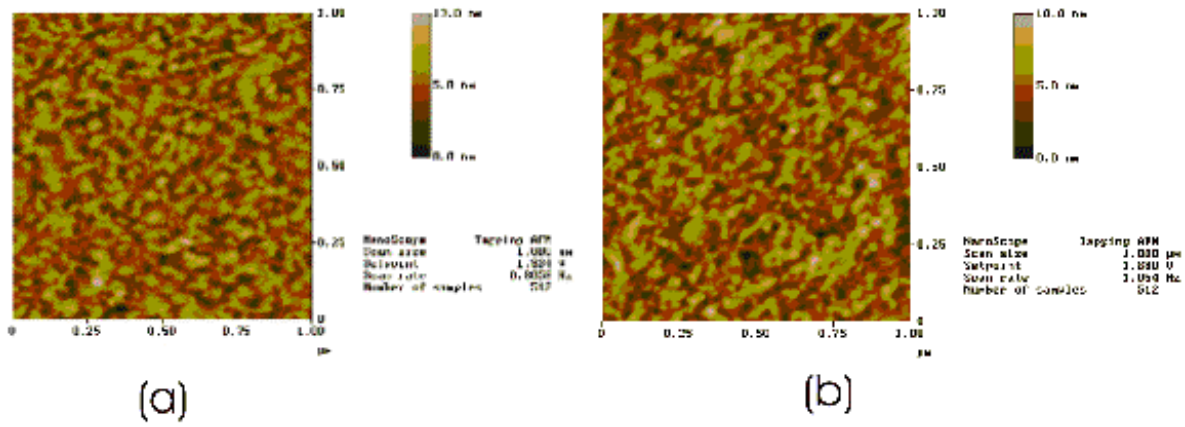

Figure 2.1.5 a and b) Tapping mode AFM images of polymerized gold surfaces using mercaptoaniline as anchor group. Polymerization cycles: 80 (a) and 10 (b) cycles.

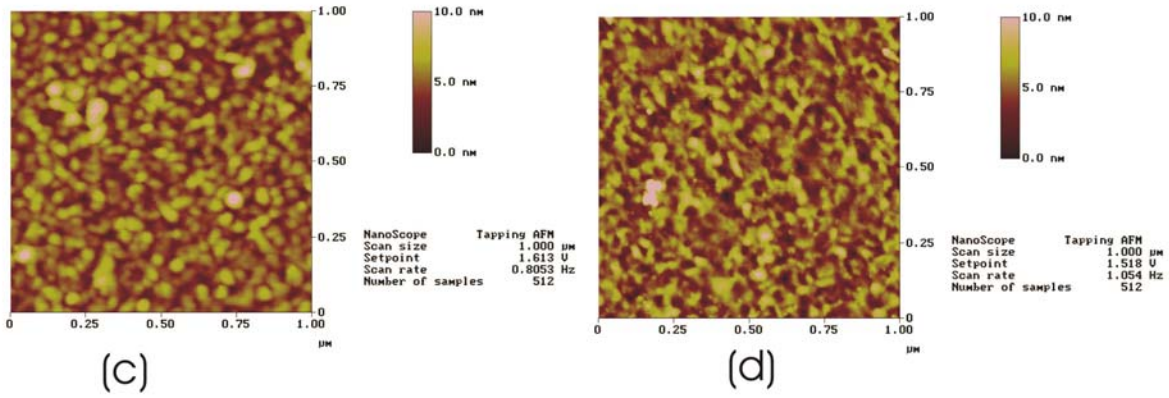

Figure 2.1.5 c) and d) Tapping mode AFM images of gold surfaces after polymerization of 10 (c) and 80 (d) cycles using cysteamine as anchor group.

2.1.2.2. Characterization of $CaCO_3$ crystals on polymerized surfaces by dipping experiments using SEM micrscopy

$CaCO_3$ can be crystallized by diffusion of CO_2 into a 10 mmol $CaCl_2$ – solution in the presence of the polymerized templates. Surfaces with mercaptoaniline as anchor group are discussed as the representative polymer surface.

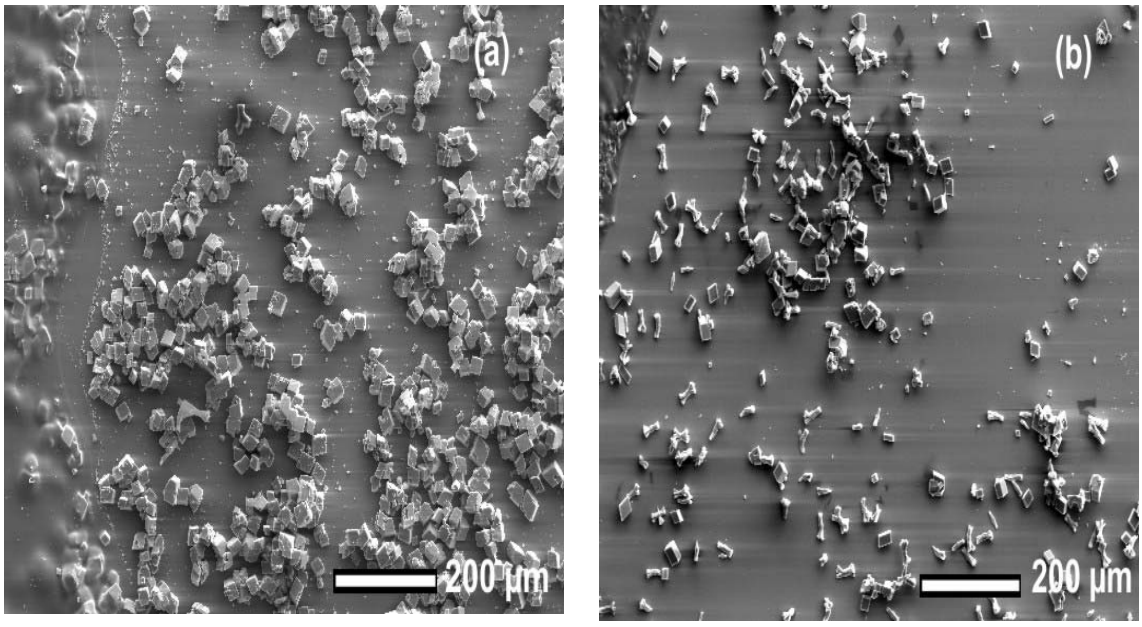

Figure 2.1.6 a) and b) Scanning electron images of calcium carbonate crystals obtained on polyaromatic amides after 10 cycles (a) and after 40 cycles (b) at 22 °C using mercaptoaniline functionalized surfaces.

Figure 2.1.6 a and b) display typical scanning electron microscopy images obtained after crystallization of $CaCO_3$ at 22 °C on aramide polymer surface using mercaptoaniline as anchor group after 10 (a) and 40 (b) reaction cycles. The typical habit [10] of calcite and a very small fraction of vaterite is observed in Figure 2.1.6 a). However, the arrangement of the crystals does not imply any mode of epitaxy or

order with respect to the substrate. An increasing amount of needle like aragonite can be seen in Figure 2.1.6 b). After 40 cycles the polymerization efficiency starts to decrease. The access of the free monomers to the functionalized headgroups are more hindered. The difference in chain length of the of the polymer chains on the same surface starts to increase. This leads to a higher roughness of the polymer surface. The formation of the aragonite phase is preferred, the amounts of calcite and vaterite are reduced. Figure 2.1.7 displays a SEM image of $CaCO_3$ obtained after crystallization at 45 °C on a polymer surface with a mercaptoaniline anchor group after 80 cycles. Figure 2.1.7 shows aragonite to be the most important phase because of the roughness of the polymer surface and the temperature effect.

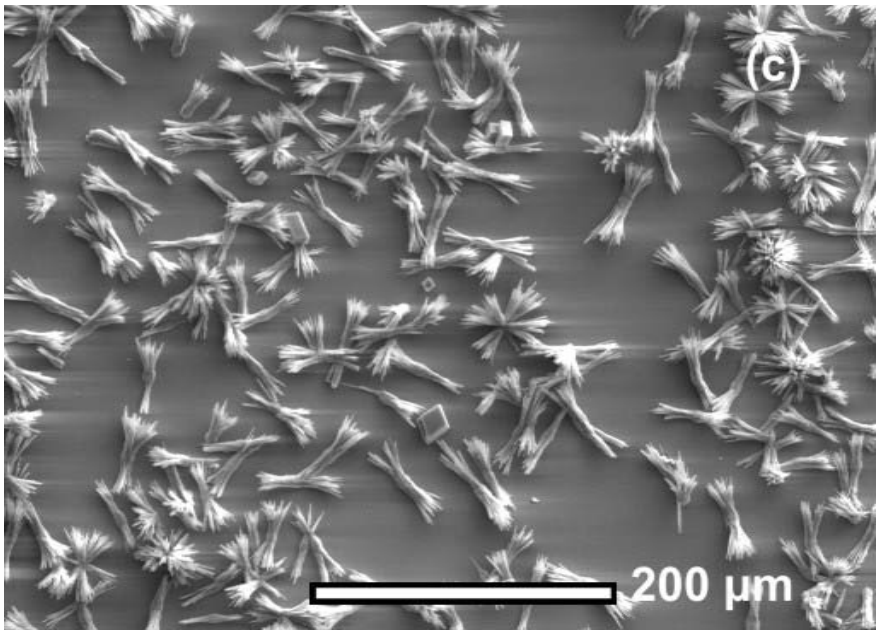

Figure 2.1.7 At crystallization experiments at 45 °C aragonite needles are the dominating amount on mercaptoaniline functionalized gold surfaces after 80 polymerization cycles (c).

2.1.2.3. Amounts of $CaCO_3$ calculated from X-ray measurements

a) Crystallization of $CaCO_3$ at 22 °C on polymer surfaces with different headgroups

In the first experiment we have used gold slides covered by different terminated polymers. The amounts of the three different phases of $CaCO_3$ were calculated. Figure 2.1.8 displays nucleation densities for $CaCO_3$ crystals on polyaromatic amides of different chain length, with differently functionalized headgroups and different aminothiols by which the polymer chains are connected to the gold surface [labeled as ET, PH: different aminothiols cysteamine or mercaptoaniline; SC, LC: length of the polymerchain (short chain or long chain); OH, COOH: nature of the headgroup (hydroxy - or carbonic acid terminated)]. The polymers were synthesized before they were anchored to the aminothiol functionalized surfaces. In this experiment the polymer films are very short compared to chain lengths obtained by the polymerization procedure directly from the surface. Film thicknesses are given in Figure 2.1.8.

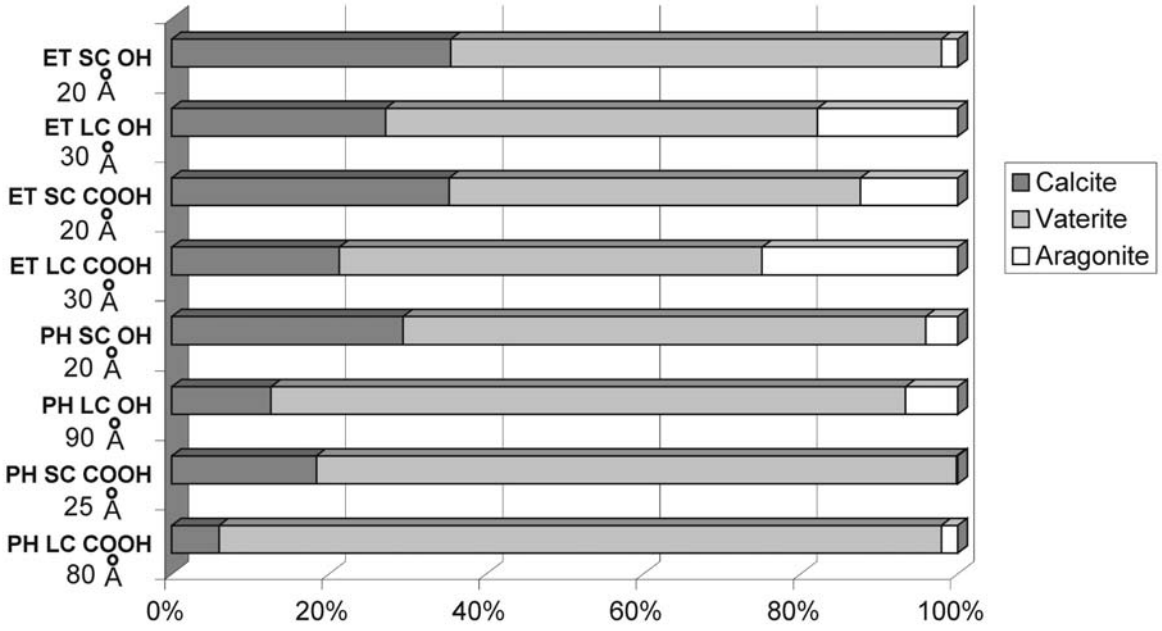

Figure 2.1.8 Histogram of weight fractions of $CaCO_3$ polymorphs obtained from Rietveld refinements of powder X-Ray profiles from crystals of $CaCO_3$ grown at 22 °C on oligomer substrates with different chain length and surface functionality. Film thickness are given.

The amounts of calcite and vaterite that were found after crystallization of $CaCO_3$ at 22 °C are comparable to those we have found in previous studies from crystallization on the COOH and OH terminated surfaces [10]. Obviously, the amount of calcite is reduced on average by a factor 2 on long chain polymer surfaces in favor of vaterite. Because of its well defined structure, the longer chain compound exerts a distinct template effect. The crystals are pre - orientated which leads to a reduced transformation from vaterite to calcite. However, the number of defects in the polymer surfaces increase because of an incomplete adsorption of long chain polymer molecules. More aragonite can be obtained on these surfaces.

b) Crystallization of $CaCO_3$ at 22 °C on polymer surfaces with different chain length

In the second experiment we have crystallized $CaCO_3$ on polymer surfaces with different chain length but same amine termination. Figure 2.1.9 a) and b) display nucleation densities for $CaCO_3$ crystals on polymer substrates after different cycles, with different connection thiols and at different temperatures. All prepared substrates have an NH_2 termination caused by the final reaction step. Figure 2.1.9 a) displays the amount of $CaCO_3$ after crystallization at 22 °C. The amount of aragonite increases with increasing thickness of the aramide polymer film. For cysteamine bound polymer chains (ET X ; X = 10 – 80) the amount of aragonite is reduced on average by a factor of 5.6 compared to surfaces where the polymer is grown on surface bound mercaptoaniline with a corresponding number of reaction cycles. This can be explained by different levels of roughness of the synthesized polymer surfaces. This effect increases if the polymer chain is growing at a rate of 1.1 layers per step and the polymer film is thick. On thin polymer surfaces growing at a rate of 0.6 layers per step this effect has a minor influence on the roughness of the surface.

c) Crystallization of $CaCO_3$ at 45 °Con polymer surfaces with different chain length

Figure 2.1.9 b) displays the results obtained after crystallization of $CaCO_3$ on polymer surfaces growing at 45 °C. The nucleation densities are again calculated from the scale factor obtained after refinement of the XRD profiles. The increase in the amount of the aragonite phase is caused by on the additional roughness with respect to previous samples using polymer films with higher thickness and by the higher temperature as well. Aragonite formation in solution is generally favored at higher temperatures [11] because of the faster decomposition of ammonium carbonate while thermodynamic conditions are changing not much at 45 °C. In notion of previous studies we found no formation of aragonite on clean gold substrate under the same conditions used here; therefore the template effect on a rougher surface might play a minor role in this case although it still has an influence on the crystallization.

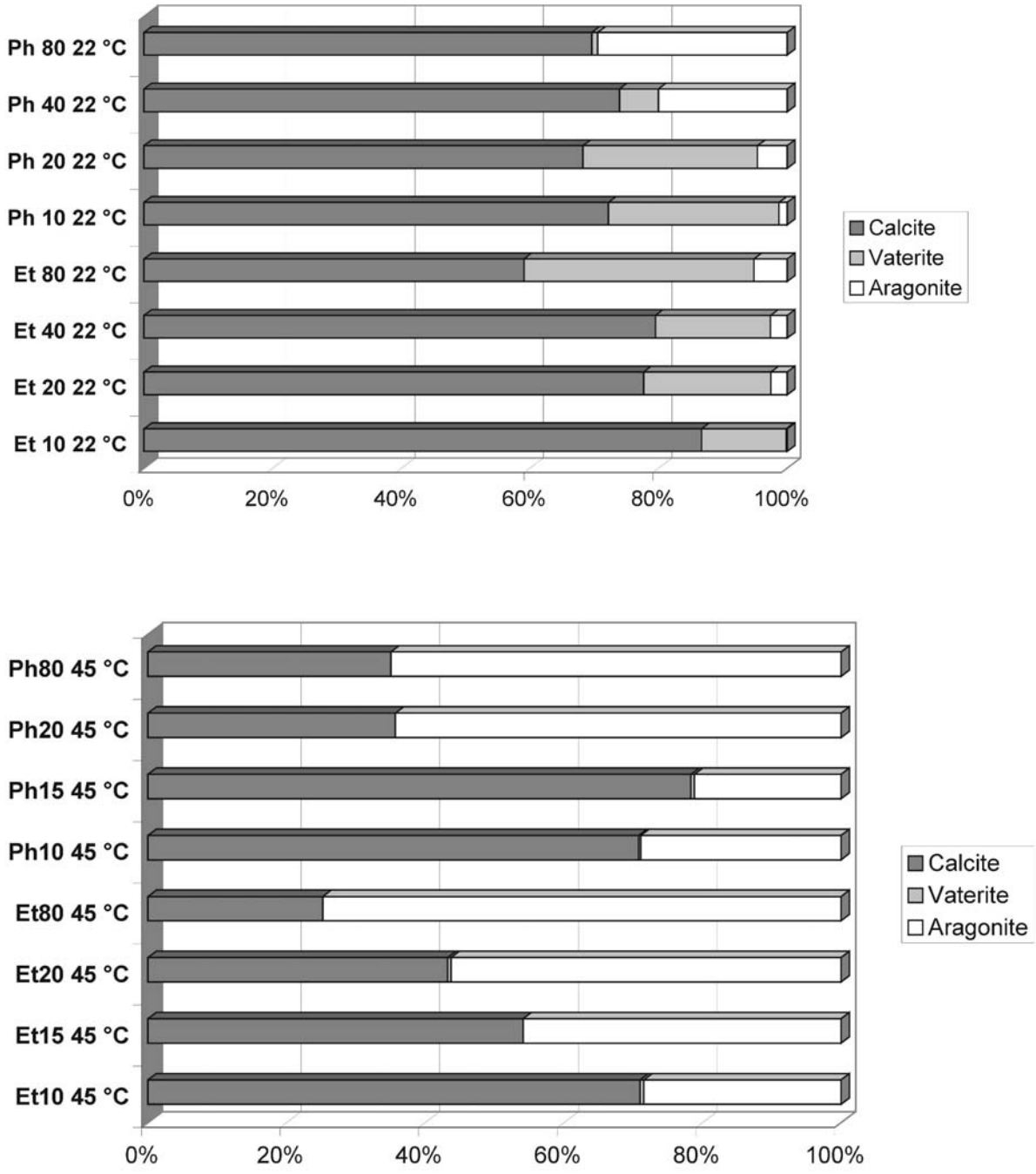

Figure 2.1.9 a), b) Histograms of obtained weight fractions of $CaCO_3$ crystals grown on NH_2 – terminated polymer substrates with different chain length at 22 °C (b) and 45 °C (c)

2.1.3. Experimental

All compounds were purchased from Acros Organics and used without further purification. The polymerization experiments were carried out in a glove box under inert gas atmosphere.

2.1.3.1. X - Ray diffraction

The XRD experiments were performed in the $\theta/2\theta$ geometry at grazing incidence using a Siemens D8 reflection powder diffractometer with Cu - $K\alpha_1$ radiation (1.540 56 Å) and Cu Cu - $K\alpha_2$ radiation (1.544 39 Å). Crystals collected from four slides were scraped from the surface and mounted on Scotch ™ tape. Data were collected from 23 – 32 ° 2 θ , with a step size of 0.02 ° and an acquisition time of 20 s per step. The acquired powder x-ray profiles were analyzed using the Rietveld [13] method incorporated in the XND [14] program. Scale factors, lattice and profile parameters, including preferred orientations were refined. The structural data were taken from the literature. [15]

2.1.3.2. SEM microscopy

Scanning electron microscopy was performed with a ZEISS digital scanning microscope 962 combined with a Kevex EDAX at acceleration potentials of 5 – 15 kV. The glass substrates were cut in small pieces and were glued on alumina sample holders with conducting carbon glue.

2.1.3.3. SPS measurement

SPS measurements were performed in the Kretschmann configuration. [16] Optical coupling was achieved with a LASFN 9 prism (n = 1.85 at λ = 632.8 nm) and index matching fluid (n = 1.70) between the prism and the BK270 glass slides. The plasmon was excited with p-polarized radiation using a He - Ne laser (632.8 nm, 5 mW). The glass slides (3,5 x 2,5 cm) were cleaned with aq. NH_3 / H_2O_2 / water (1 / 1 / 5) 10 minutes at 80°C and coated with gold using a Balzers BAE250 vacuum coating unit under pressure of less than 5 x 10^{-6} hPa, typically depositing 48 nm of gold after first depositing 3 nm of Cr. The slides were exposed to the organic thiol solution (10 mmol, Cysteamine or 1,4 mercaptoaniline) for 24 h.

2.1.3.4. Polyaramides

Different types of functionalized oligomers from polyaramides were prepared. These oligomers had a carbonyl chloride group at one end and a hydroxyl or one or two carboxylic groups at the other end.

2.1.3.5. Preparation of short chain oligomers

Iso - phthaloyl chloride (0,203 g) was reacted with aminobenzoic acid (1.137 g) or 5 –amino isophthaloyl acid (0.181 g) or hydroxyaniline (0,109 g) in the presence of triethylamine (0,20 g) in dimethylacetamide (80 ml) as solvent. The solution of acid chloride in dimethylacetamide (35 ml) was prepared under rigorously anhydrous conditions and in a conical flask equipped with a mechanical stirrer. The mixture of amines was dissolved in dimethylacetamide (45 ml) in the dropping funnel and was added dropwise to a rigorously stirred acid chloride solution at 0-5 °C. After the addition was completed the mixture was stirred for another 2 h. The resulting mixture was used directly for the reaction with the functionalized gold substrates.

2.1.3.6. Preparation of long chain oligomers

Iso - phthaloyl chloride (0.406 g) was reacted with a mixture of p – phenylendiamine (0,108 g) and 1 mmol of one of the following: aminobenzoic acid (0.137 g) or hydroxyaniline (0,109 g), in the presence of triethylamine (0,41 g) in dimethylacetamide as solvent. The reaction was carried out as described above.

2.1.3.7. Preparation of long chain polymers (automatic dip reaction)

Iso – phthaloyl chloride (0,4677 g) and 1,4 – phenylendiamine (0,4451) were separately dissolved in dimethylacetamide (each 40 ml). Triethylamin (0,41 g) were added to the amine solution. Both reaction mixtures were placed in different reaction flasks of a ISEL Microstep dip machine [17]. The machine was placed in a glove box to protect the reaction from moisture and oxygen. Gold coated glass slides functionalized with one of the two linker thiols were inserted into the ma-

chine. The glass slides were washed between the two reaction steps with dimethylacetamide automatically. Fresh solvent was pumped through the cleaning flasks over the whole reaction period. The functionalized gold slides were dipped into the reaction mixtures for 20 min. and washed for another 10 min. The first reaction step was assigned to the dipping into the acid chloride solution, phenylendiamine solution for the final one. An increasing film thickness was achieved by repeating 10, 20, 40 and 80 cycles of this reaction. One cycle sequence incorporates one reaction with acid chloride, one reaction with diamine and two washing steps in between.

2.1.3.8. Crystallization experiments

The crystallization of $CaCO_3$ was performed using published methods [11]. The templates were placed face down into a reaction flask which was filled with 10 mmol $CaCl_2$ (300 ml) solution. The flask was transferred into a desiccator and stored at 22 °C or 45 °C. The precipitation was initiated by placing a Petri dish with $(NH_4)_2CO_3$ at the bottom of the desiccator. The crystallization was carried out for 48 h.

2.1.4. Conclusion

Here, it is demonstrated the formation of $CaCO_3$ on polyaromatic amide surfaces obtained by a step - wise condensation polymerization. This reaction was performed in two ways: (I) polymerization of iso-terephthalic acid with phenylene diamine to yield a polymer which was connected to functionalized gold surfaces. (II): polymerization on the functionalized gold substrates under automated conditions. Using different anchor groups the roughness of the adsorbed polymer film can be tuned. The formation of the high pressure phase of $CaCO_3$, Aragonite, was already found at lower temperature at 22 °C. The amount was found to increase

dramatically when polymer films with higher thickness were used. To point out this effect, defined polymer surfaces were produced via a step-polymerization using a automatic dipper maintain equal conditions during the polymerization experiments. The crystallization densities of $CaCO_3$ were calculated from scale factors obtained from Rietveld refinements of XRD profiles. The results that can be drawn are: (I) Short chain oligomers with hydroxy or hydroxy - carbonyl termination behave like their corresponding alkyl thiols. They favor vaterite and calcite. The amount of aragonite is increased when oligomers with longer chain length were used. (II) At ambient temperatures the amount of the aragonite phase can be increased by using long chain polymers that lead to higher surface roughness. Faster reactions lead to the formation of surfaces with higher roughness. This can be found predominantly on polymers connected to the stiffer amino thiol mercaptoaniline. (III) Crystallization of $CaCO_3$ at 45 °C obtained more aragonite (effect of temperature) but there is also an increasing effect of roughness.

2.1.5. References

[1] H.A. Lowenstam and S. Weiner, *On Biomineralization,* Oxford University press, **1997,** 7, 689

[2] S. Mann, *J. Mater. Chem.* **1995**, 5, 935

[3] S. Mann, J. M. Didymus, N. P. Sanderson, B. R. Heywood, *J. Chem. Soc. Faraday Trans*. **1990,** 86, 1873

[4] S. Mann, *Angew. Chem. Int. Ed. Engl*. **2000**, 39, 3392

[5] S. Rajam, B. R. Heywood, J. B. A. Walker, S. Mann, *J. Chem. Soc. Faraday Trans.* **1991**, 87, 727; B. R. Heywood, S. Mann, *Adv. Mater.* **1994**, 6, 9

[6] L. Addadi, S. Weiner, *Angew. Chem. Int. Ed. Engl.* **1992**, 31, 153

[7] P. A. Bianconi, J. Lin, A. R. Strzelecki, *Nature* **1991,** 349, 315

[8] D. Walsh, S. Mann, *Adv. Mater.* **1997**, 9, 658

[9] J. Küther, M. Bartz, R. Seshadri, G. B. M. Vaughan, W. Tremel, *J. Mater. Chem.* **2001**, 11, 503; J. Küther, R. Seshadri, W. Tremel, *Angew. Chem. Int. Ed. Engl*. **1998,** 37, 3044 and references therein

[10] J. Küther, R. Seshadri, W. Knoll, W. Tremel, *J. Mater. Chem.* **1998**, 8, 641

[11] J. Küther, W. Tremel, *Chem Commun.* **1997**, 2029

[12] J. Küther, R. Seshadri, G. Nelles, H.-J. Butt, W. Knoll, W. Tremel, *Adv. Mater.* **1998**, 10, 401

[13] H. M. Rietveld, *J. Appl. Crystallogr*. **1969**, 186, 300

[14] J. F. Berar and P. Garnier, in *Accuracy in Powder Diffraction, Proc II, Intl. Conf. Gaithersburg*, **1992**, 846, 212

[15] H. Chessin, W. C. Hamilton, *Acta Cryst.* **1965**, 18, 689 (Calcite); J. P. R. De Villiers, *Am. Mineral.* **1971**, 56, 758 (Aragonite); S. R. Kamhi, *Acta Cryst.* **1963**, 16, 770 (Vaterite)

[16] E. Kretschmann, *Z. Physik* **1971**, 241, 313

[17] ISEL – Automation, Im Leibolzgraben 16, D – 36132 Eiterfeld

2.2. Stamping of monomeric SAMs as a route to structured crystallization templates: Patterned titania films.

2.2.1. Introduction

Gold-coated glass slides have be patterned by using self - assembled monolayers (SAM) of alkane thiols. Through the use of a special thiol terminated with a styrene monomer, microstructures of 5 to 10 μm width and 70 Å height have been formed on the surface by graft polymerization of styrene. These patterned gold slides have then been used to template the precipitation of thin titania films from ethanolic solutions of titanium isopropoxide to create microstructured architectures in the film. Plasmon resonance spectra have established the presence of different steps in the process and have been used to follow the kinetics of the precipitation of titania on the surface. The structured TiO_2 films have been characterized by scanning electron microscopy

There is currently an intensive effort to develop materials with a wide range of properties that open up new opportunities in fields such as catalysis, separation technology, [1], [2] electronics [3] or optics. [4] Many of these materials are made by using self - organizing systems, such as surfactant liquids and biological systems as templates for the deposition of inorganic materials in the form of thin films. Titanium dioxide has been of special interest because of its relatively high refractive index (n = 2,88 at λ = 620 nm). Another challenge is to produce patterned materials, for example as photonic materials. Several methods have been employed towards this end. Surfactants have been used to pattern micropores in titania [5] , microlithography [6] and colloidal suspensions [7] that spontaneously form colloidal crystals were employed for the template growth of porous material. In this contribution, it has been suggest the possibility to structure titania thin films by micropatterning, a

powerful method which has been used most widely for preparing organic films (self assembled monolayers, SAMs) with specific surface properties. Microstructures can be obtained by soft lithographic patterning, usually involving combinations of chemical etching, stamping and photolithography.[8] In previous studies it has been employed SAMs of various thiols for a number of applications such as direct crystallization or polymerization catalysis. [9] The use of thiol monolayer surfaces on gold has been extended by us to the use of thiol coated gold colloids. This has opened new dimensions in the chemistry of protected surfaces as colloids show a similar behavior as molecules, that is they can be precipitated or redissolved. On the other hand they still display many properties of extended surfaces. Water soluble colloids have been prepared through the use of thiols that serve as an in-situ agent for protection and capping. [10] The crystallization of biominerals like calcium carbonate [11] and iron hydroxides [12] on gold surfaces modified with different thiols has been extended to the use of protected colloids as crystallization nuclei. [13] Sticky colloids that can be used in the construction of complex composites have been prepared by means of protecting groups. [14] Whitesides and coworkers used micropatterning techniques to crystallize calcium carbonate in structured regions on self - assembled monolayers. The crystallization can be made very sensitive to the structure and the patterned surface induces the nucleation itself. [15] Knoll and coworkers have established the chemical deposition of thin lead sulfide films. The self - assembled monolayers control the deposition rate of PbS, the size and the orientation of the PbS thin film. [16]

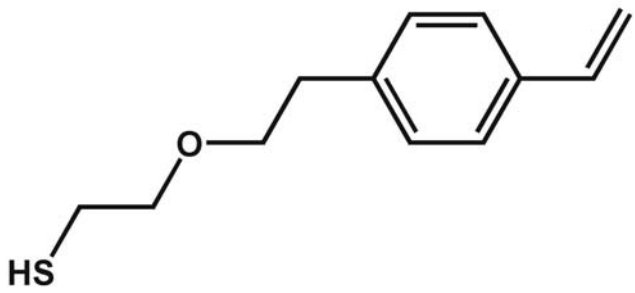

T 2

In the present work, it is introduced a new styrene monomer **T 2** which combines a monomeric moiety that can be polymerized, with a functionality that permits cleavage of the polymer from the surface through breaking an ether bond. Our thiol has been inspired by reports by Ulman and coworkers on the possibility of anionic polymerization of styrene-derived thiols on gold surfaces. [17] The resulting layers are invested with high stability and high grafting density, and are preferred in nano applications which require structurally rigid and compact behavior of the monolayer. Polymers such as polystyrene and polyethyloxazoline can be photochemically attached to surfaces over fixed benzophenone derivatives. [18] Zhao and Brittain have established the synthesis of block – polymers on surfaces by carbocationic and atom transfer radical polymerization. [19] Well defined polymer – nanoparticles can be obtained by living radical polymerization on SiO2 nanoparticles. [20]

Self - assembled monolayers can be made on gold (111) surfaces by exposing glass slides evaporated with a fresh gold film to alkane thiol solutions. Thiol monolayers are fixed chemically to gold surfaces with a strong gold - thiol bond. [21] The monomer **T 2** was modified to carry a free mercapto group for linking it to gold surfaces. Because the gold-thiol linkage is not easily cleavable, a breakage was introduced through an ether bond. This special structural feature opens various possibilities for modifying surfaces in general. Thiols with more than one functionality in one molecule promise many ways to new nano-material technologies.

By using the stamping technique [22] the mercapto - styrene monomer could be patterned on the gold surface. This very hydrophobic monomer is not soluble in solvents such as alcohols, water. By using hydrophilic stamps, we patterned gold surfaces with a nonfunctionalized alkane thiol, which is soluble in ethanol and spreadable on the stamp surface. Then the functionalized mercapto styrene monomer was spontaneously assembled from toluene solution. [23] After anionic

polymerization with unfunctionalized styrene, structures of polystyrene appear on the surface which correspond to the original stamp structure. These structures can not be removed from the surface both by simple washing or even by harsher methods such as soxhlet extraction with boiling toluene.

The assembly of the thiol monomer (on normal gold surfaces) can be followed by plasmon resonance spectroscopy, as can the polymerization, and the cleavage of the polymer from the surface through breaking the ether linkage. Kinetic experiments monitoring the precipitation of titania were also made using plasmon resonance spectroscopy, by following the thickness of titania as a function of time. But this technique demonstrated in this work can be used in tailoring crystal structures by using selected monomeric SAMs.

2.2.2. Results and Discussion

Figure 2.2.1 shows the schematic procedure to produce structured thin titania films. Starting with monomer/alkane thiol structured gold slides, the polymerization leads to a pre-structured surface. Titania can be precipitated by diffusing water into an ethanolic titanium isopropoxide solution. The inorganic material covers the entire surface. The film formed in this fashion is physically stable and strong enough to withstand the following chemical modifications on the surface.

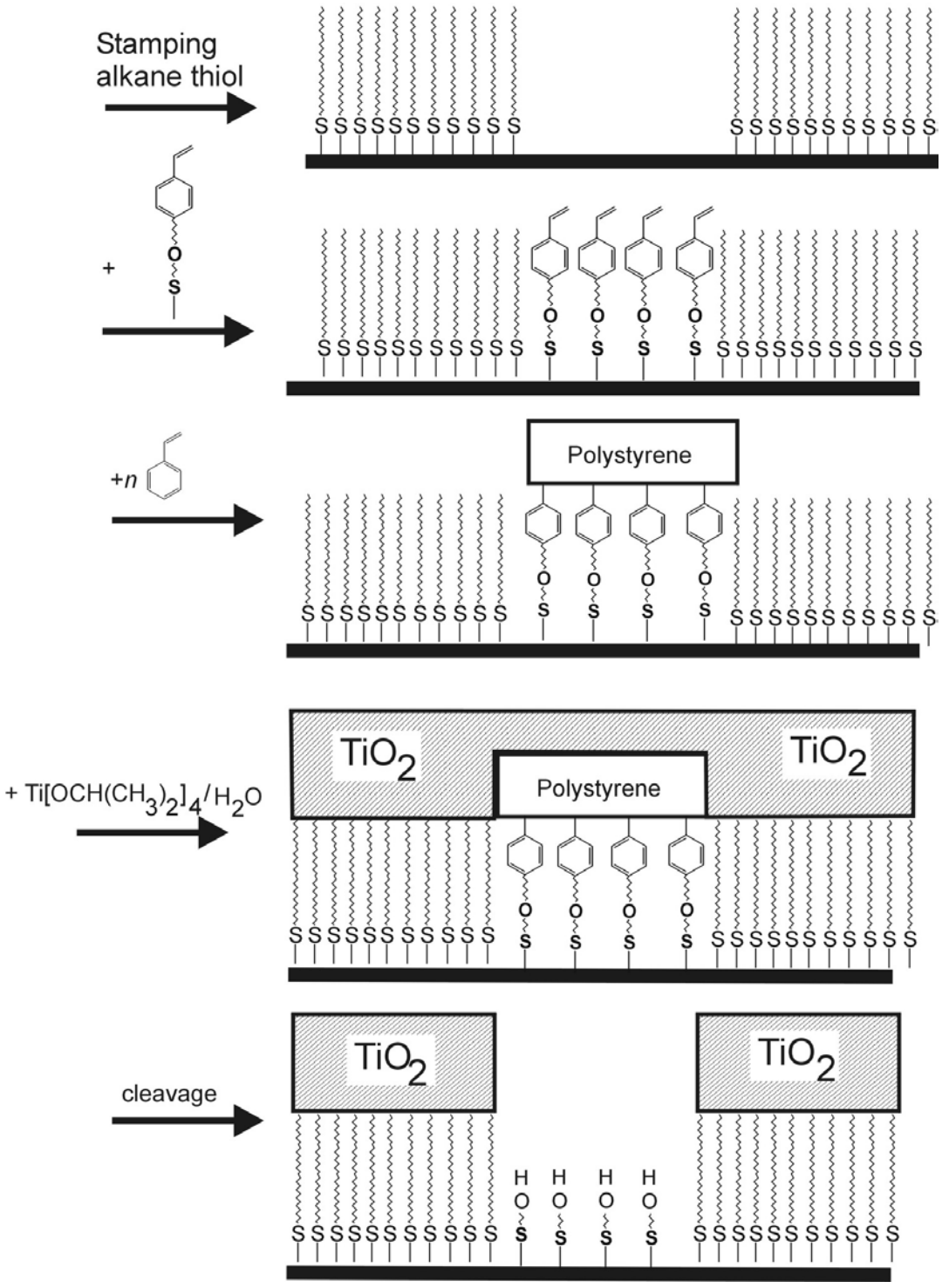

Figure 2.2.1 Schematic illustration of the formation of thin, structured titania films. The gold surface is patterned with an alkane thiol and then with the monomer **T 2**

After polymerization, blobs of polystyrene are obtained in the area of the patterned monomer. The other areas are not affected by the manipulation. Titania is then precipitated all over the surface. After the cleavage of the polymer, the titania over the polymer blobs is removed.

2.2.2.1. Cleavage of polystyrene on gold surfaces

The plasmon resonance spectrum was collected against ethanol on bare gold slides, after coating with the thiol monolayer **T 2**, after polymerization of the assembled monomer **T 2,** and after cleavage of the polymer from the surface. Figure 2.2.2 displays the corresponding SP spectra of the experiments (b) and a closer view of the corresponding minima (a). The shifts of the plasmon curves corresponding to angular changes of 0.6° (monomer - bare gold), 0.9° (polymer - bare gold) and 0.43° (removed polymer - bare gold) and could be fitted using the Fresnel formula. Assuming that the refraction indices of thiol **T 2** and of the polystyrene layer are not different from that of bulk styrene (n = 1.5470) and bulk polystyrene (n = 1.5760), the thickness of both SAMs on gold were determined to 16 **Å** in case of the monomer and 70 **Å** in case of the polymer. After removing the polymer layer from the surface a thickness of the resulting SAM of 9 **Å** was determined, assuming that their refraction index is not significantly different from those of a hydroxyalkane thiol SAM (n = 1.5360) on the surface. Modeling the structures of the monomer and a hydroxyethane thiol using molecular mechanics at the MM2 level (as implemented in Chem 3D™ version 3.5) of the thiol **T 2** suggests that the chain expansions of as much as 14.3 **Å** are reasonable from an energetic point of view.

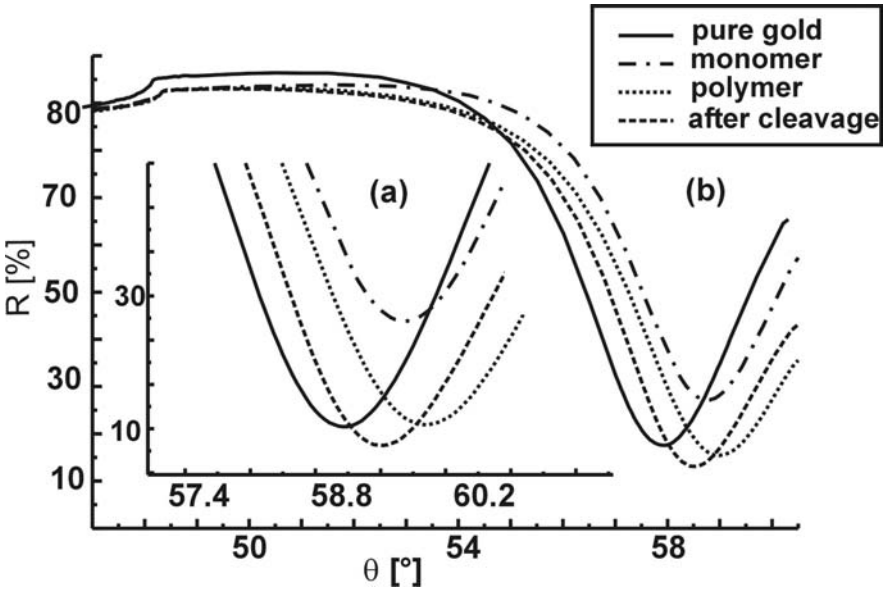

Figure 2.2.2 Surface plasmon resonance spectra of the bare gold - coated surface (___) after self assembly of the monomer (---), after polymerization (....) and after cleavage of the polymer (-..-). (a) closer view of the corresponding minima Full of spectra (b).

In case of the hydroxyethane thiol a chain expansion of 5.6 **Å** is expected. It is assumed that the polymer is not quantitatively removed from the surface. Considering additional gold - sulfur bonding for the adsorbed thiols, we conclude that nearly complete monolayer coverage of the gold surface has been achieved.

2.2.2.2. Precipitation of titania on surfaces:

The kinetics of the precipitation of titania on the self assembled monolayer surfaces could be followed by using plasmon spectroscopy. Figure 2.2.3 displays the deposition through hydrolysis of titania on the polymer surface from ethanolic solution of titanium isopropoxide. Here the changes in the plasmon reflectivity have been pursued using a minimum search routine monitoring the experiment as a

function of time. The initial time for this experiment was taken as the time of exposure of the monolayer surface to the titanium isopropoxide solution (10 mmol) to a moist atmosphere. It can be seen that the near-saturation in the reflectivity takes as long as 120 minutes. Plasmon spectroscopy experiments showed shifts of the plasmon curves after 200 minutes reaction time, which corresponds to a film thickness of 14 **Å** assuming a refractive index which is not much different to that of titania (n = 2.8300).

The experiment shows that the reaction time has an influence on the film thickness, only in the beginning. After saturation standardized films of titania can be obtained which can be deduced from insignificant changes of the film thickness after 2 hours.

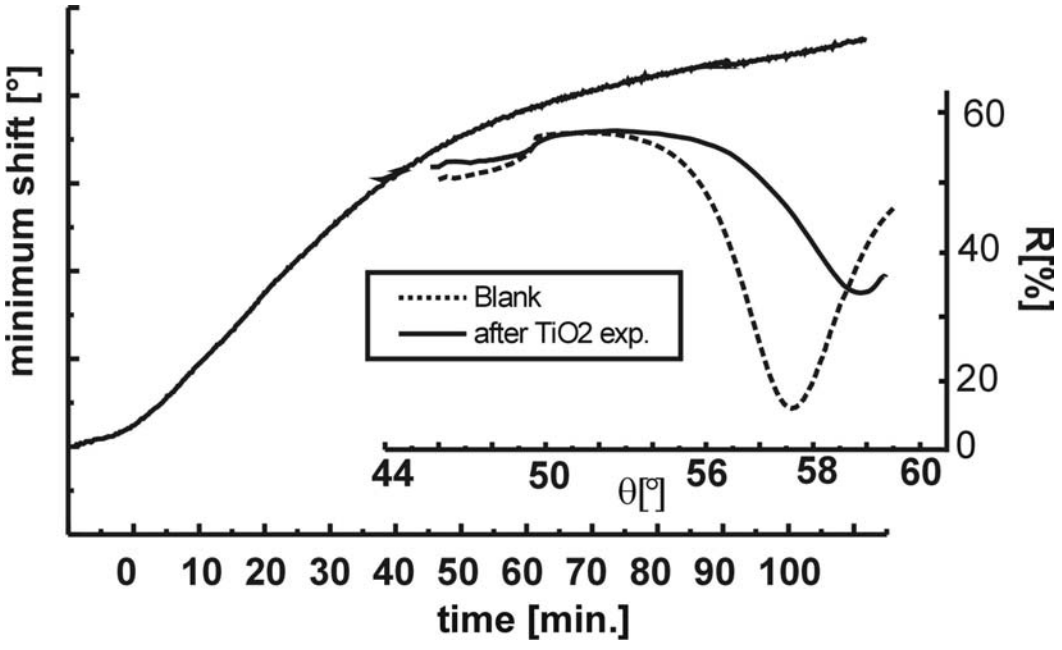

Figure 2.2.3 Plasmon resonance kinetic experiment of precipitation of titania from ethanolic solution on polymer surface. The final shift in the plasmon minimum corresponds to a film thickness of 14 **Å** after 140 minutes.

2.2.2.3. Scanning electron microscopy

Titania can be precipitated from a 10 mmol solution of titanium isopropoxide in ethanol under conditions described in the Experimental section. Figure 2.2.4 displays a scanning electron micrograph of spheres of titania thus obtained. The size of these filled particles ranges from 1 to 2.5 μm. They aggregate on the bottom of the reaction vessel as a porous material.

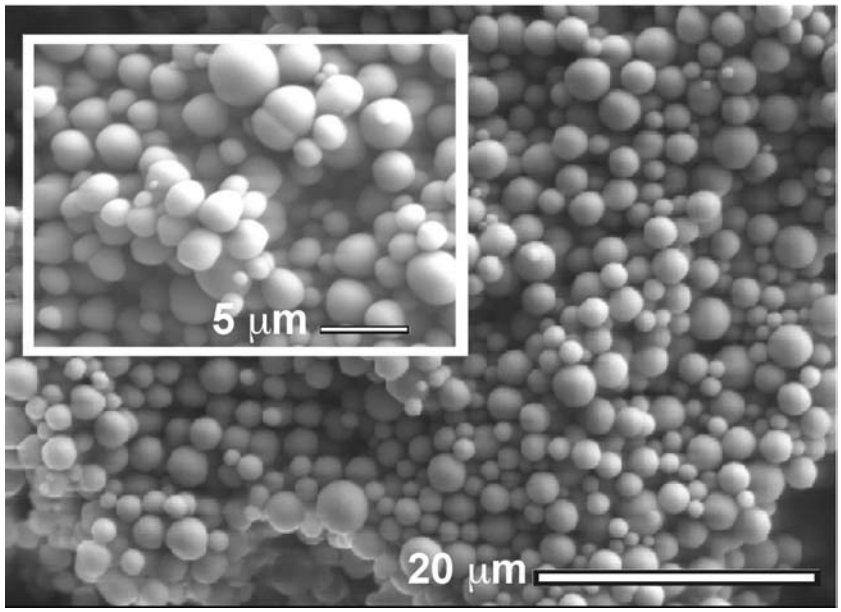

Figure 2.2.4 Scanning electron micrographs of the precipitation of titania from ethanolic solution in absence of a self assembled monolayer surface.

Gold surfaces were patterned with hexadecane thiol and were then placed in a 10 mmol toluene solution of the prepared monomer **T 2**. These patterned areas can be polymerized in toluene using butyl lithium and additional styrene monomer. The SE micrograph in Figure 2.2.5 displays the resulting surface after the polymerization. The obtained regular polymer dots have a size of 10 μm which corre-

sponds to the size of the stamp pattern. The surfaces thus prepared can be used to precipitate titania under the same conditions as discussed above.

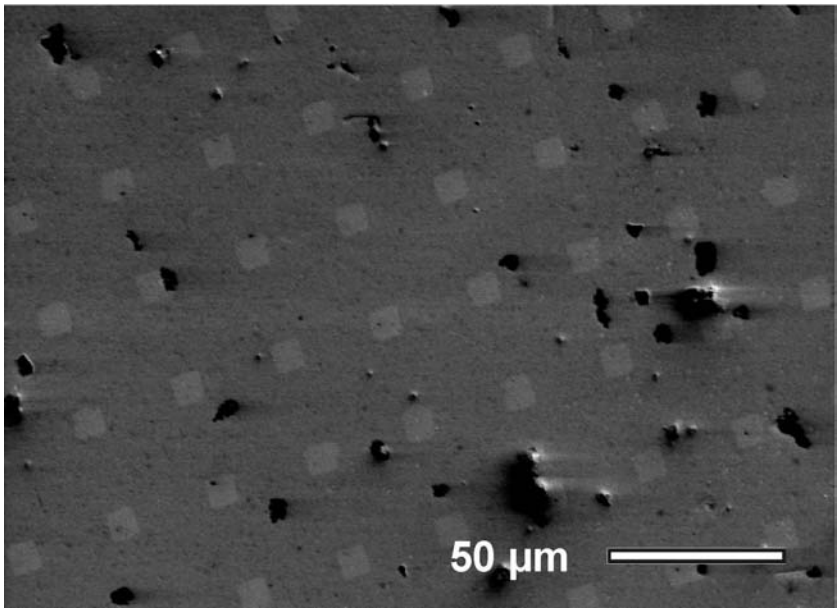

Figure 2.2.5 Scanning electron micrograph of a patterned gold surface after polymerization. The light dots correspond to the polymer, the dark area to the stamped alkane thiol structure.

FTIR measurements of the obtained poly styrene film can be taken from bulk material and from measurements directly from the surface in reflectance mode. (Figure 2.2.6)

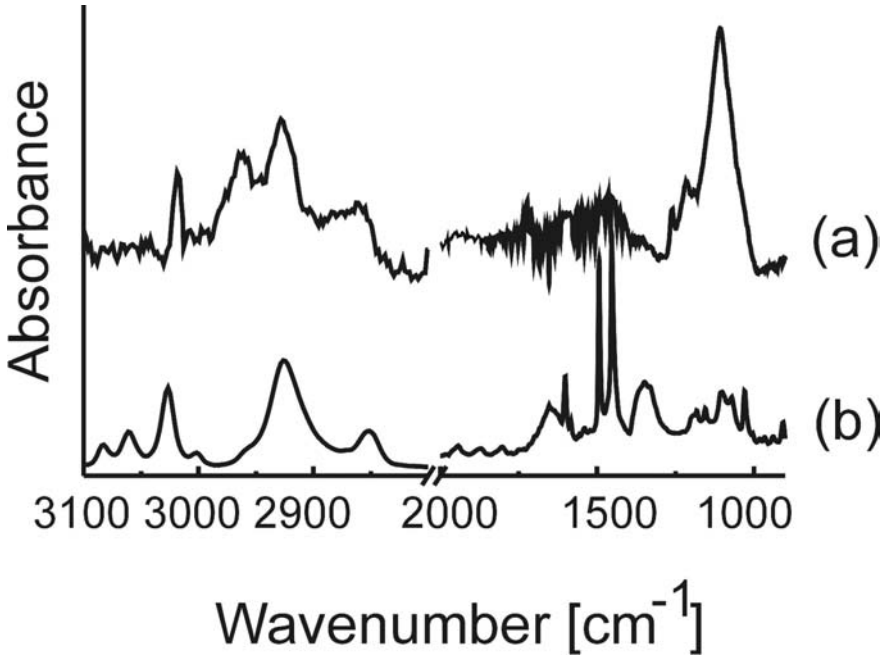

Figure 2.2.6 FTIR measurements of the obtained poly styrene film from the surface (a) and from bulk material (b)

Figure 2.2.7 displays a SE micrograph of titania obtained on the templated surface. At this stage, titania aggregates on the surface in the form of a continuous thin film, and the surface is fully covered. After 24 h the gold slides were washed with fresh ethanol and transferred into a reaction vessel which contained a solution of trimethyl silyl chloride in dichloromethane to split the polymer layer with titania above from the gold slide surface.

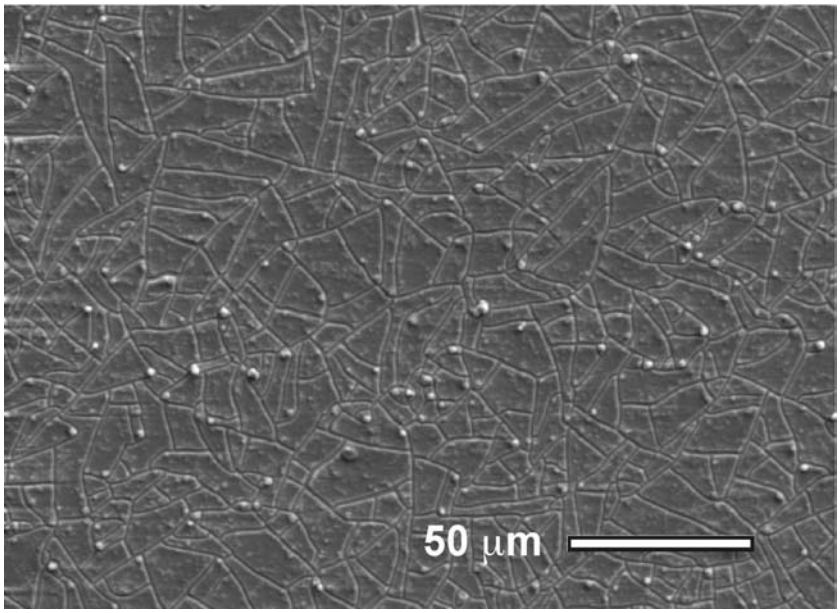

Figure 2.2.7 Scanning electron micrograph of a patterned and polymerized gold surface after precipitation of titania from ethanolic solution of titanium isopropoxide.

A surface which results normally after the cleavage procedure is displayed in Figure 2.2.8 and Figure 2.2.9 The dark hollows correspond to the patterned polymer surface. The patterned structure is seen to be quite sharp with the edge resolution being better than 1 μ. From the SE micrographs, we venture to say that the patterns in the titania films nearly as well defined as the patterns in the original stamp. EDX measurements, which can be made simultaneously during the scanning electron microscopy experiment, verify the absence of titania in the hollows and presence in the area around. (Figure 2.2.10)

As the electrostatic charging of the insulating titania leads to dark spots in the SEM image the area around the hollows can be assigned to the titania covered surface. Using simple SAM surfaces (without forming polymers on them) surface titania could not be removed through cleavage of the ether bond breaking.

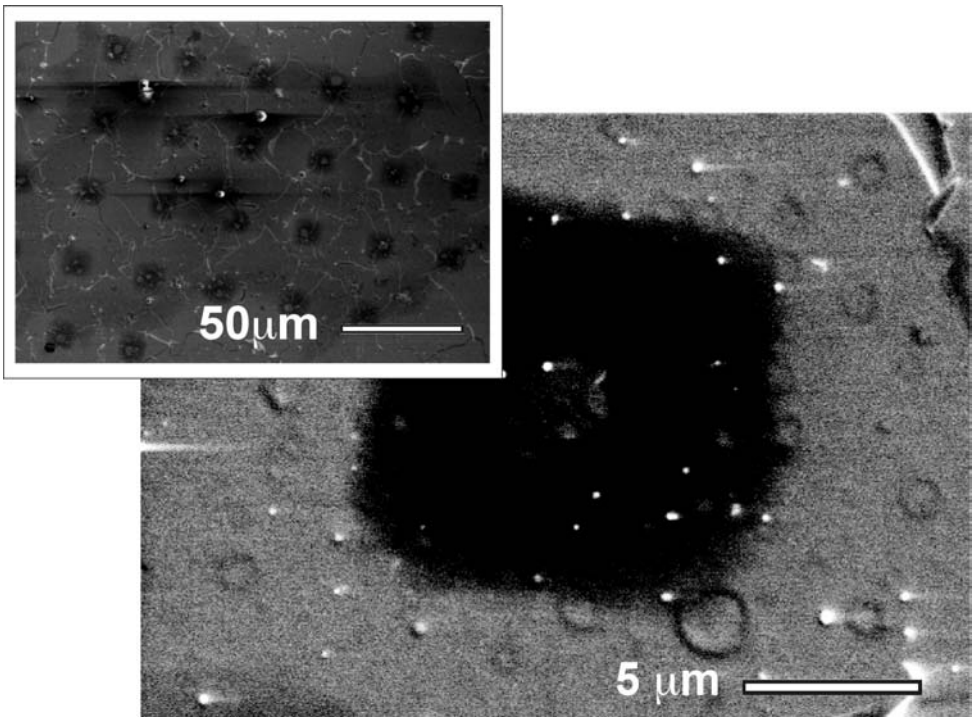

Figure 2.2.8 Scanning electron micrograph after cleavage of the ether bond in the previous surface. Regular hollows are obtained in the thin titania film.

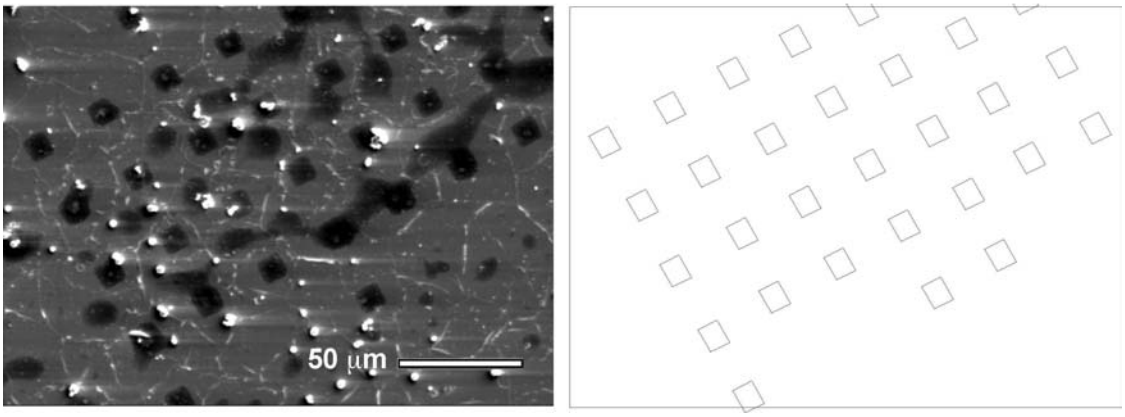

Figure 2.2.9 Scanning electron micrograph displaying obtained structure combined with theoretical drawing of expected structure.

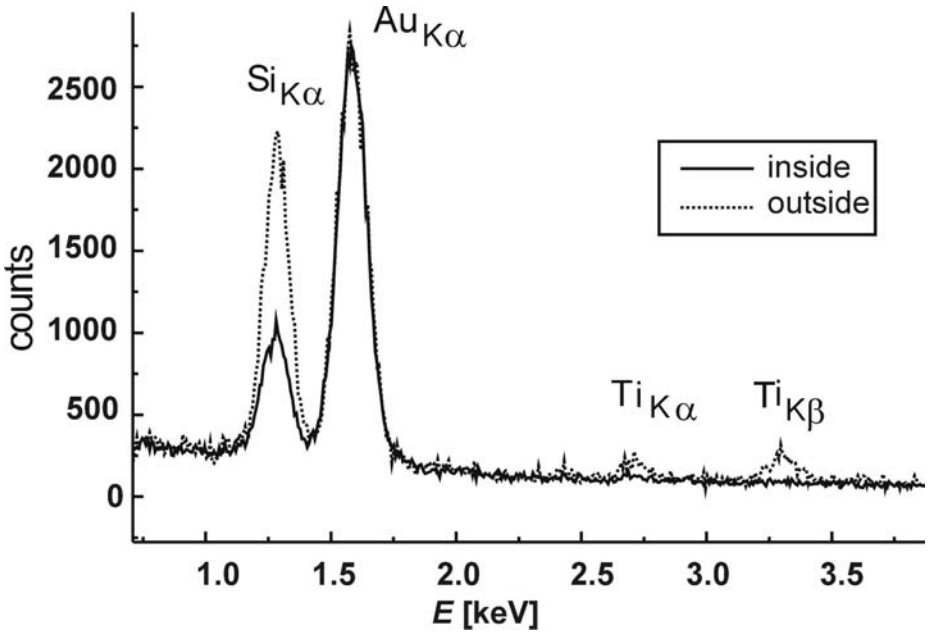

Figure 2.2.10 Energy dispersive X-ray measurement from the area inside the hollows (dots) and from the outside area (solid). Titanium K_α and K_β peaks cannot be found inside the hollows after removing of the polymer/titania surface.

AFM measurements can verify the obtained structure after cleavage of the polymer film. Figure 2.2.11 displays an AFM measurement in contact mode of one the obtained hollows in the thin titania film. Corresponding sizes can be found through SEM and AFM measurements.

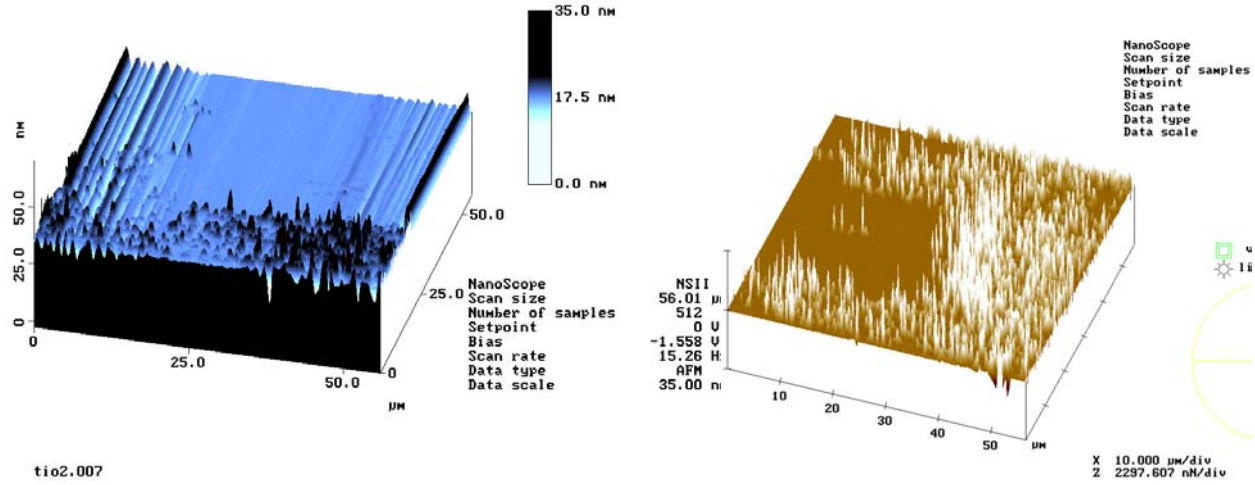

Figure 2.2.11 Contact mode AFM images of the one hollow of the titania structured surface after cleavage of the polystyrene film

2.2.3. Conclusion

In this paper we have presented a new way to pattern thin films of inorganic oxides using templates of self - assembled polymeric monolayers. Their architectures are obtained through combination of organic synthesis and stamping techniques. Organic thiols posses a high stability on such gold surfaces and lend themselves well for further manipulations to yield surfaces with new characteristics. It was shown that it is possible to polymerize prestructured areas filled with monomeric thiol molecules. These patterned surfaces can be used as templates for crystallization, and in this work, titania was presented as an example. This work also shows that it is possible to perform a wide range of modifications of surface - bound organic compounds after crystallization has taken place. The thin inorganic films have the specific structure of the stamp. It is obvious that these patterned films have a

number of potential applications, the only limitation being the number of structures that can be made with stamping techniques.

2.2.4. Experimental

All preparations were carried out an inert gas atmosphere. Solvents were purchased from Riedel de Haën Chemicals and used without further purification. Toluene was dried over sodium before use in polymerization. Styrene (Aldrich Chemicals) was freshly distilled to remove the stabilization agent.

2.2.4.1. Instrumental techniques

SPS measurements were performed in the Kretschmann configuration [24] against ethanol. Optical coupling was achieved with a LASFN 9 prism (n = 1.85 at λ = 632.8 nm) and index matching fluid (n = 1.70) between prism and the BK270 glass slides. The plasmon was excited with p-polarized radiation using a He - Ne laser (632.8 nm, 5 mW). The glass slides (3,5 x 2,5 cm) were cleaned with aq. NH_3 / H_2O_2 / water (1 / 1 / 5) 10 minutes at 80°C and coated with gold using a Balzers BAE250 vacuum coating unit under pressure of less than 5 x 10^{-6} hPa, typically depositing 48 nm of gold after first depositing 3 nm of Cr. The slides were exposed to the organic thiol solution (10 mmol) for 24 h.

Scanning electron microscopy was performed with a ZEISS Digital Scanning Microscope 962 combined with a Kevex EDAX at acceleration potentials of 5-15 kV. The glass substrates were cut in small pieces and fixed with conducting glue on alumina sample holders and used without further coating.

2.2.4.2. Preparation of the thiol T 2

The monomer was achieved by using modified procedures of Braun and Keppler, [25] Sieber and Ulbricht. [26] The thiol group was obtained using the Bunte salt method. [27], [28],[29]

2.2.4.3. (2-Hydroxy-ethyl)-phenethyl-ether (a)

A mixture of sodium (8 g) and phenyl ethanol (100 g) were heated up to 70° C. After sodium was fully dissolved the reaction mixture became solid. Then bromo-ethanol (2.5 g) were slowly added and stirred at 100° C . After 1 hour the mixture was heated up to 130° C and was stirred for further 2.5 hours. After cooling to room temperature the precipitated salt was filtered off and the oily filtrate was distilled under reduced pressure ($3*10^{-2}$ mbar). After repeated distillations (a) was obtained (50 %).

b.p: 110-120° C, ($3*10^{-2}$ bar); ^{1}H NMR (400 MHz, $CDCl_3$, 25° C, TMS): δ = 2.82 (t, ^{3}J (H,H) = 6.7, 2H; $ArCH_2$), 3.47(t, ^{3}J (H,H) = 6.7, 2H; OCH_2), 3.78 (t, ^{3}J (H,H) = 6.7; 4 H, CH_2O-, CH_2OH), 7.19(m, 5H; ArH); MS (EI-MS): m/z (%) = 166.1 (10) M^+ .

2.2.4.4. (2-Brom-ethyl)-phenethyl-ether (b)

(a) (8 g) was added to a solution of HBr (40 mL) and glacial acetic acid (40 mL). The mixture was stirred under reflux for 12 hours. After cooling to RT the mixture was neutralized with saturated Na_2CO_3 - solution. The organic product was collected by shaking the aqueous solution with $CHCl_3$. The organic layer was dried

with sodium sulfate and the solvent was evaporated. The resulting product was used without further purification (77 %).

^{1}H NMR (400 MHz, $CDCl_3$, 25° C, TMS): δ = 2.82 (t, ^{3}J (H,H) = 7.6, 2H; $ArCH_2$), 3.53 (t, ^{3}J (H,H) = 7.6, 2H; $BrCH_2$), 3.70 (m, ^{3}J (H,H) = 7.6, 4 H; CH_2OCH_2), 7.17 (m, 5H; ArH); IR (KBr): $\bar{\nu}$ = 3087 - 3007 (ArH), 2960 (CH_2, CH_3), 1120 cm^{-1} (C-O-C).

2.2.4.5. (2-Bromo-ethyl)-acetophenethyl-ether (c)

$AlCl_3$ (2.2 g) was suspended in CS_2 (8 mL) and acetyl chloride (1 mL) was added. A solution of (b) (4 g) and acetyl chloride (4 mL) was dropped slowly to the mixture in such a way that the reaction temperature was kept at 0° C. After stirring for 3 hours at 0° C the mixture was poured into a solution of ice and 37 % HCl (4:1). The organic layer was separated, and the aqueous layer was washed with $CHCl_3$ twice. The organic phases were combined and dried with sodium sulfate, the solvent was evaporated and the residue was chromatographed from silica gel with eluant petrol ether/ethyl acetoacetate (5:1) to yield (c) (44 %).

^{1}H NMR (400 MHz, $CDCl_3$, 25° C, TMS): δ = 2.55 (s, 3H; CH_3), 3.1 (t, ^{3}J (H,H) = 6.7, 2H; $ArCH_2$), 3.57 (t, ^{3}J (H,H) = 6.7, 2H; CH_2Br), 3.87 (m, ^{3}J (H,H) = 6.7, 4H; CH_2OCH_2), 7.22 (d, ^{3}J (H,H) = 7.6; 2H; ArH), 7,89 (d, ^{3}J (H,H) = 7.6; 2H; ArH); MS (EI-MS): m/z (%) = 272.0 (50) M-H^+ .

2.2.4.6. p-(2-brome-ethyl)-styrylethyl-ether (d)

A solution of (c) (2.5 g) in isopropanol (15 mL) was added to a mixture of aluminiumisopropoxide (2.1 g) in isopropanol (15 mL). The mixture was distilled over a vigreux - column (20 cm length) at a bath temperature of 130-140° C. The distillation was kept up until the distillate became free of acetone (proofed with 2,4 - dinitrophenyl hydrazine). Then the isopropanol was distilled off and the residual was poured into 6 N H_2SO_4 (100 mL). The aqueous layer was extracted with diethyl ether 3 times and the combined organic layers were washed with 1 N NaOH (50 mL), and subsequently 3 times with water (100 mL). Then $KHSO_4$ (3 g) were added to the ether solution, and the mixture was kept at room temperature. After 10 hours the ether was evaporated and the residue was distilled at 200 mbar. Water was set free at 130° C bath temperature. After the distillation of water stopped the bath temperature was increased to 170° C and a colorless oil obtained at 99-105° C in oilpump vacuum ($3*10^{-2}$ bar) (42%).

^{1}H NMR (400 MHz, $CDCl_3$, 25° C, TMS): $\delta =$ 3.10 (t, ^{3}J (H,H) = 6.7, 2H; $ArCH_2$), 3.50 (t, ^{3}J (H,H) = 6.7, 2H; CH_2Br), 3.55 (m, ^{3}J (H,H) = 6.7, 4H; CH_2OCH_2), 5.19 and 5.73 (dd, ^{3}J (H,H) = 7.4, 2H; CHC**H**$_2$), 6.66 (m, ^{3}J (H,H) = 7.4, 1H; C**H**CH_2), 7.22 (m, 4 H; ArH); MS (EI-MS): m/z (%) = 256.2 (30) M-H^+ .

2.2.4.7. p-(2-mercapto-ethyl)-styrylethyl-ether (T 2)

(d) (0.5 g) were dissolved in ethanol (10 mL) and stirred under reflux. A solution $Na_2S_2O_3$ (0.8 g) in water (10 mL) was added dropwise. The mixture was stirred under reflux for 4 hours. The solvent was evaporated and 1 N HCl (50 mL) were added to the residue. The mixture was heated under reflux for 2 hours. The aqueous layer was extracted with CH_2Cl_2 for 3 times, the organic phases were com-

bined, dried with Na_2SO_4 and the solvent was evaporated. The product obtained as a yellowish oil (72 %).

^1H NMR (400 MHz, $CDCl_3$, 25° C, TMS): $\delta =$ 2.72 (m, ^3J (H,H) = 6.7, 4H; $ArCH_2$, CH_2SH), 3.88 (m, ^3J (H,H) = 6.7, 4H; CH_2OCH_2), 5.19 and 5.73 (dd, ^3J (H,H) = 7.4, 2H; CHC**H**$_2$), 6.66 (m, ^3J (H,H) = 7.4, 1H; ArCH), 7.22 - 7.89 ppm (m; 4 H; ArH)); MS (EI-MS): m/z (%) = 209 (30) M-H^+ .

2.2.4.8. Polymerization of structured templates

Gold slides were prepared immediately before use as described in the experimental section and hexadecane thiol was stamped in a patterned manner on the gold surface according to published methods. [15] The gold slides were then placed into a solution of **T 2** (10 mmol) in $CHCl_3$ for 10 hours. The slides were washed with $CHCl_3$, dried in a N_2 stream and transferred into dry toluene. Two glass slides were placed in a reaction vessel and n-butyllithium (0.5 mL) and styrene (0.2 mL) were added. The reaction mixture was stirred for 30 minutes at room temperature. Then styrene (1.5 mL) was further added to give a dark orange solution and the mixture was stirred for 1 hour. The polymerization was stopped by adding methanol (3 mL). The templates were cleaned with $CHCl_3$ and methanol, and dried in a N_2 stream. Surface IR measurements correspond to polystyrene films as published by Ulman and coworkers. [17]

2.2.4.9. Crystallization of titania:

The templates were placed face down into a reaction flask. [30] The flask was filled with ethanol (100 mL), then titanium isopropoxide (3 mL) were added. The flask was transferred into a desiccator and stored at room temperature. The precipitation was initiated by placing a Petri dish with water at the bottom of the desiccator. The diffusion experiment was stopped after 10 hours, the samples were removed, washed with ethanol and dried in air.

2.2.4.10. Cleavage of the ether bond

A solution of dry $CHCl_3$ (100 mL) and trimethylsilyl chloride (100 μL) was placed in a reaction vessel fitted with a gas inlet and outlet. N_2 was passed through the mixture for 15 minutes. Then the titania coated templates were placed and the mixture was stirred for 1 hour under N_2 atmosphere. After this time the samples were removed, cleaned with toluene and dried on air.

2.2.5. References

[1] T. Kresge, M. E. Leonowicz, W. J. Roth, J. C. Vartuli, J. S. Beck, *Nature* **1992**; 359, 710

[2] N. K. Raman, M.T. Anderson, C. J. Brinker, *Chem. Mater.* **1996**, 8, 1682

[3] G. Schmid, *Chem. Rev.* **1992**,92,1709

[4] B. O´Regan, M. Grätzel, *Nature* **1991**, 353, 737

[5] A. Imhof, D. J. Pine, *Nature* **1997**, 389, 948

[6] F. Krauss, R. M. De La Rue, S. Brand, *Nature* **1996**, 383, 699

[7] W. L. Vos, R. Sprik, A. van Blaaderen, A. Imhof, .A. Langdijk, G. H. Wegdam, *Phys. Rev. B* **1996**, 53, 16231 - 16235; *Phys. Rev. B* **1997** , 55, 1903

[8] M. K. Erhardt, R. G. Nuzzo, *Langmuir* **1999**, 15, 2188

[9] M. Bartz, J. Küther, R. Seshadri, W. Tremel, *Angew. Chem Intl. Ed. Engl* **1998**, 37, 2466

[10] M. Bartz, J. Küther, G. Nelles, N. Weber,. R. Seshadri, W. Tremel, *J. Mater. Chem.* **1999**, 9, 1121

[11] J. Küther, R. Seshadri, W. Knoll, W. Tremel, *J. Mater. Chem.* **1998**, 8, 641; J. Küther, G. Nelles, R. Seshadri, M. Schaub. H.-J. Butt, W. Tremel, *Chem. Eur. J.* **1998**, 4, 1834

[12] M. Nagtegaal, J. Küther, J. Ensling, P. Gütlich, W. Tremel, *J. Mater. Chem.* ***1999***, 9, 1115

[13] J. Küther, R. Seshadri, W. Tremel, *Angew. Chem. Int. Ed.* **1998**, 37, 3044

[14] M. Bartz, N. Weber, J. Küther, R. Seshadri, W. Tremel, *J. Chem Soc. Chem.* Commun. **1999**, 2085

[15] J. Aizenberg, A. J. Black, G. M. Whitesides, Nature **1998**, 394, 868

[16] F. C. Meldrum, J. Flath, W. Knoll, *J. Mater. Chem.* **1999**, 9, 711

[17] R. Jordan, A. Ulman, J. F. Kang, M. H. Rafailovich, J. Sokolov, *J. Am. Chem. Soc.* **1999**, 121, 1016

[18] O. Prucker, C. A. Naumann, J. Rühe, W. Knoll, C. W. Frank, *J. Am. Chem. Soc.* **1999,** 121, 8766

[19] B. Zhao, W. J. Brittain, *J. Am. Chem. Soc.* **1999**, 3557

[20] T. von Werne, T. E. Patten, *J. Am. Chem. Soc.* **1999**, 7409

[21] A. Ulman, *Chem. Rev.* **1996**, 96, 1533

[22] Y. Xia, X.-M. Zhao, E. Kim, G. M. Whitesides, *Chem. Mater.* **1995**, 7, 2332; A. Kumar, H. A. Biebuyck, G. M. Whitesides, *Langmuir* **1994**, 10,

[23] P. E. Laibninis, G. M. Whitesides, D. L. Allara, Y. T. Tao, A. N. Parikh, R.G. Nuzzo, *J. Am. Chem. Soc.* **1991**, 113, 7152

[24] E. Kretschmann, *Z. Physik*, **1971**, 241, 313 - 324

[25] D. Braun, H.-G. Keppler, *Mh. Chem.* **1963**, 94 1250

[26] G. Sieber, I. Ulbricht, *J. prakt. Chem.* **1963**, 20, 14

[27] W. Fabianowski, L. C. Coyle, B. A. Weber, R. D. Granata, D. G. Castner, A. Sadownik, L. Regen, *Langmuir* **1989**, *5*, 35

[28] N. Nakashima, Y. Takada, M. Kunitake, O. Manabe, *J. Chem. Soc., Chem. Commun.* **1990**, 845

[29] I. Rubinstein, S. Steinberg, Y. Tor, A. Shanzer, J. Sagiv, *Nature* **1988**, *332*, 426

[30] J. Küther, W. Tremel, *Thin Solid Films* **1998**, 327-329, 554

3. 3- Dimensional Structures

3.1. Monothiols derived from glycols as agents for stabilizing gold colloids in water: Synthesis, self-assembly and use as crystallization templates.

3.1.1. Introduction

Tetraethylene glycol (HO-$(C_2H_4O)_4$-H) can be monofunctionalized by replacing one of the terminal hydroxyl groups with the thiol SH group. The resulting molecule can be self - assembled on gold (111) surfaces. More importantly, this molecule allows the simple one-step preparation of protected, water-soluble gold colloids within a single aqueous phase. Attempts are made to use such protected water-soluble colloids as nucleating "seeds" around which calcium carbonate can be crystallized.

Interest in preparation, characterization, properties and use of self assembled monolayers (SAMs) has grown tremendously in the last few years. [1], [2], [3] Amongst the different applications of thiol self - assembly to form monolayers on gold surfaces is the possibility of preparing stable gold colloids which display *quasi*-molecular behavior. [4] Gold colloids have been prepared and studied at least since the time of Faraday but the colloids in question always required stabilization through dispersion in a liquid medium. [5] There was usually no possibility of precipitating the gold colloids and then redispersing them – precipitation usually resulted in the formation of bulk gold particles. This also happened when one attempted to prepare sols of gold colloids in high concentrations. Only in recent times, through the use of protecting groups including long chain thiols, has it be-

come possible to prepare colloidal materials in high sol concentrations, and more importantly, obtain them as solids that can be redissolved.

The availability of these molecular nanocrystals has opened a range of possibilities for novel chemical architectures. In our group we have used different ω-terminated thiols assembled on flat gold-coated glass slides for the templated crystallization of calcium and strontium carbonates [6] and of iron oxide - hydroxides. [7] We have recently been able to carry over such crystallization into homogeneous media by using thiol-stabilized gold colloids instead of gold-coated glass slides for templating the crystallization. [8] By carrying over SAM chemistry to colloids, we have the advantage of being able to perform many chemical manipulations within the homogeneous medium and to follow the individual steps using conventional analytical techniques. [9] This has for example permitted us to immobilize homogeneous catalysts on gold colloids to obtain systems that combine the advantages of heterogeneous and homogeneous catalysts. [10] While protected gold colloids possess nearly molecular behavior, they retain the (111) surface of bulk gold. [5] They therefore form a class of materials that bridge the world of discrete molecules and the world of extended solids. [11]

This study presents the synthesis and use of a monothiol derived from tetraethylene glycol **T** 3 for preparing protected gold colloids in water. The thiol is water soluble without being polar. This has been an important motivation for the present study – our previous attempts [8] to make stable water-soluble colloids involved the use of phenolic thiols with the problem that they only dissolved at a rather high *p*H, or involved the use of sulphonate salts with the associated problem of polarity of the colloids so formed.

The self-assembly of the thiol on flat gold surfaces has been followed using surface plasmon spectroscopy. Gold salts can be reduced in the presence of the thiol to yield stabilized colloidal gold particles in solution. The colloids so formed retain the water-solubility of the thiol. Dispersing the colloids through spin-casting on a

mica surface has permitted their characterization by tapping-mode atomic force microscopy. It was attempted to use the protected gold colloids as seeds for the nucleation of calcium carbonate from solution. The products of such crystallization have been examined by powder x-ray diffraction and scanning electron microscopy.

3.1.2. Results and discussion

3.1.2.1. Self-assembly of the thiol on gold-coated glass substrates

Figure 3.1.1 shows angle dispersive surface plasmon spectra of a clean gold surface in water, and the plasmon spectra of a gold surface exposed to the thiol **T** 3. The shift of the plasmon curve is corresponding to an angular change of 0.4° and could be fitted using the Fresnel formula. Assuming the refractive index of the thiol **T** 3 to be no different from that of bulk tetraethylene glycol (n = 1.4598) a thickness of 18 Å for the SAM of **T** 3 on gold was determined. Modeling the structure of the thiol using molecular mechanics at the MM2 level (as implemented in Chem3D™ version 3.5) of the thiol **T** 3 suggests that chain expansions of as much as 15 Å are reasonable from the point of view of energetics. Considering additional gold - sulfur binding for the adsorbed thiol, we obtain the result that nearly complete monolayer coverage of the gold surface by the thiol has been achieved.

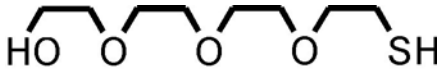

T 3

The kinetics of the thiol binding could be followed from changes in the surface plasmon. Figure 3.1.2 displays the adsorption of the thiol on flat gold surfaces followed from changes in the plasmon reflectivity at fixed scattering angle. The initial time for this experiment was taken as the time of exposure of the gold surface to the thiol (1 mM in water).

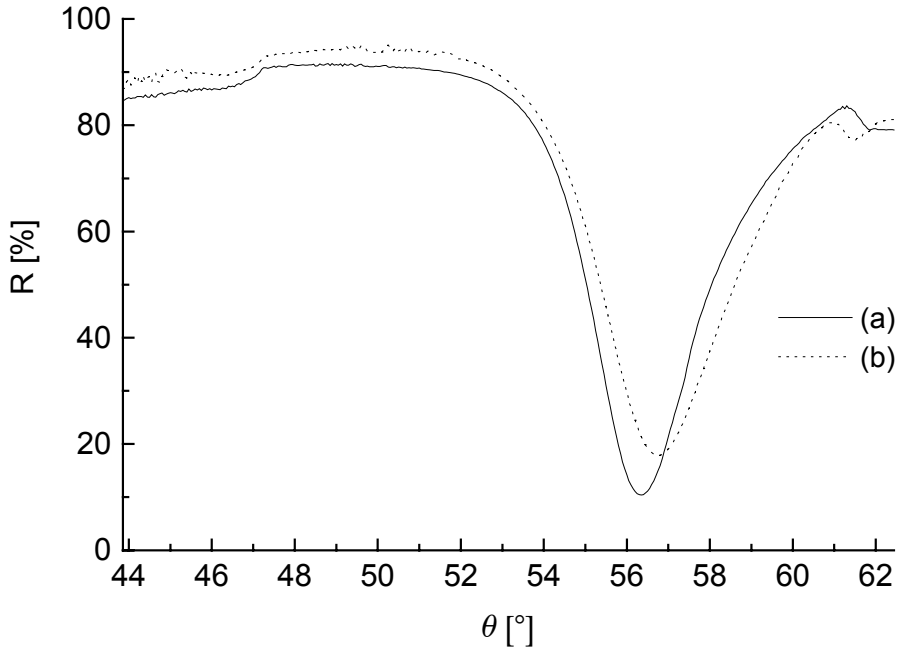

Figure 3.1.1 Surface plasmon resonance spectra of (a) the bare gold-coated glass surface and (b) after the coverage by the thiol **T** 3.

It is seen that near - saturation in the reflectivity takes as long as 100 minutes. After 150 minutes no further changes in the reflectivity are seen and the complete spectrum recorded after this time is consistent with a monolayer of the thiol being present. In comparison, long chain alkylthiols adsorb much more rapidly from ethanolic solution. A second trace corresponding to the kinetics of ω-mercapto- hexadecanoic acid adsorption (from ethanol, 1 mM concentration) is also shown in this figure. It seems that the adsorption kinetics for the glycolic thiol **T** 3 are much

slower than those for the alkylthiol perhaps as a result of much stronger solvent - thiol interactions in the case of the glycolic thiol. After 2 h in both cases the monolayers seem to be complete.

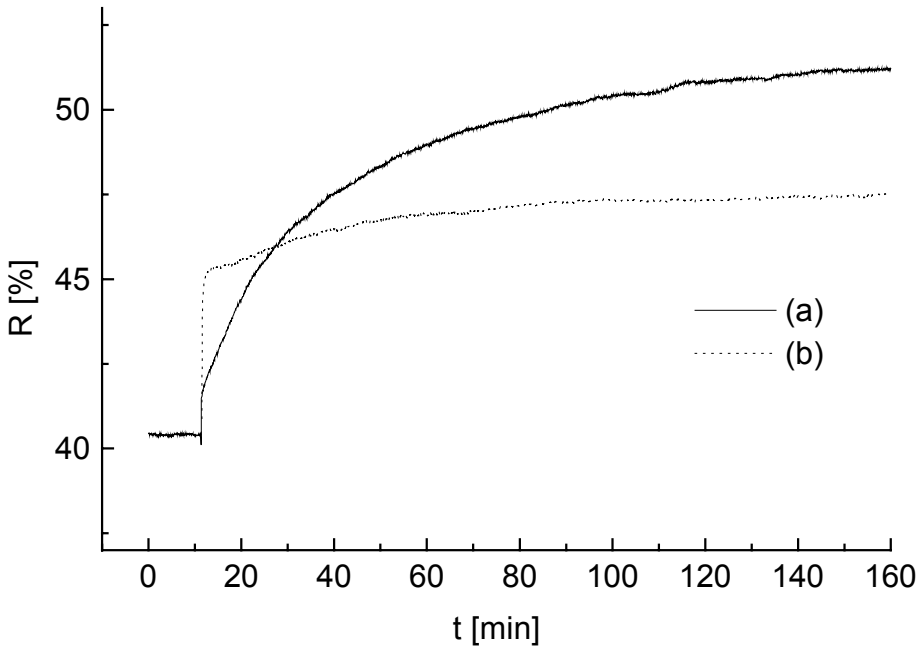

Figure 3.1.2 Kinetics of monolayer formation followed from the surface plasmon reflectivity. (a) is the thiol **T** 3 adsorbed from water and (b) for comparison is ω-mercapto-hexadecanoic acid adsorbed from ethanol.

Water contact angle measurements on the flat gold – coated glass slides after thiol adsorption yielded an advancing contact angle of 65.1° and a receding angle of 59.5°. The hysteresis is surprisingly small and the contact angles themselves are much higher than what would normally be expected for such a hydrophilic surface. OH terminated surfaces have contact angles usually smaller than 10°. [12] At the present time, neither the small hysteresis (which normally indicates very well-ordered surfaces) nor the large contact angles can be explained.

3.1.2.2. Gold colloids protected by the thiol T 3

The reduction of chloroauric acid in the presence of the thiol **T** 3 yields protected gold colloids in solution. These can be dried by evaporating the solvent water and then redissolving in water. This behavior is usually considered to be indicative of complete protection of the gold colloid by the thiol monolayer. The recorded IR - spectra of these functionalized and dried gold colloids are presented in Figure 3.1.3. The spectra are consistent with those of the free thiol, and of the thiol SAM on flat gold - coated glass substrates (taken in specular reflectance mode). These are also displayed in Figure 3.1.3.

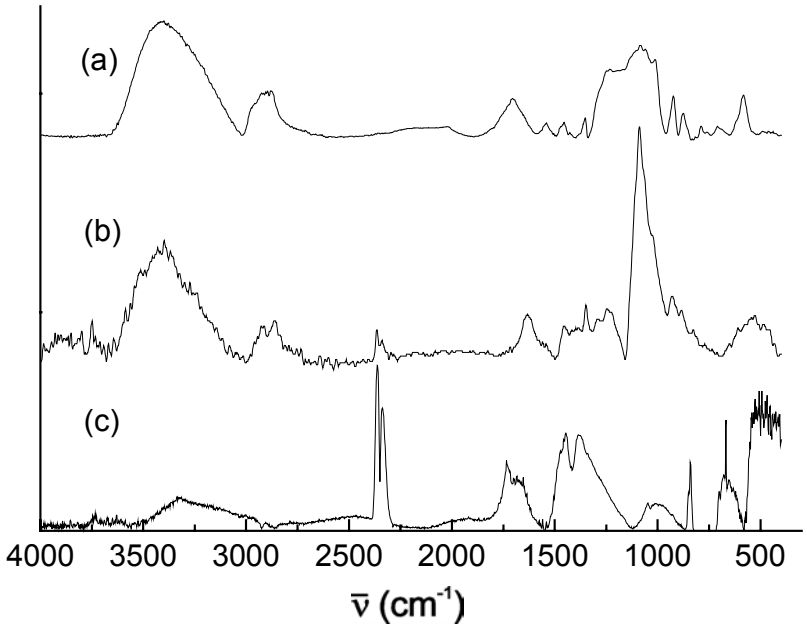

Figure 3.1.3 FT-IR spectra of (a) the thiol **T** 3 in transmission (b) gold colloids protected by the thiol **T** 3 in transmission and (c) the thiol **T** 3 adsorbed on gold-coated glass substrates taken in specular reflectance. The asterisk indicates the absorption of sorbed CO_2.

The panels of Figure 3.1.4 display atomic force micrographs of the glycol - thiol protected gold colloids that were spin - cast on mica surfaces. Panel (a) shows an AFM top view and panel (b) the surface plot. Both images display the heights of the objects. Two kinds of spherical objects on the surface can be observed, the first are clusters of the colloids forming spherical aggregates around 10 nm in diameter [from the heights surface plot in panel (b)]. These large aggregates are seen not to have smooth profiles but show up the individual colloidal particles which they comprise. The second feature are the individual colloidal particles with diameters around 2 - 3 nm [from the heights surface plot in panel (b)]. Elsewhere [13], we have examined the utility of tapping-mode AFM to examine gold colloids spin-cast on mica-surfaces through comparison with TEM images. Consistent sizes and morphologies through the two techniques can be found. Tip - sample convolution in determining the sizes of these colloidal particles does not seem to be a problem.

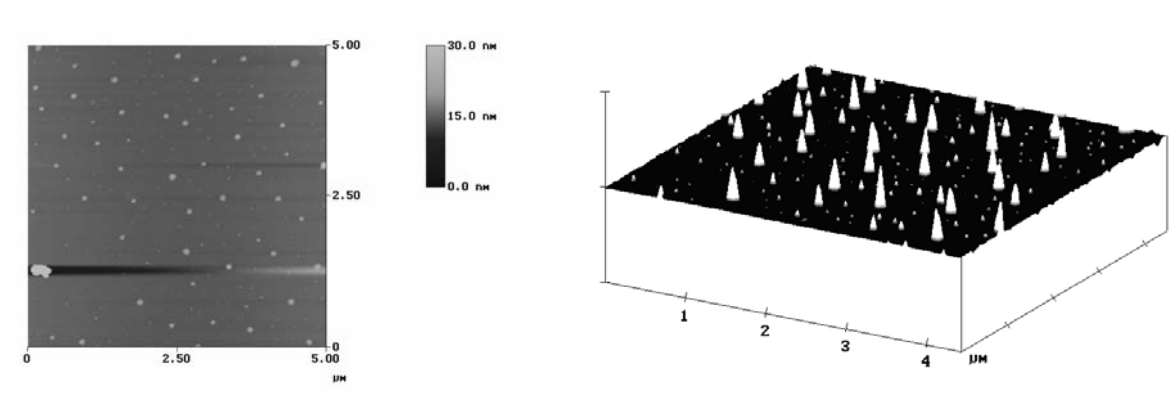

Figure 3.1.4 Tapping mode AFM images of the thiol-protected gold colloids deposited on a mica substrate. (a) is a top view and (b) the surface plot.

3.1.2.3. Calcium carbonate crystallization in the presence of the colloids

At a *p*H of 8.5 calcium carbonate crystallizes in its three modifications aragonite, vaterite and calcite. Typical scanning electron micrographs of materials collected after the crystallizations are displayed in Figure 3.1.5. Panel (a) shows rhombohedral calcite crystals with the typical (104) habit grown in the absence of the protected gold colloids. Panels (b) displays a micrograph of a typical aggregate obtained after calcium carbonate crystallization in the presence of the protected gold colloid seed (100 mg/l in terms of the Au). Analysis of the phase composition of the material collected from such a crystallization was followed through Rietveld refinements of the X-ray powder diffraction profiles as previously reported. [6] The analysis suggested that the ratio of calcite : vaterite : aragonite was 73 : 7 : 20 compatible with the ability of aragonite to form at this *p*H. However we focus on the calcite crystals in the micrograph displayed in this panel. While in our previous work, we have been able to infer unambiguously that (at a *p*H around 12) calcite crystals form spheroidal aggregates around the colloidal nuclei, from the micrograph in Figure 3.1.5 (b), it was unable to arrive at such a conclusion, here. Indeed, it would seem that the thiol - protected colloids, rather than acting as nuclei, act in this case as growth and habit modifiers. The precise plane on which the colloid acts is difficult to determine from this image. To confirm that the colloids indeed act as modifiers, the $CaCO_3$ crystallization in the presence of tetraethylene glycol (6 μM) was performed. In Figure 3.1.5 (c), a typical crystal aggregate after such crystallization is shown. There is significant inhibition causing the normally facetted calcite crystals to develop with edges that are rounded, making the calcite crystals form quasi - spheroidal morphologies.

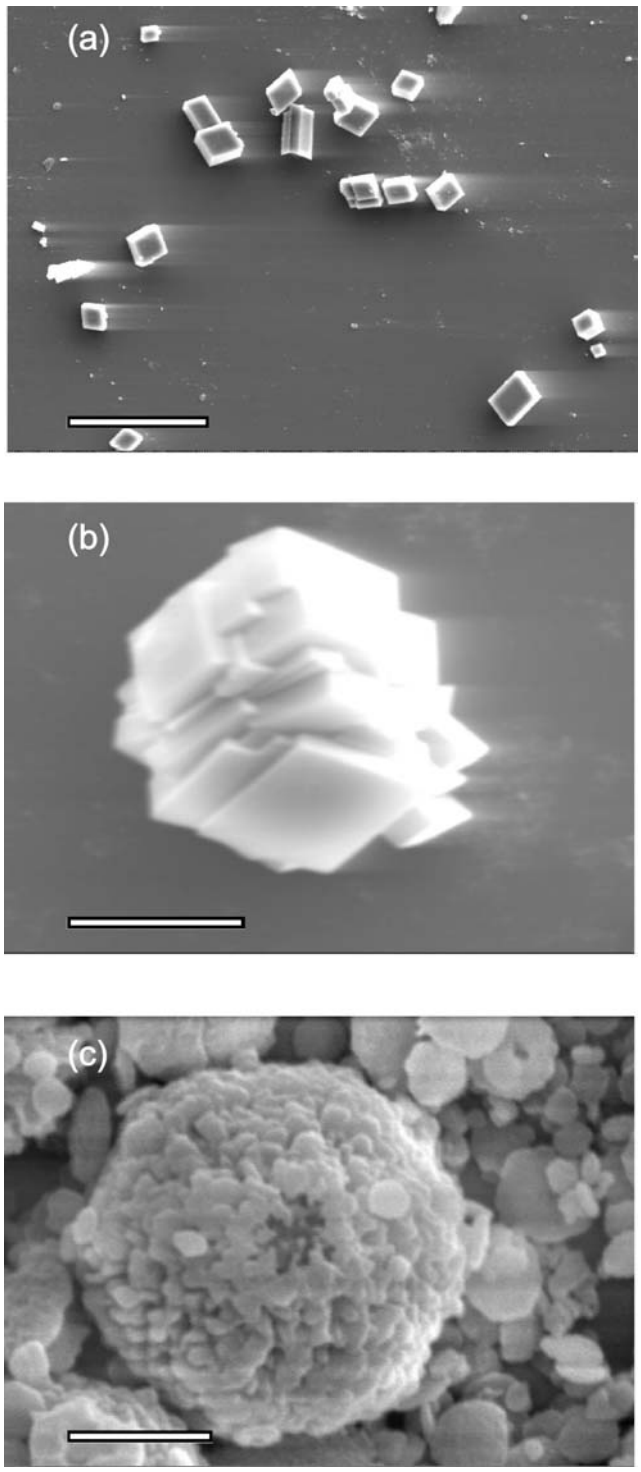

Figure 3.1.5 Scanning electron micrographs of the crystallizations performed at a *p*H of 8.5. (a) shows the crystals formed in the absence of the colloid, (b) in the presence of the thiol-protected colloids and (c) in the presence of tetra-ethylene glycol. The scale bars are (a) 50 μm, (b) 5 μm and (c) 5 μm.

When the *p*H is raised to 12, the only phase formed is calcite as verified from the x-ray powder diffraction profiles.Figure 3.1.6 (a) shows calcite crystals precipitated from solutions in the absence of thiol - protected gold colloid seeds. The crystal aggregates formed in the presence of the colloids are shown in Figure 3.1.6 (b). The nature of the rhombohedral crystals arranged in spheroidal aggregates suggests that the crystallization has indeed taken place around the colloidal nuclei. In this, the results correspond more to the kind of assemblies previously studied have been observed in crystallizations around *p*-mercaptophenol coated gold colloids [8]. The same problem, that aragonite is suppressed under a high *p*H, is retained. The present work provides additional impetus to the use of gold colloids as controlled seeds for the crystallization of inorganic materials from solution. Glycol seems to inhibit $CaCO_3$ crystallization, and a future direction to the present work would be to functionalize the exposed glycol group in order to obtain organic interfaces that are more compatible with the growth of the inorganic crystals.

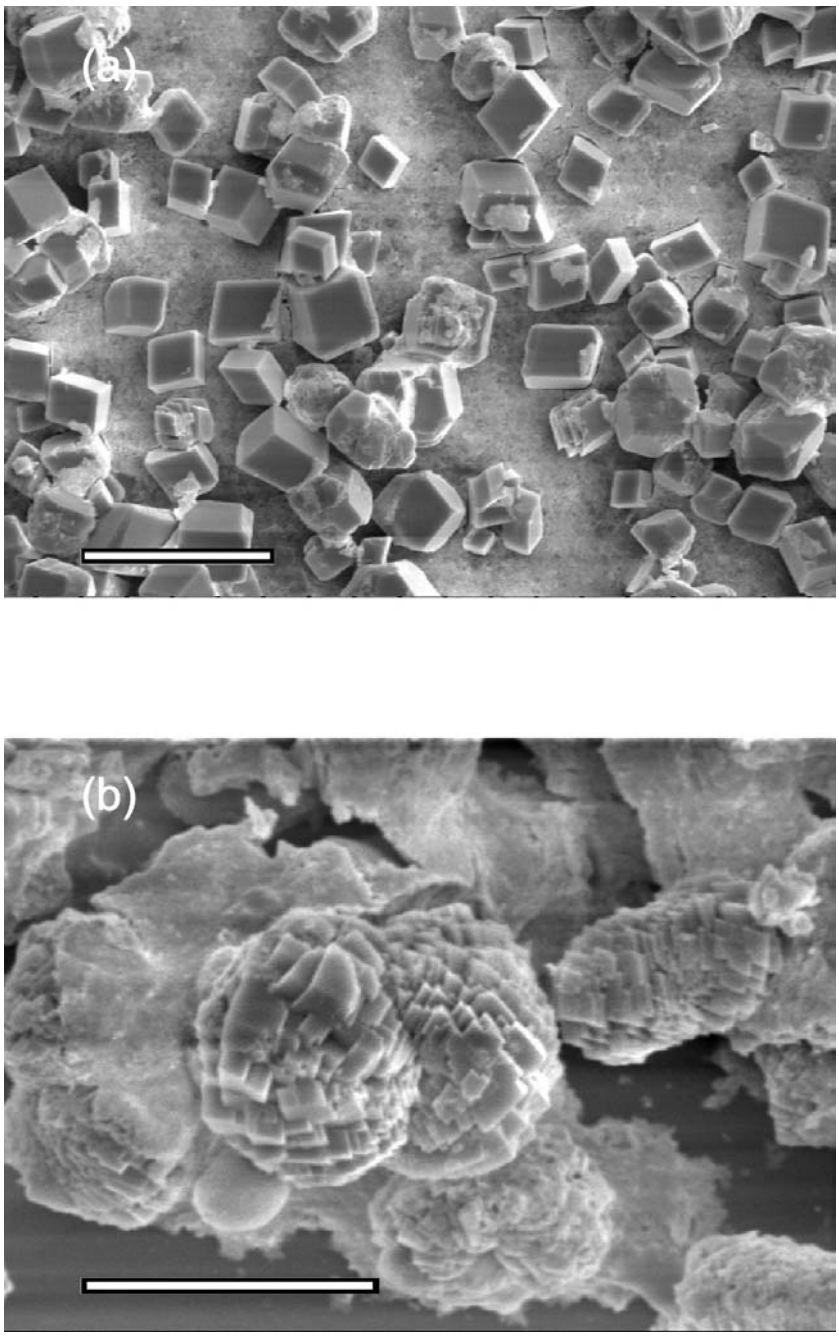

Figure 3.1.6 Scanning electron micrographs of crystallizations performed at a *p*H of 12. (a) is in the absence of colloids and (b) in the presence of the thiol-protected colloids. The scale bars are (a) 50 μm and (b) 20 μm.

3.1.3. Experimental

3.1.3.1. Instrumental techniques

X-ray diffraction patterns were obtained using a Siemens D5000 powder diffractometer equipped with a Ge(111) monochromatized CuKα_1 radiation (λ=1.54056 Å) in $\theta/2\theta$ transmission geometry. The crystals were collected by scratching the surfaces of the glass slides and were mounted on Scotch-Tape. Measurements were taken from $20° \leq 2\theta \leq 40°$ with a step size of 0.02° and a step time of 60 sec. SPS measurements were performed in the Kretschmann configuration [14]. Optical coupling was achieved with a LASFN9 prism (n=1.85 at λ=632.8 nm) and index matching fluid (n=1.70) between the prism and the BK270 glass slide. The surface plasmon was excited with *p*-polarized electromagnetic light using a He-Ne laser (632.8 nm, 5 mW). Kinetic experiments of the assembly of the thiol on gold-coated glass slides were monitored by following the plasmon reflectivity corresponding to an initial reflectivity of 40 %. The initial time was taken to correspond to the injection of the solution into the cuvette. Tapping-mode atomic force microscopy (AFM) images using silicon cantilevers were acquired on colloidal samples that were spin-cast onto mica substrates from aqueous solution. A Nanoscope IIIa was used for this purpose. FTIR spectra were recorded in transmission mode (KBr pellets) using a Mattson Instrument Galaxy 2030 IR-spectrometer. FTIR spectra in reflection mode were obtained by using a Nicolet (5DXC) GI-FTIR spectrometer equipped with a Spectra-Tech specular reflectance cell and a MCTA – detector with a angle of incidence of 85 °.

3.1.3.2. Preparation of the thiol T 3

The thioglycol was obtained by a modified reaction described by Tsymbal et al. [15] from the tetraethylene glycol by reaction with tosyl chloride. The mono- and bifunctionalized glycols were separated by column chromatography on silica gel and the mono–functionalized product was treated with LiBr to give the monobromoglycol. This was converted to the monothiol **T** 3 with $Na_2S_2O_3$ and HCl by using the Bunte salt method. [16], [17], [18] Details are presented in appendix A.

3.1.3.3. Study of the self-assembly of 1 on Au surfaces

After resistive evaporation (using a Balzers Baltec instrument at a pressure of 10^{-5} hPa) of a 2 nm adhesion layer of Cr on clean glass substrates, a further 50 nm of Au was deposited. The rate of deposition was monitored using a quartz crystal microbalance. The freshly prepared Au-glass substrates were placed in solutions of the thiol **T** 3 in ethanol (1 mM) overnight for studies by surface plasmon spectroscopy.

3.1.3.4. Gold colloids protected by T 3

A 5 ml solution of $HAuCl_4$ (2 g /100 ml water) was diluted with water to 40 ml. 50 µl of the thiol **T** 3 were added then. A solution of $NaBH_4$ (0.01 g) in water (10 ml) was added slowly with vigorous shaking until the mixture exhibited a dark red color. In the absence of the thiol, there is immediate precipitation of fine, black gold particles under these conditions. It was also verified that the simple tetraethylene glycol (without the thiol functionality) provides no protection to the gold col-

loids. Excess thiol and salts left over from the reduction could be removed by containing the solutions of the thiol-protected colloids in cellophane dialysis bags and washing with copious quantities of water.

3.1.3.5. Crystallization of $CaCO_3$ in the presence of gold colloids protected by the thiol T 3

A 10 mM solution of $CaCl_2$ was prepared in water (250 ml) and a freshly prepared solution of the colloid (50 ml, 0.2 g/100 ml) was added. Glass slides were placed at the bottom of the vessel containing the solution. The vessel was placed in a closed desiccator with solid $(NH_4)_2CO_3$ at the bottom for 2 days at 22° C. In the CO_2 rich atmosphere, crystallites precipitate from solution. The precipitated material was collected on the glass slides and dried at 50 °C in air before being examined by scanning electron microscopy and powder x-ray diffraction.

3.1.3.6. 12-(p-toluenesulfonyl)-3,6,9,12-tetraoxa-1-dodecanol (a)

10 g of tetraethylene glycol (0.05 mol) and 5.06 g of triethylamine (0.05 mol) were dissolved in acetonitrile (150 ml). 9.5 g of p-toluenesulfonyl chloride (0.05 mol) were added dropwise over 1 h. The reaction mixture was stirred for 14 h at 25 °C. The white precipitate of triethylamine hydrochloride was filtered off and washed with acetonitrile. The solution was evaporated and the residue was chromatographed from silica gel with the eluant chloroform/acetone 10:3. The second fraction was the monosulfonate (2). Yield: 8.7 g (50%). (^{1}H) NMR: 7.79 – 7.73 (m, 4H arom.), 4.14 – 3.51 (m, 16 H, OC**H**$_2$), 2.42 (s, 3H, C**H**$_3$), 2.14 (s, 1H, -CH_2O**H**).

3.1.3.7. 12-Bromo-3,6,9,12-tetraoxa-1-dodecanol (b)

17 g LiBr (0.2 mol) were dissolved in p.a. acetone (200 ml). 8 g of (a) (0,023 mol) were added and the mixture was stirred over 4-5 h at 80 °C. The mixture was then cooled to room temperature and stirred overnight. The solvent was evaporated and 100 ml chloroform was added to the residue. A white precipitate was filtered and the solution was washed two times with water. The organic layer was dried with Na_2SO_4 and the solvent was evaporated. Yield: 3.9 g (65 %). (^{1}H) NMR: 3.72 (t, 2 H C**H**$_2$OH), 3.63 – 3.49 (m, 12 H, OC**H**$_2$), 3.36 (t, 2 H, C**H**$_2$Br). EI-MS m/z(%) = 256.41 (54.4%), 258.39 (21.2%)

3.1.3.8. 12-Mercapto-3,6,9,12-tetraoxa-1-dodecanol (c)

20 g of (b) ($7.8*10^{-2}$ mol) were dissolved in Ethanol (200 ml) and stirred under reflux. A solution of 2.5 g of $Na_2S_2O_3$ (0.11 mol) in water (200 ml) was added dropwise. The mixture was stirred at 20° C for 48 h. The solvent was evaporated and 1 N HCl (60 ml) was added to the residue. The mixture was heated under reflux for 2 h. The solvent was evaporated and the residue was dissolved in dichloromethane (50 ml) and dried with Na_2SO_4. The solvent was evaporated and the residue was dissolved in acetone (5 ml). A yellow precipitate was filtered of. The solution was evaporated and the product obtained as a yellow oil. Yield: 6.7 g (40 %). (^{1}H) NMR: 3.72 (t, 2H, CH_2OH), 3.57 (m, 12H OCH_2), 2.8 (m, 2 H, CH_2S). IR 3410 (-OH), 2925 – 2850 (-CH_2), 1454 (CH_2), 1300 – 1020 cm^{-1} (C-O-C).

3.1.4. References

[1] A. Ulman, *Chem. Rev.* **1996,** *96*, 1533

[2] S. Flink, B. Boukamp, A. van den Berg, F. van Veggel, D. Reinhoudt, *J. Am. Chem. Soc.* **1998,** *120*, 4652

[3] R. Clegg, S. Reed, J. Hutchinson, *J. Am. Chem. Soc.* **1998**, *120*, 2486

[4] M. Brust, M. Walker, D. Bethell, D. Schiffrin, R. Whyman, *J. Chem. Soc. Commun.* **1994**, 801; M. Brust, D. Bethell, D. J. Schiffrin, C. J. Kiely, *Adv. Mater.* **1995**, *7*, 795

[5] A. I. Kirkland, P. P. Edwards, D. A. Jefferson, D. G. Duff, *Ann. Rep. C* The Royal Society of Chemistry: Cambridge, 1988, 247; J. Prost, F. Rondelez, *Nature* **1991,** *350*, suppl. mater., 11

[6] J. Küther, G. Nelles, R. Seshadri, M. Schaub, H.-J. Butt, W. Tremel, *Chem. Eur. J.* **1998**, *4*, 1834; J. Küther, R. Seshadri, W. Knoll, W. Tremel, *J. Mater. Chem.* **1998**, *8*, 641; J. Küther, R. Seshadri, G. Nelles, H.-J. Butt, W. Knoll, W. Tremel, *Adv. Mater.* **1998**, *10*, 401

[7] M. Nagtegaal, P. Stroeve, J. Ensling, P. Gütlich, M. Schurrer, H. Voit, J. Flath, J. Käshammer, W. Knoll and W. Tremel, *Chem. Eur. J.* accepted

[8] J. Küther, R. Seshadri, W. Tremel, *Angew. Chem.* **1998**, *110*, 3196; *Angew. Chem. Intl. Ed. Engl.*, **1998**, *37*, 3044

[9] R. Terril, T. Postlethwaite, C. Chen, C. Poon, A. Terzis, A. Chen, J. Hutchinson, M. Clark, G. Wignall, J. Londono, R. Superfine, M. Falvo, C. Johnson Jr., E. Samulski, R. Murray, *J. Am. Chem. Soc.* **1995**, *107*, 12537

[10] M. Bartz, J. Küther, R. Seshadri, W. Tremel, *Angew. Chem.* **1998**, *110*, 2646; *Angew. Chem. Intl. Edn. Engl.* **1998,** *37*, 2466

[11] R. L. Whetten, J. T. Khoury, M. M. Alvarez, S. Murthy, I. Vezmar, Z. L. Wang, P. W. Stephens, C. L. Cleveland, W. D. Luedtke, U. Landmann, *Adv. Mater.* **1996**, *8*, 428

[12] C. D. Bain, G. M. Whitesides, Angew. Chem. **1989**, 101, 522; Angew. Chem. Intl. Ed. Engl., **1989**, 110, 506

[13] J. Kütther, R. Seshadri, G. Nelles, W. Assenmacher, H.-J. Butt, W. Mader, W. Tremel, *Chem. Mater.* **1999**, 11, 1317

[14] E. Kretschmann, *Z. Physik* **1971**, 241, 313

[15] L. Markoviskii, D. Rudkevich, V. Kal´chenko, I. Tsymbal, *J. Org. Chem USSR (engl. transl.)* **1990**, *26*, 2094

[16] S. Regen, W. Fabianowski, L. Coyle, B. Weber, R. Granata, D. Castner, A. Sadownik, *Langmuir* **1989**, *5*, 35

[17] N. Nakashima, Y. Takada, M. Kunitake, O. Manabe, *J. Chem. Soc., Chem. Commun.* **1990**, 845

[18] I. Rubinstein, S. Steinberg, Y. Tor, A. Shanzer, J. Sagiv, *Nature* **1988**, *332*, 426

3.2. ´´Sticky´´ gold colloids through protection-deprotection and their use in complex metal-organic-inorganic architectures.

3.2.1. Introduction

Exposing bare gold colloids to long-chain dithiols results in their precipitation due cross-linking of the thiol groups with the gold surfaces. Here we demonstrate that through the use of a dithiol that has one of the thiol groups protected, we can, through attachment followed by deprotection, prepare gold colloids with exposed thiol. The uses of such ´´sticky´´colloids in creating complex architectures is demonstrated by using them to template the growth of PbS particles.

The notion that gold colloids in the nanometer range provide surfaces on which thiol self-assembly can be achieved has been employed by us for a variety of new functionalizations. Using suitable thiols, we have for examples, attached polymerization catalysts on colloid surfaces. [1] The use of thiol monolayer surfaces on gold in templating the crystallization of inorganic minerals such as calcium carbonate [2], [3] has been extended by us to the use of thiol-coated colloids as crystallization nuclei [4], [5]. This has opened a new dimension surface-templated crystallizations since a dispersed, spherical colloid offers a very different geometry from a large, planar surface.

In coating gold colloids with thiols in solution, there are a few points that need to be examined. The first is that the thiol should protect the colloid and keep in solution. The second is that the surface functionality of the thiol (the ω group on the long chain) should be compatible with the use to which the colloids are put. For example, in a previous work, we used long chain glycol-based thiols to take colloids into aqueous solution but the surfaces so formed on the colloids inhibit the crystal-

lization of calcium carbonate. [5] We have been interested in coating dithiols on gold colloids since particles so coated would offer an SH functionality on the surface (the ω group) that would be compatible with inorganic sulfides. However, if dithiols are added to a gold colloid sol, immediate precipitation results due to the cross-linking of the thiols with the colloid surfaces. [6]

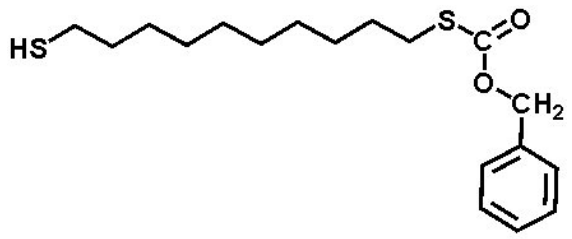

T 4

The strategy that we present in this communication borrows from peptide chemistry and uses a protection group for the thiol functionality. [7] We have prepared half-protected dithiols 1 with n = 6, 10 and 12 #. The self-assembly of these thiols on flat gold surfaces and the possibility to deprotect the ω – thiol functionality with aq. NH_3 has been established using Surface Plasmon Resonance Spectroscopy (SPS), as has the propensity of the deprotected surface to stick gold colloids. The thiols have been assembled on gold colloids in a toluene solution. The colloids are precipitated by and washed with methanol following which they are redissolved in CH_2Cl_2 where the protection group is removed with aq. NH_3. These ´´sticky´´ colloids are then dissolved in THF and PbS is deposited around them. The templated growth of PbS particles on SAM surfaces has been studied extensively by Meldrum *et al.* [8]

3.2.2. Results and Discussion

Figure 3.2.1 displays the SP spectra of a clean gold surface and the surface after various steps of thiol self-assembly, deprotection, exposure to colloids etc. as explained in the caption and the scheme. These establish the possibility to deprotect the surface as well as to then stick gold colloids.

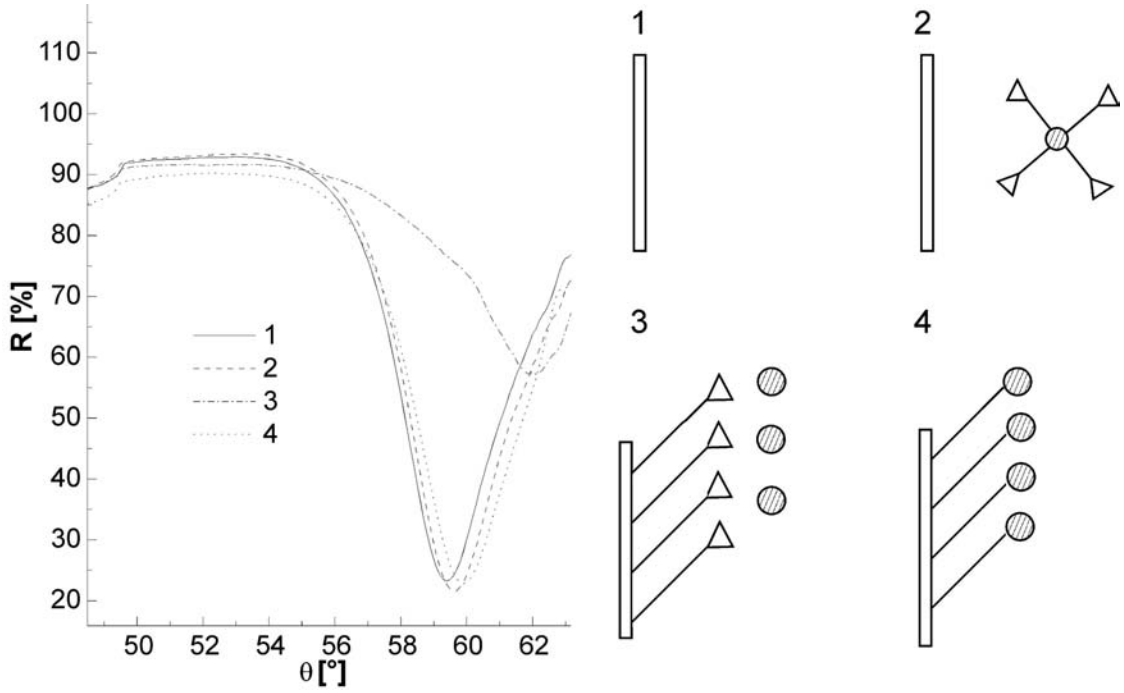

Figure 3.2.1 Surface plasmon spectra of a clean gold surface (1), a clean gold surface exposed to protected gold colloids (2), a gold surface modified with the half protected decanedithiol and exposed to bare gold colloids (3) and a gold surface after deprotection of the dithiol and exposure to bare gold colloids (4). The schemes on the right correspond to the different SP spectra with rods indicating the thiol, spheres the gold colloids and triangles, the protecting groups.

Figure 3.2.2 displays SE micrographs of PbS particles grown from THF solutions in the absence (a) and in the presence of dithiol-coated gold colloids (b,c). The thiol – group in Figure 3.2.2 b is still protected so the significant modification in the morphology of the particles, and the spherical shape suggests that the particles are grown around the colloids with unprotected thiol groups in (c). At the present time, we are unable to establish whether it is a single colloidal particle that nucleates the growth of a PbS shell or a cluster of particles. We have determined that it is not the thiol alone that results in the morphologies displayed in (c) (through the inhibition of certain surfaces for example) so the colloid does play a critical role.

PbS is a semiconductor and the thiol layer is insulating. Links between the structures of MOSFETs and of the metal colloid, thiol, PbS architectures presented here are recognized. The materials that are the subject of the present communication could perhaps be referred to as ´´MOSFETs in a test tube´´.

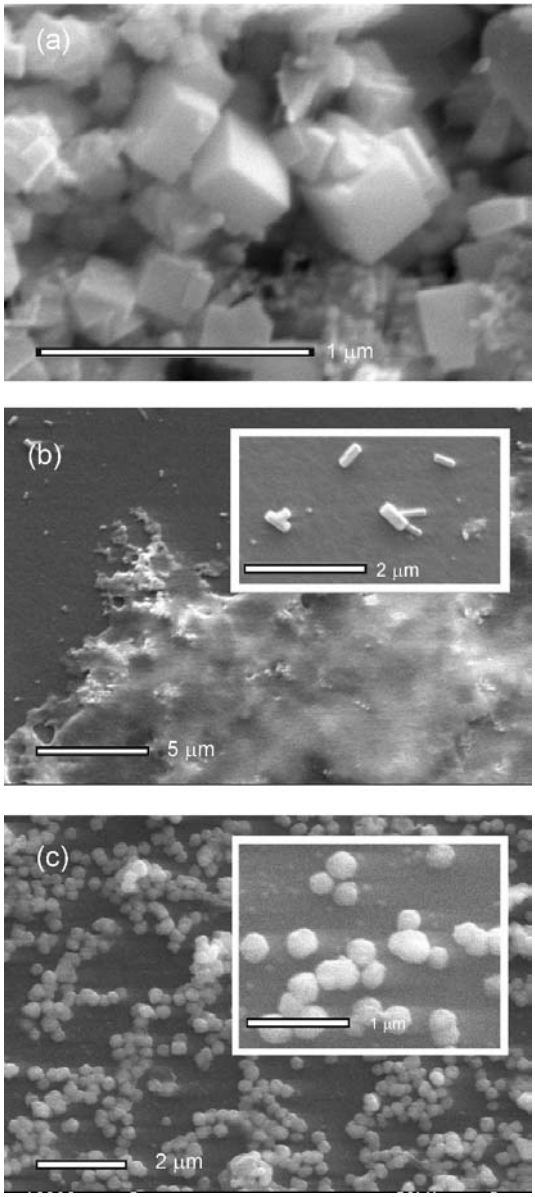

Figure 3.2.2 Scanning electron micrographs of the products obtained after crystallization of PbS. (a) crystallization in the absence of gold colloids. The crystals formed correspond to the cubic system of lead sulfide. (b) Pictures of products crystallized in the present of protected gold colloids. (c) Round Particles found after crystallization PbS in the presence of unprotected gold colloids.

Figure 3.2.3 displays a scanning electron micrograph image of obtained PbS particles in the presence of deprotected gold colloids in higher resolution. The spherical nature of the particles corresponds to results explained

above. However, colloidal particles of PbS, obtained on the surface , roughen the surface texture.

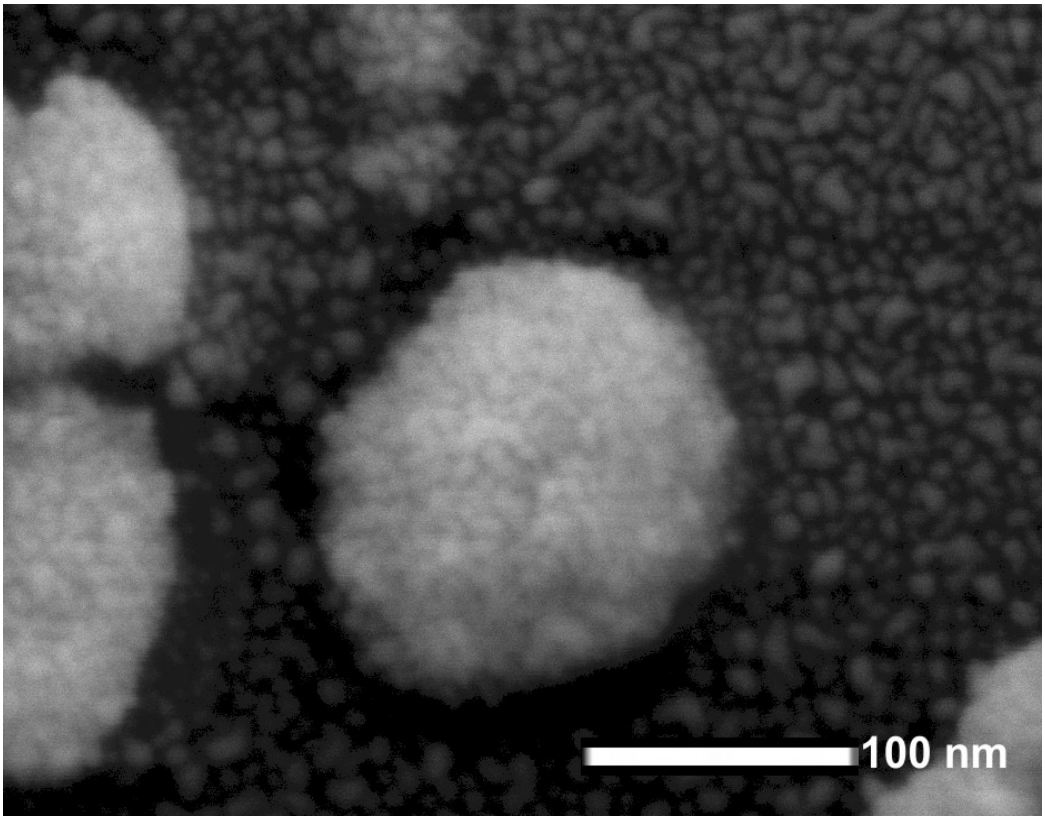

Figure 3.2.3 Scanning electron microscope images in higher resolution of PbS particles in the presence of unprotected gold colloids

The panels of Figure 3.2.4 display atomic force micrographs of the PbS particles precipitated in the presence of gold colloids fixed through dimercaptodecane on gold substrates. The left panel displays the heights of the objects, the right one displays the same region in force mode. The colloidal surface was functionalized with additional dithiol with the subsequencal precipitation of PbS. Spherical objects can be observed with 100 nm in diameter corresponding to observed sizes before.

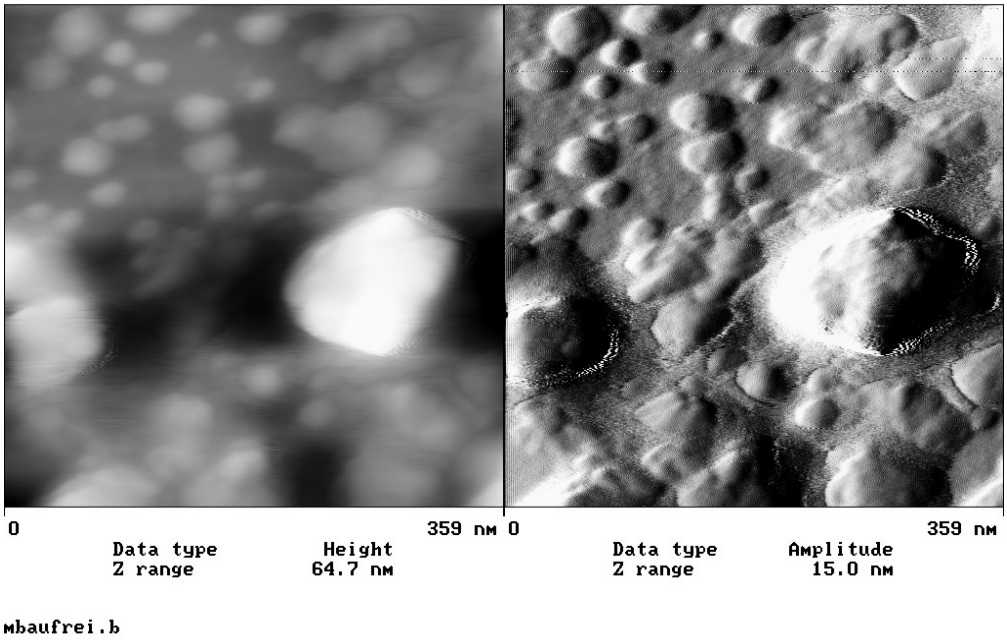

Figure 3.2.4 Tapping mode AFM images PbS – gold colloid composites, dithiol fixed on gold substrates. The left panel displays objects obtained in height mode, the right panel displays the same region in force mode.

3.2.3. Experimental

3.2.3.1. Instrumental techniques

SPS measurements were performed in the Kretschmann configuration [9]. Optical coupling was achieved with a LASFN9 prism (n = 1.85 at λ = 632.8 nm) and index matching fluid (n = 1.70) between prism and the BK270 glass slides. The plasmon was excited with p-polarized radiation using a He-Ne laser (632.8 nm, 5mW). The glass slides were cleaned with aq. NH_3/H_2O_2/water (1/1/7) 10 min. at 80 °C and coated with gold using a Balzers BAE250 vacuum coating unit under pressure of less than 5 x 10^{-6} hPa, typically depositing 48 nm of gold after first depositing 2 nm of Cr. The slides were exposed to the organic thiol solution (10 mmol) for 24 h.

3.2.3.2. Half protected dithiols

The dithiols were prepared from 1, *n*-dibromo alkanes using the Bunte Salt method. [1], [10] The protection of one of the thiol groups using the benzoyloxocarbonyl group was achieved using a procedure of Scott *et al.* after modification. [11] Briefly, to the dithiol (5 g) in acetone (50 ml) with 2N NaOH in water (60 ml), benzoyloxycarbonyl chloride (2.8 g) in acetone (20 ml) and 2N NaOH (40 ml) in water are added simultaneously dropwise, over 30 min. while cooling with ice. After stirring overnight at room temperature, the acetone was removed and the residue was worked up with ether. The organic layer is separated and chromatographed on silica to separate 1 from the unprotected and deprotected compounds. Gold colloids were prepared in toluene following the method of Brust *et al.* [12][11]

3.2.3.3. Deprotection

Deprotection could be carried out with aq. NH_3 (40 ml) in CH_2Cl_2 (40 ml), stirring overnight. The deprotected colloids in the organic layer are collected after removing the solvent and dissolved in THF for the crystallization experiments.

3.2.3.4. Crystallization of PbS

Crystallization of PbS was carried out using aqueous solution (3 mmol) of $PbNO_3$ (3 ml) in THF (100 ml) and deprotected gold colloids (0.1 g) were added. After glass slides were placed at the bottom of the vessel it was exposed to an H_2S – atmosphere in desiccator for 24 h. The solvent was removed, sucked off and the glass slides were dried at room temperature. The material collected on the slides were studied by X-ray diffraction (Siemens D5000, transmission, $CuK\alpha_1$ to confirm the NaCl structure of PbS and by SE microscopy (Zeiss DSM 962).

3.2.4. References

[1] M. Bartz, J. Küther, R. Seshadri and W. Tremel, *Angew. Chem.*, 1998, 110, 2646; *Angew. Chem. Int. Edn. Engl.* **1998**, 37, 2466

[2] J. Küther, R. Seshadri, W. Knoll and W. Tremel, *J. Mater. Chem.* **1998,** 8, 641

[3] J. Küther, G. Nelles, R. Seshadri, M. Schaub, H.-J. Butt and W. Tremel, *Chem. Eur. J.* **1998,** 4**,** 1834

[4] J. Küther, R. Seshadri and W. Tremel, *Angew. Chem.*, **1998**, 110, 3196; *Angew. Chem. Int. Ed.* **1998**, 37, 3044 ; J. Küther, R, Seshadri, G. Nelles, W. Assenmancher, H.-J. Butt, W. Mader and W. Tremel, *Chem. Mater.* **1999**, 11, 1317.

[5] M. Bartz, J. Küther, G. Nelles, N. Weber, R. Seshadri and W. Tremel, *J. Mater. Chem.* **1999,** 9**,** 1121

[6] M. Brust, D. Bethell, D.J. Schiffrin and C.J. Kiely, *Adv. Mater.*, **1995**, 7, 795

[7] T.W. Greene, *Protective Groups in Organic Synthesis*, John Wiley & Sons, **1981**

[8] F.C. Meldrum, J. Flath and W. Knoll, *Langmuir* 1997, 13(7), 2033-2049; F.C. Meldrum, J. Flath and W. Knoll, *J. Mater. Chem.* **1999**, 10, 711

[9] E. Kretschmann, *Z. Physik* **1971**, 241, 313

[10] H. Distler, *Angew.* Chem. 1967, 11, 520; H. Wolf, PhD Thesis, Universität Mainz, **1995**

[11] P.W. Scott and I.T. Harrison, *J. Org. Chem.* **1981**, 46, 1914

[12] M. Brust, M. Walker, D. Bethell, J. Schiffrin and R. Whyman, *J. Chem. Soc. Chem. Commun.* **1994**, 801

3.3. Synthesis of tubular titania composites: The use of human hair as template.

3.3.1. Introduction

The engineering of inorganic materials with special structures in the micrometer range has opened a variety of new applications, i.e. for new catalyst systems, [1] in separation technology / flow behavior tuning [2] and optoelectronics. [3] The generation of such materials often requires a template whose structure can be transferred onto the inorganic material. Such structures are fabricated in the laboratory with techniques like photo lithography, [2] CVD, stamp techniques combined with self assembly methods etc.. [4] However, because of its large repertory of complex morphologies, nature is perhaps the best source of structural templates for the formation of new material architectures. Natural structures can be imitated at the laboratory level by using sol - gel methods, foams, or polymers as templates. [2] Additives can control the morphology of calcium carbonate (calcite) crystals. These additives can bind onto selected crystal phases. [5] The combination of colloidal templating and self assembly processes lead to the formation of 3 D architectures in the micrometer or sub micrometer range by using polymer lattices as templates. [6,7] Tubular structures which are important for the transport of liquids and gases or which can be used as micro- or nanoreactors can be synthesized by several techniques e.g. polyester fibers, carbon fibers, metal wires, rapid cooling, chemical vapor deposition etc.. [8] A self organization reaction has permitted Matsui and Nakamura [9] to produce silica nanotubes. Microtubes of aluminum nitride formed when AlN coated aluminum foil is treated with diluted hydrochloric acid [8].

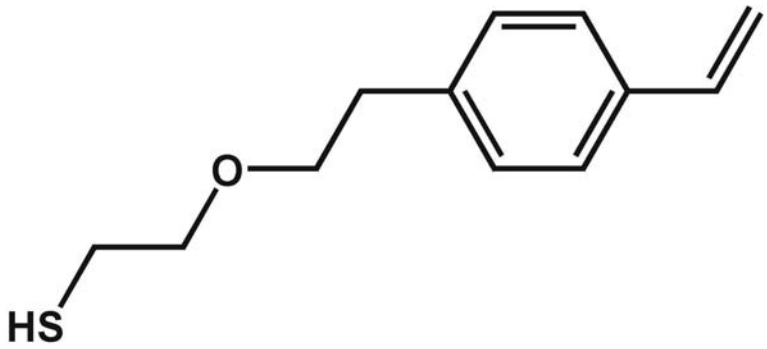

T 2

3.3.2. Results and discussion

In this paper we suggest the use of human hair as the structure-directing template to produce tubular inorganic materials. The strategy of the synthesis is displayed in Figure 3.3.1. We have prepared a thiol functionalized styrene monomer **T 2** which combines the monomeric moiety with the possibility that thiols can be attached to gold surfaces [10] with a strong chemical bond. A human hair was glued[1] on both ends to glass slides in such a way that it forms a loop. Subsequently, it was coated with gold (usually 70 – 100 nm thickness) similar to gold coating experiments described elsewhere. [11] The loop facilitates gold coating on the full surface of the biological template. The monomer was assembled on the gold surface using **T 2** routine procedures. [11] In this case dichloromethane was used as solvent. Subsequently, the glue was removed from the glass slides. After the anionic polymerization of styrene with the surface bound monomer **T 2,** a polystyrene film of about 70 **Å** (measured on clean flat gold substrates) can be obtained after reaction times of 30 minutes. Then thin titania surfaces of about 14 **Å** (measured on polymer flat coated gold substrates) can be produced by adding the polymerized hair templates into a glass vessel containing an ethanolic solution (100 ml) of titanium isopropoxide (300 μl). The precipitation of titania was initiated by atmospheric moisture (for

[1] UHU Sekunden Alleskleber Gel

more details see reference [12]). Exploiting the fact that a hair, peptides and other biological structures can easily be dissolved in sodium hypochlorite solution, the prepared composites were transferred in a 13 % hypochlorite solution for 30 minutes. After dissolving the biological template, tubular structures of titania / polystyrene composites can be obtained. The tubular structure is stabilized by the presence of the polymer between the gold and titania layers.

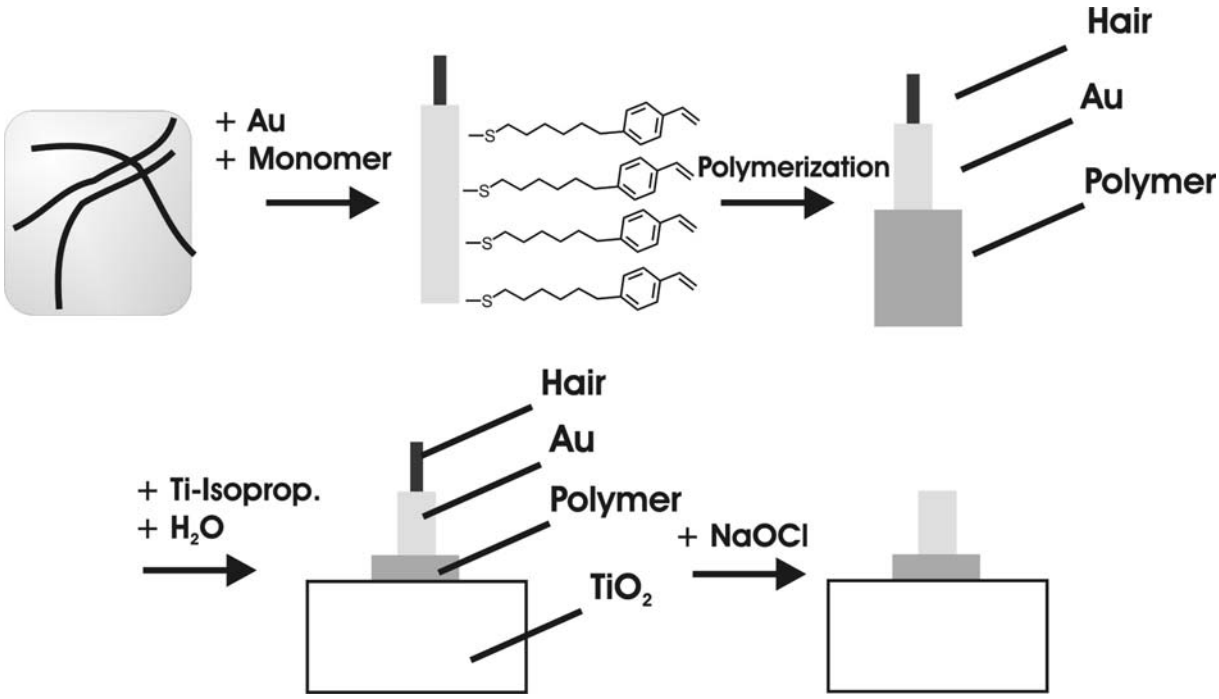

Figure 3.3.1 Scheme for the synthesis of an inorganic – organic composite in a microtubular structure. The biological template (human hair) was coated with a 70 – 100 nm gold layer. After thiol adsorption the surface was functionalized with styrene molecules which can be polymerized in the following step. The polymer film stabilizes the inorganic titania surface after removing the biological template.

Figure 3.3.2 a and b display scanning electron microscopy images (ZEISS Digital Scanning Microscope 962 combined with a Kevex EDAX at acceleration potentials of 5 – 15 kV) of the tubular titania composites obtained after dissolving the biological template and drying in air. For the scanning electron microscopy measurements the samples were fixed on carbon conducting stripes.

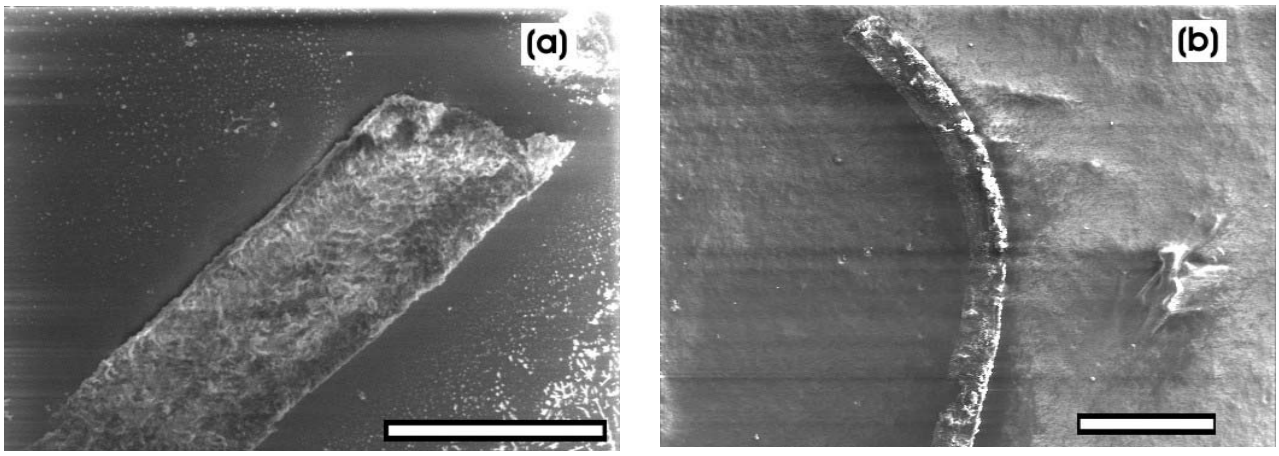

Figure 3.3.2 a) Scanning electron microscopy images of the product obtained after removing the human hair. The tubes were air - dried and pressed on conducting carbon stripes, which causes them to obtain a larger diameter than they had in solution. b) Typical EDX measurement taken from the tubular surface. Characteristic peaks corresponding to Ti K_α and K_β are indicated. Scale bars correspond to a) 200 µm and b) 500 µm

The human hair used in these experiments had a diameter of approximately 100 µm. The higher diameter obtained in the composites is caused by the sample preparation for the microscope. Energy dispersive x - ray measurements, which can be made simultaneously during the scanning electron microscopy experiment were taken from these structures and were collected from several places of the tubular surfaces. Figure 3.3.3 displays a characteristic EDX measurement and verifies the presence of titania on top the surface. Figure 3.3.4 displays light microscope images in transmission and reflection mode visualizing the tubular structure in liquid solution.

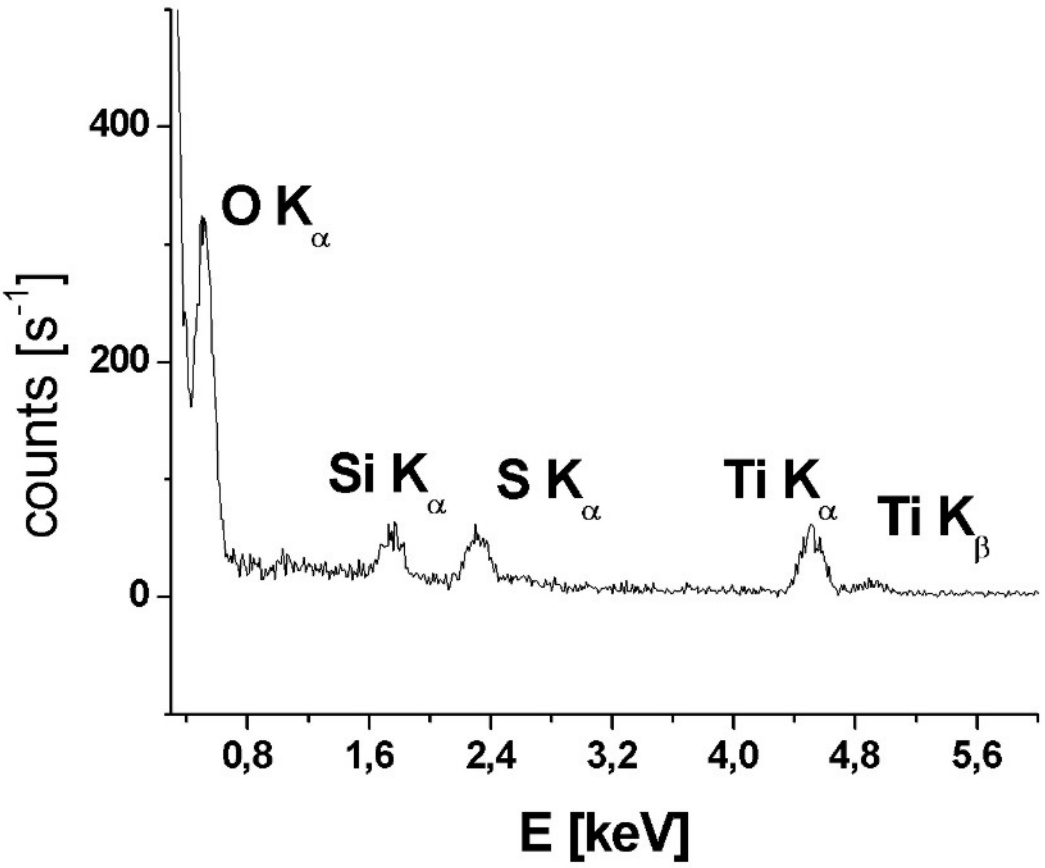

Figure 3.3.3 Energy dispersive x-ray measurement of the surface of obtained tubular composites. Ti K_a and Ti K_b are indicated

The thickness of the obtained structure is in range of 120 – 130 μm in correspondence to the thickness of the biological template. The lined gold film cannot be removed physically because of the chemical binding to the polymer film. The physical interaction of the biological template to the gold film effects the formation of the tube. It is noticed that an incomplete gold coverage on the template surface leads to incompletely closed tubes. The formation of "half tubes" increases if the thickness of gold coating is less than 70 nm.

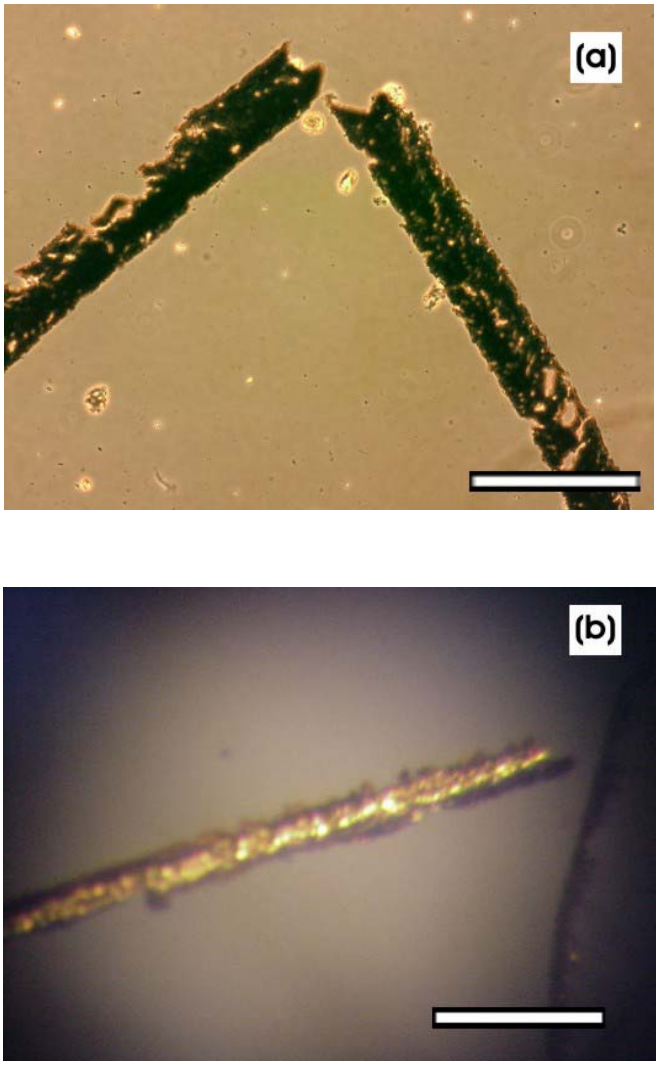

Figure 3.3.4 Light microscopy images in (a) transmission and (b) reflection mode of the obtained tubular structures in aqueous solution . The original size in diameter in the range of 120 – 130 µm corresponds to the original template size. Scale bars correspond to 300 µm.

3.3.3. Experimental

3.3.3.1. Monomer Synthesis

The monomer **1** was achieved by using modified procedures of Braun and Keppler, Sieber and Ulbricht [13]. The thiol group was introduced using the Bunte Salt method [14]. The detailed preparation procedure is described elsewhere [12].

3.3.3.2. Polymerization and Preparation for Microscopy

All preparations were carried out in a glove box under inert and dry gas atmosphere. The gold coated biological template was transferred in a reaction vessel containing 10 ml of toluene. The toluene was dried over sodium (5 g) and was freshly distilled before use. n -butyllithium (0.5 ml) was added and freshly distilled styrene (1 ml) was added dropwise over a period of 30 minutes. The reaction was terminated by adding of methanol. The template was moved out of the glove box, was washed with toluene and dried in a N_2 stream.

The obtained tubes were sucked into a pipette and transferred into distilled water twice to remove the sodium hypochlorite.

3.3.3.3. References

[1] M. G. L. Petrucci, A. K. Kakkar, *J. Chem. Soc. Chem. Commun.* **1995**, 1577; M. G. L. Petrucci, A. K. Kakkar, *Adv. Mater.* **1996**, 8, 251; M. G. L. Petrucci, A. K. Kakkar, *Chem. Mater.* **1999**, 11, 2

[2] S. Mann, *Angew. Chem. Intl. Ed. Engl.* **2000**, 39, 3392

[3] C. T. Kresge, M. E. Leonowicz, W. J. Roth, J. C. Vartuli, J. S. Beck, *Nature* **1992**; 359; N. K. Raman, M.T. Anderson, C. J. Brinker, *Chem. Mater.* **1996**, 8, 1682; G. Schmid, *Chem. Rev.* **1992**,92,1709; B. O´Regan, M. Grätzel, *Nature* **1991**, 353, 737

[4] W. Fritsche, K. J. Böhm, E. Unger, J. M. Köhler, *Appl. Phys. Lett.* **1999**, 75, 2854;S. Mann, W. Shenton, M. Li, S. Conolly, D. Fitzmaurice, *Adv. Mater.* **2000,** 12, 147; S. R. Hall, W. Shenton, H. Engelhardt, S. Mann, *Chem. Phys. Chem.* **2001**, 3, 184

[5] S. Mann, J. M. Didymus, N. P. Sanderson, B. R. Heywood, *J. Chem. Soc. Faraday Trans.* **1990**, 86, 1873

[6] F. Caruso, *Chem. Eur. J.* **2000**, 6, 413

[7] E. Donath, G. B. Sukhorukov, F. Caruso, S. A. Davis, H. Möhwald, *Angew. Chem. Intl. Ed. Engl.* **1998**, 37, 2201

[8] M. Akiyama, K. Shobu, C. – N. Xu, K. Nonaka, T. Watanabe, *J. Appl. Phys.* **2000,** 88, 4434

[9] H. Nakamura, Y. Matsui, *J. Am. Chem Soc.* **1995**, 117, 2651

[10] A. Ulman, *Chem. Rev.* **1996**, 96, 1533

[11] J. Küther, R. Seshadri, W. Knoll, W. Tremel, *J. Mater. Chem.* **1998**, 8, 641

[12] M. Bartz, A. Terfort, W. Knoll, W. Tremel, *Chem. Eur. J.* **2000**, 6, 4149

[13] D. Braun, H.-G. Keppler, *Mh. Chem.* **1963**, 94 1250; G. Sieber, I. Ulbricht, *J. prakt. Chem.* **1963**, 20, 14

[14] W. Fabianowski, L. C. Coyle, B. A. Weber, R. D. Granata, D. G. Castner, A. Sadownik, L. Regen, *Langmuir* **1989**, *5*, 35; N. Nakashima, Y. Takada, M. Kunitake, O. Manabe, *J. Chem. Soc., Chem. Commun.* **1990**, 845; I. Rubinstein, S. Steinberg, Y. Tor, A. Shanzer, J. Sagiv, *Nature* **1988**, *332*, 426

3.4. Preparation of Nanowires from Gold Colloids Using Biogenic and Synthetic Silica Nanotubes as Templates

3.4.1. Introduction

Biological silica nanotubes as well as synthetic silica nanotubular structures can act as templates for a following procedure to obtain wires of gold colloid / alkane thiol composites in a nanometer scale of diameter an 20 – 200 μm length . The preparation involves filling of the silica nanotubes with freshly prepared gold colloids (with a diameter in 2-10 nm range). These gold colloids can be precipitated in the inner part of the tubular silica template and the silica can be dissolved with hydrofluoric acid. The tubular structure is retained by the precipitated gold colloids in form of a nanowire which has the same diameter of 100 – 500 nm as interior of the silica template.

The controlled assembly of inorganic materials on a nanometer scale is an important factor for the synthesis of materials with interesting properties. In particular, there is much interest in the preparation of nanotubes and nanowires in the emerging area of nanoelectronics. [1] One - dimensional nanostructures have been receiving increasing attention in the last few years due to the wide range of properties they exhibit [2], [3], [4] The development of general techniques for the preparation of tools for nanoelectronics and for molecular machines will perhaps by a key scientific problem for the next 10 years.[5] Nanowires link the microscopic world of atoms and the macroscopic extended world. The synthesis of such structures can be achieved, in principal, via chemical vapor deposition or laser ablation methods. Scanning tunnel microscopes[6] and electron-beam irradiation [7] in ultrahigh vacuum electron microscopes have been used to produce wires in nanometer size. However, there are very few general methods [8] for the synthesis of nanowires and these procedures are often not easily accessible. We have been examining two - dimensional structured surfaces using functionalized thiols on gold coated glass

slides combined with the PDMS stamp technique [9] as a route to microstructures.[10]

Making use of the fact that thiol - functionalized gold colloids (with a diameter in 2-10 nm range) behave like molecules and at the same time, possess a surface not unlike the (111) surface of bulk gold, the nanoparticles perfectly bridge the world of molecular chemistry and the macroscopic world of extended solids. [11] We have used special functionalized gold colloids [12] as crystallization templates for the precipitation of lead sulfide. The material formed in this manner is spherical and in the nanometer range and has an architecture not unlike that of a MOSFET. [13]

3.4.2. Results and discussion

In this paper we demonstrate the preparation of nanowires from gold colloids using nanotubular silica isolated from marine sponges, as well as synthetic nanotubular silica as templates. The preparation involves filling of the nanotubes with freshly prepared gold colloids in toluene solution by capillary forces. The gold colloids are then precipitated inside the silica tubes by cross-linking through the addition of dithiol. After such precipitation, the siliceous portion of the material is dissolved with hydrofluoric acid (HF). (Scheme 1) The structure of the silica tubes is retained by the precipitated gold colloids in the form of a nanowire which has the same dimensions as the silica template used. The nanostructures obtained in this manner have been characterized by scanning electron microscopy (SEM) and EDX measurements.

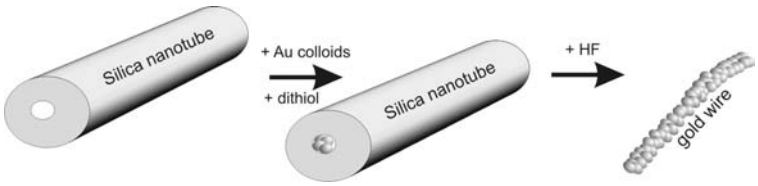

Scheme 1

Using sol – gel methods, [16] silica nanotubes were synthesized from an ethanolic solution of DL - tartaric acid and tetra ethyl orthosilicate (TEOS) by adding am-

monia solution. The white precipitate obtained after drying was analyzed by SEM. Figure 3.4.1 a displays a scanning electron micrograph of the silica tubes. The tubular character visualized at higher magnification Figure 3.4.1 b). The hollow core of the tube is approximately 500 nm in diameter.

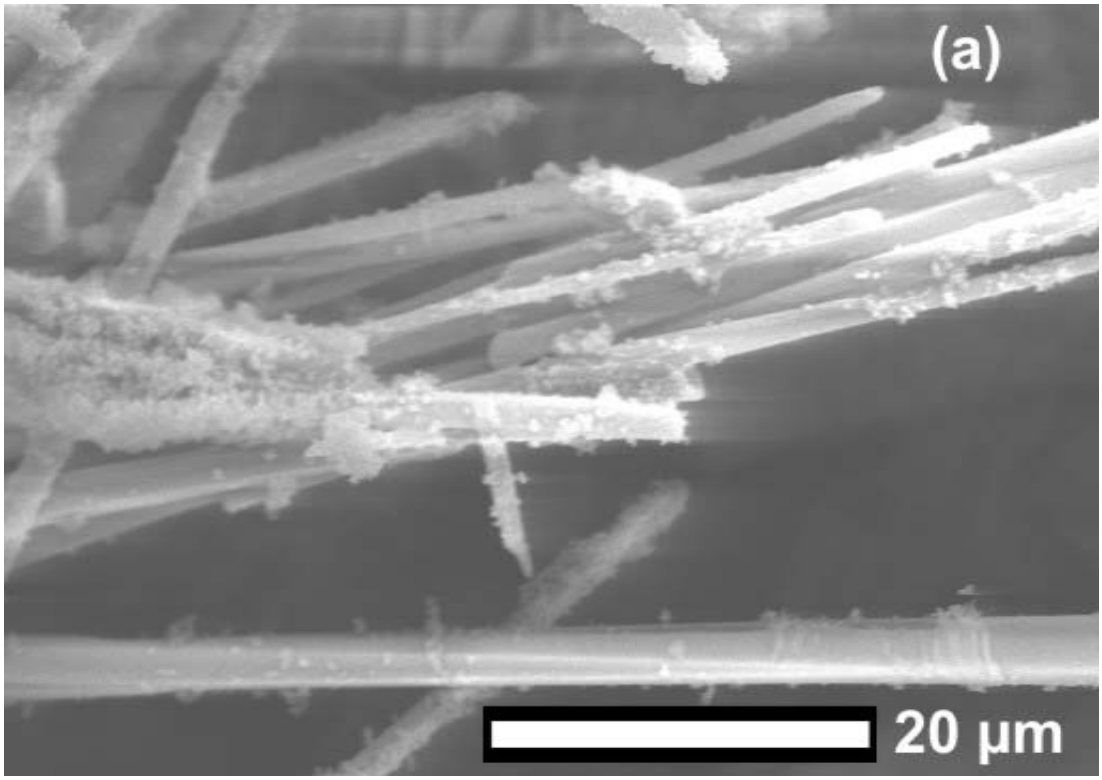

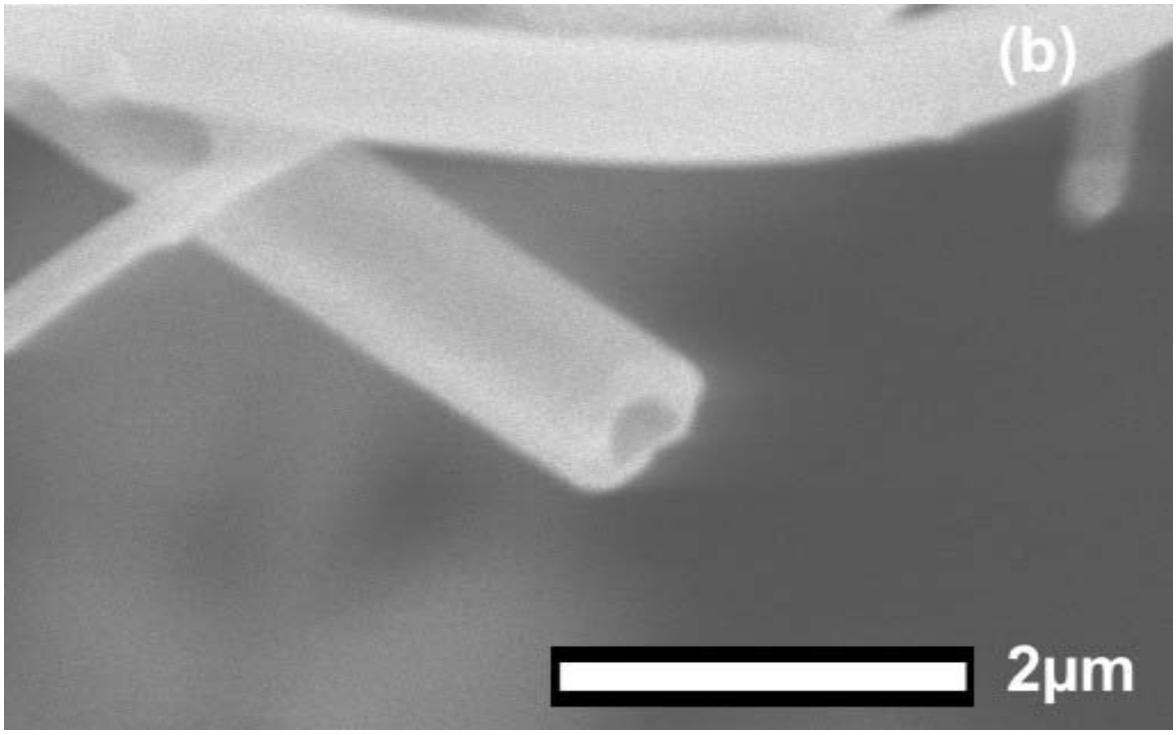

Figure 3.4.1 Scanning electron microscopy images of the SiO_2 – nanotubes obtained after reaction of TEOS with aqueous ammonia solution containing DL – tartaric acid (a). (b) Picture in higher magnification. The interior of the tube has a diameter of approximate 500 nm.

The SiO_2 synthesized contains both spherical and tubular particles. As the presence of spherical SiO_2 particles did not interfere in the formation of gold nanowires, the SiO_2 sample is used as prepared without further separation of spherical particles from the tubes.

The formation of gold nanowires failed when tetrachloro gold acid was reduced in the presence of silica nanotubes, instead of a black gel a powder (analyzed by SEM) (see Figure 2b) was obtained. However, gold wires of 10 – 20 µm in length and less than 100 to 500 nm in diameter were formed when the gold colloids were precipitated by a dithiol in the presence of the silica template (Figure 3.4.1a). Figure 3.4.1 a) also reveals the presence of unstructured gold powder along with the gold

nanowire. The formation of these powders is attributed to the precipitation of gold colloids on the outside of the tubular and spherical SiO_2. Nanowires are not form in the absence of the template with dithiols only (Figure 3.4.2 b). The diameter of the nanowires clearly shows that the structures must have been formed in the interior and not on the exterior of the template (in this case structures in the micrometer range should be expected) (see Scheme 1). Nevertheless the gold colloids structured by the SiO_2 tube and dithiol linker form compact nanowires with a smooth surface. Figure 3.4.2 c) displays a nanowire at higher magnification. In general, the diameter of these nanowires is in the range between 100 and 500 nm. The thickest wire found in different samples had a diameter of 500 nm. The length is approximately of about 20 μm.

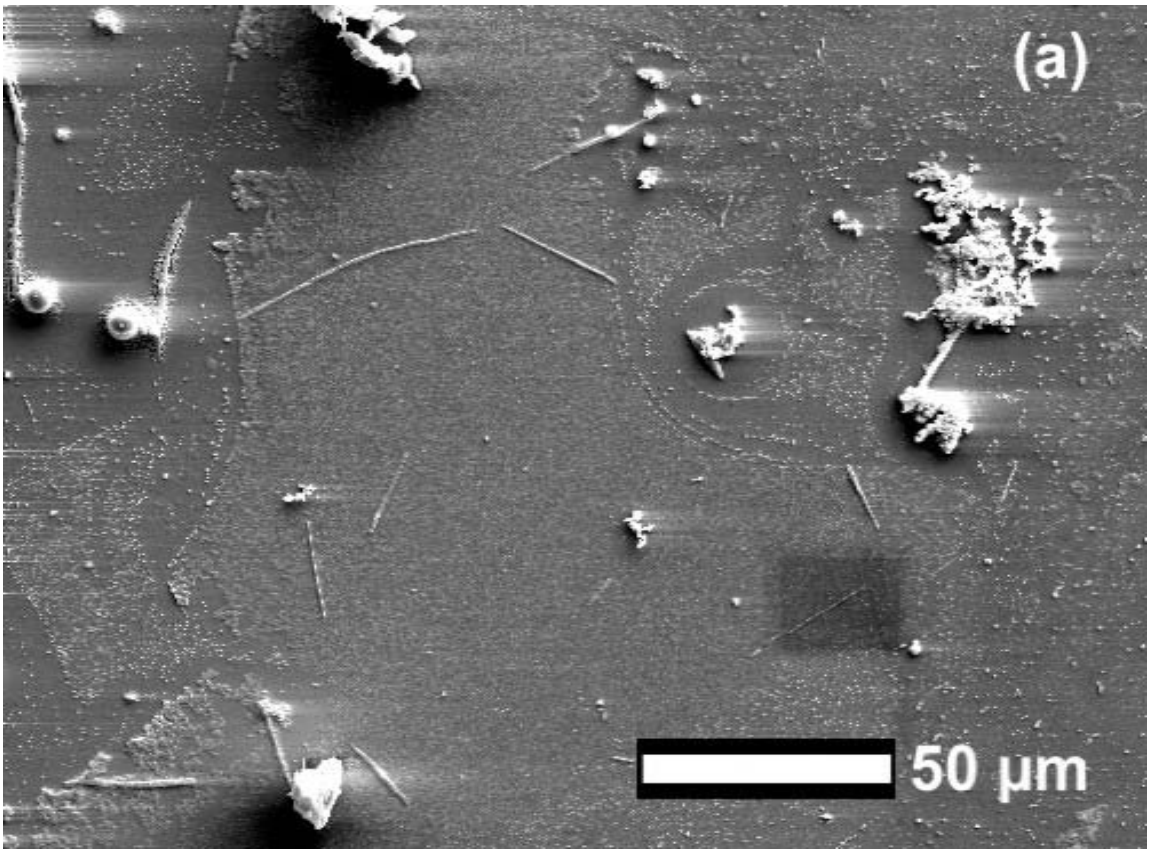

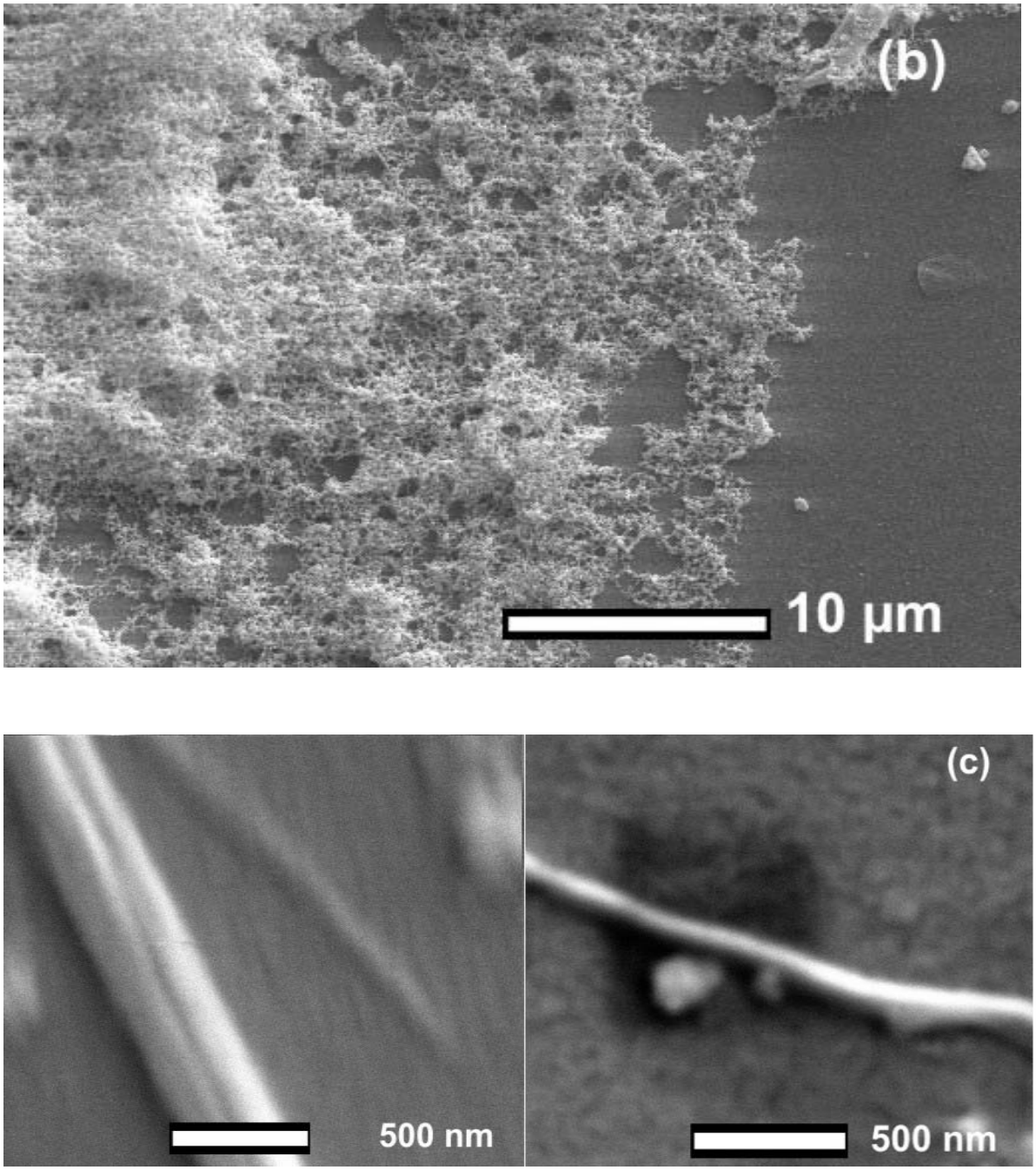

Figure 3.4.2 Scanning electron microscopy images of the obtained gold wires after treatment of the SiO_2 – template with HF (a). Image (b) displays the formation of unstructured gold colloids obtained after precipitation adding a dithiol solution in absence of a silica template. Figure 2 c displays the range in diameter from 100 nm to 500 nm of the gold wires.

EDX measurements of non sputtered samples can be made simultaneously during the scanning electron microscopy experiments. Figure 3.4.3 displays a typical EDX spectrum taken directly from the surface of the nanowires displayed in Figure 3.4.2.c). The extended silica K_α peak obtained in the spectrum is due to the glass substrate background on which the wires are collected. This peak does not appear wen samples which are collected on conducting carbon stripes are measured (not shown).

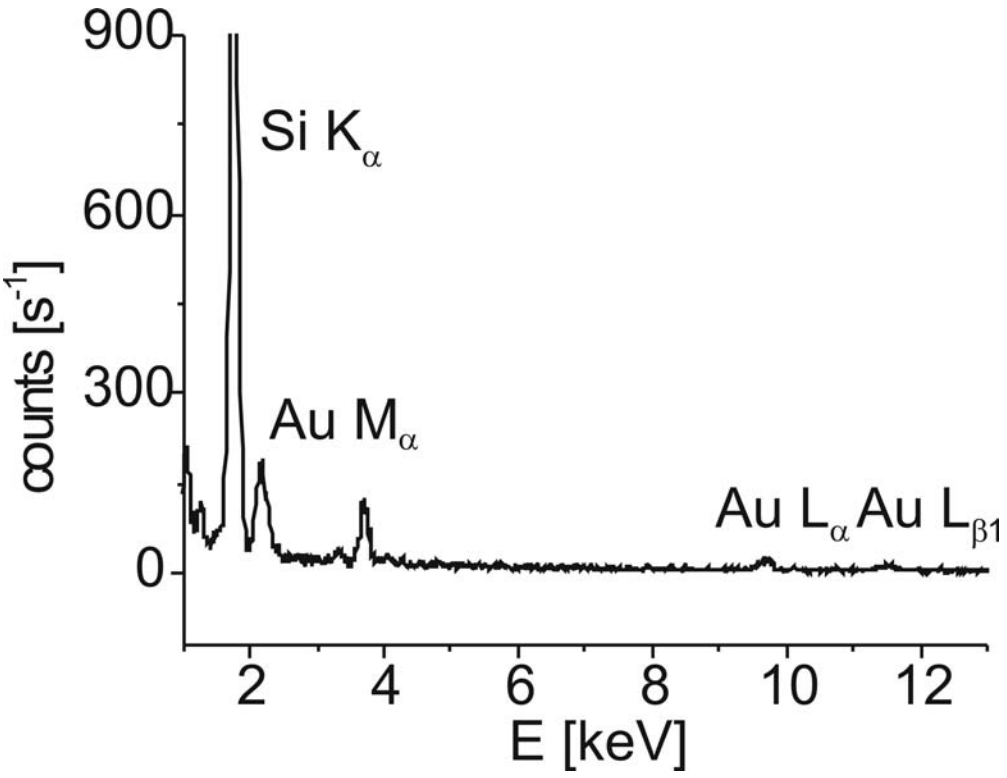

Figure 3.4.3 Energy dispersive X-ray measurement of obtained nanowires. Characteristic gold peaks verify the specific nature of the in Figure 3.4.2 c) displayed samples.

Figure 3.4.4 a) displays a SEM image of nanotubular silica of 200 μm length isolated from a marine sponge *Suberites domuncula*. The spherical head and the needle - like end are removed by sonication or crushing the sample powder. The open spi-

cules are used as templates following to the procedure described above, the inner diameter of the tube being no more than 300 nm. (Figure 3.4.4 b).

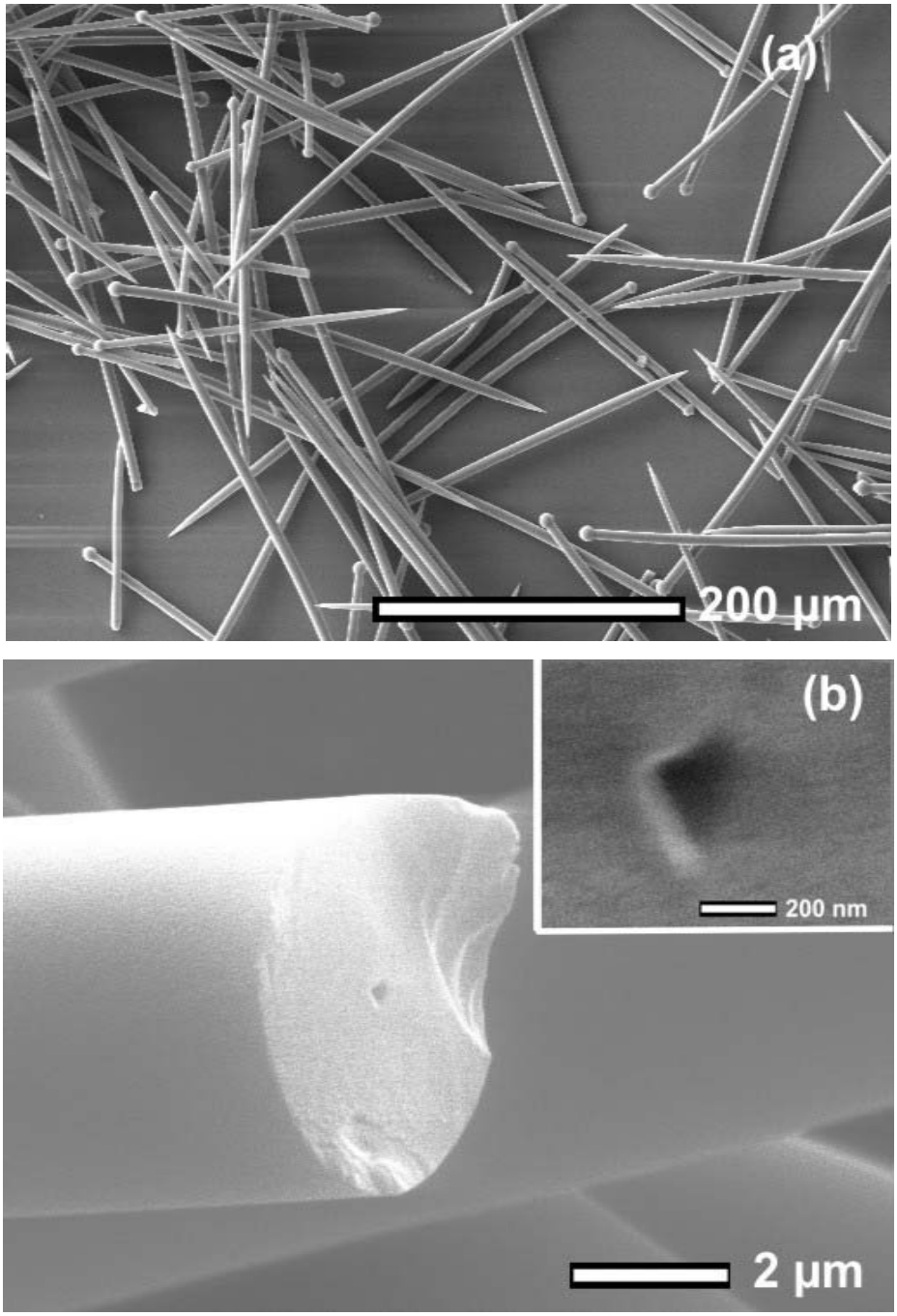

Figure 3.4.4 Scanning electron microscopy images of isolated spicule from marine sponges (a). Closer view of an open spicule after both ends are removed (b). The interior of the tube is about 200 nm in diameter.

The resulting gold nanowires are displayed in Figure 3.4.5. This overview picture shows the large number of gold wires. Figure 3.4.5 b) displays the same area using the secondary electron and the back scattering electron detector. The high material contrast is consistent with the presence of a bulk gold wire (instead of a thin colloidal film on remnants of the silica templates). Figure 3.4.5 c) is a closer view visualizing the diameter size of around 200 nm.

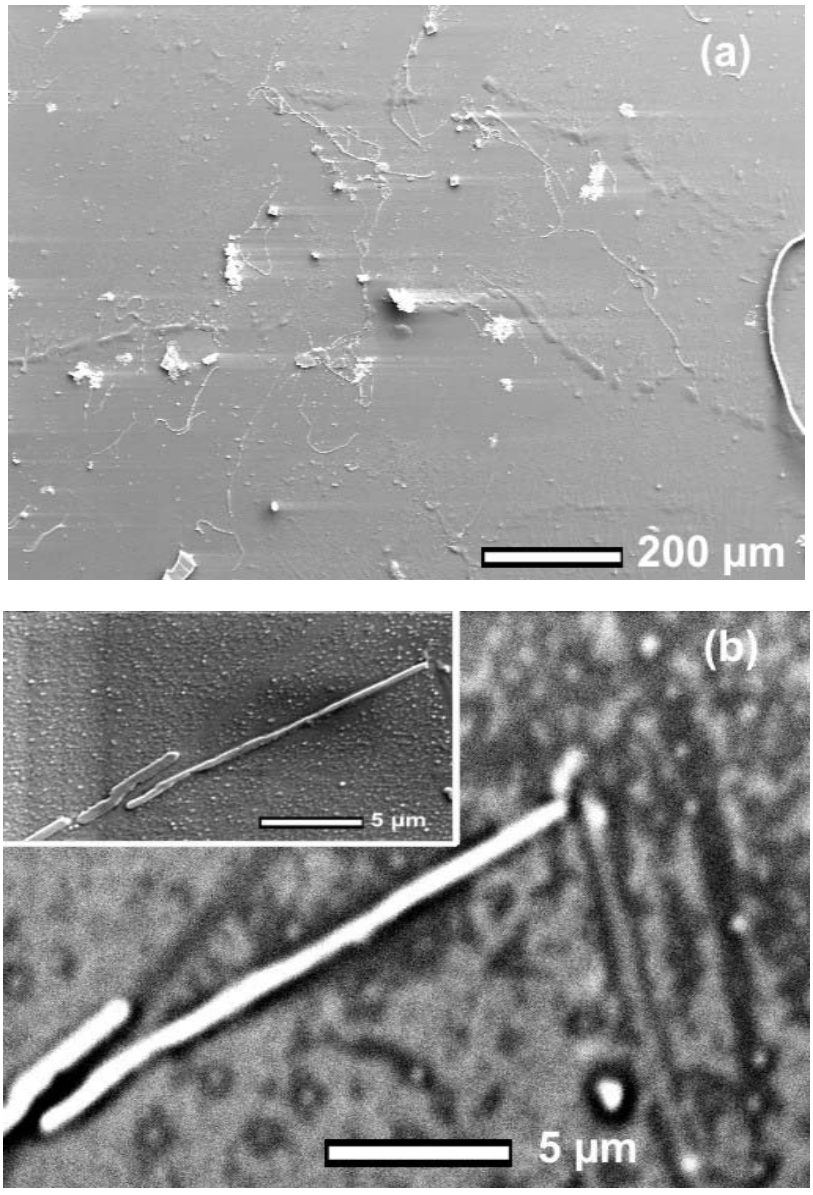

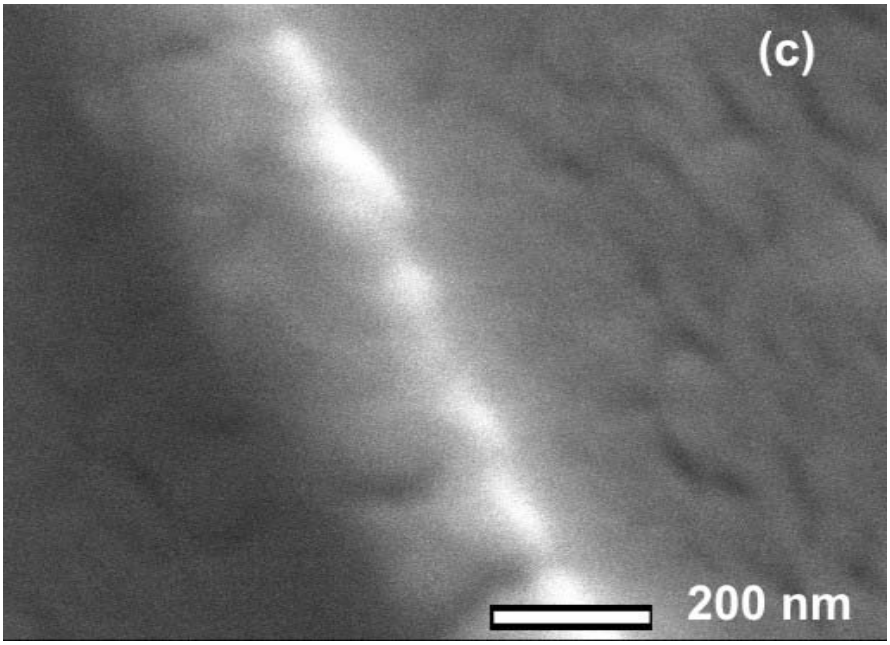

Figure 3.4.5 Scanning electron microscopy images of nanowires which were obtained when marine spicules were used as template. The length of the wires is about 200 μm and the thickness about 200 nm in diameter is corresponding to the template structure.

3.4.3. Experimental

3.4.3.1. Scanning electron microscopy

Scanning electron microscopy was performed with a ZEISS digital scanning microscope 962 combined with a Kevex EDAX at acceleration potentials of 5-15 kV. The SiO_2 samples were transferred onto a carbon glue pad and sputtered with gold before analysis. In the case of gold nanowire the glass plate was cut into a small piece and pasted on a aluminum sample holder using a conducting glue before sputtering with gold.

3.4.3.2. Gold Colloids (A)

Gold Colloids were prepared following the standard procedure described elsewhere [14] by putting a aqueous solution of HAuCl4 (1g /250 ml H_2O) (20 ml) into a separation funnel. Toluene was added along with tetraoctylammonium bromide (1.2 g). The acid was transferred to the organic phase by shaking the separation funnel. By adding $NaBH_4$ the gold colloids were obtained by reduction at the water/toluene interface. The aqueous layer was removed and the toluenic solution was pure enough for the following reaction.

3.4.3.3. 1,12 – Dodecandithiol (B)

1,12 – Dodecandithiol was obtained via the Bunte Salt method described by Küther et al. [15]. 1, 12 – Dibromdecan (11.6 g) was dissolved in ethanol (50 ml). The mixture was heated up to reflux. Natriumthiosulfat – Pentahydrat (19.2 g) was dissolved in water (50 ml) and was added dropwise. The reaction mixture was stirred for 2 h and the white precipitate was filtered after cooling to 4 °C. The dried Bunte salt (16 g) was suspended in a mixture of water (100 ml) and ethanol (5 ml). HCl conc. (16 ml) was degassed in a nitrogen stream for 15 min. and was added to the Bunte salt suspension. The mixture was heated up to reflux for 2 h under a nitrogen atmosphere. After cooling to 4 °C the white precipitate was filtered and dissolved in CH_2Cl_2. The organic solution was washed 3 times with an aqueous solution of NaCl (3 mol) and finally with water. After drying with Na_2SO_4 the solvent was removed IR 2924, 2849 (CH), 2564 (SH), 1470 (CH), 718 (CS) cm^{-1}. (^1H) NMR (400 MHZ, $CDCl_3$, 25°C, TMS): δ = 1.2 –1.5 (m, 20H; CH_2), 2.4 –2.5 (4H; CS) ppm.

3.4.3.4. SiO_2 – Nanotubes (C)

SiO_2 – Nanotubes were prepared following the report by Nakamura and Matsui.[16] DL tartaric acid (0.2 g) and water (0.6 g) were dissolved in ethanol (50 ml) by sonication and slightly heating to 40 – 50 °C. TEOS (7.3 g) was added and the mixture was allowed to stand 30 min. to form SiO_2 gel. Ammonia (25% NH_3 solution) (50 ml) was added, the white precipitate formed was filtered after 30 min, dried at 80 °C and was used without further purification.

3.4.3.5. Biogenic Spicule (D)

Biogenic Spicule were isolated by using standard methods [17]. Cells of the marine sponge *Suberites domuncula* fragments (3 – 5 mm^3) were transferred into Ca^{2+} and Mg^{2+} - free artificial seawater containing EDTA (CMFSW – E) (10 mmol) and was shaken for 30 minutes and centrifuged 10 minutes (1900 rpm). The supernatant was removed and fresh CMFSW - E was added. The mixture was shaken again for 30 minutes and then filtrated through a 60 μm nylon net. The residue was collected and washed by adding distilled seawater 2 times to remove dissolved organic matter.

The spicules were opened by sonication for 10 min until a dispersed spicule powder was obtained. The inside tubes, containing organic matter were then cleaned by transferring them into a 13 % hypochlorite solution and the mixture was shaken for 12 h. The powder was removed by centrifugation was washed 2 times with water and once with acetone and subsequently dried at 45 °C.

3.4.3.6. Gold Nanowires (E)

Gold Nanowires were prepared by adding a freshly prepared gold colloid solution (A) (20 ml) to the SiO_2 nanotube powder (C) (1.15 g). 1,12 – dodecandithiol (B) (0,02 g) was added and the solvent was removed by filtration. The precipitate was dissolved in HF (20 %, 10 ml), toluene (10 ml) was added to achieve the black colored precipitate between the two phases. The precipitate can be collected by very carefully removing the water phase and 8 ml of the toluene phase. The residual was transferred onto glass slides and was dried for microscopy in air at room temperature.

3.4.4. References

[1] M. S. Fuhrer, J. Nygard, L. Shih, M. Forero, Y. – G. Yoon, M. S. C. Mazzoni, H. J. Coi, J. Ihm, S. G. Louie, A. Zettl, P. L. McEuen, *Sciene* **2000**, 288, 494

[2] Y. Kondo, K. Takayanagi, *Phys. Rev. Lett.* **1997**, 79, 3455

[3] X. Peng, L. Manna, W. Yang, J. Wickham, E. Scher, A. Kadavanich, A. P. Alivisatos, *Nature* **2000**, 404, 59

[4] M. Li, H. Schnablegger, S. Mann, *Nature* **1999**, 402, 393

[5] W. Tremel, *Angew. Chem.* **1999**, 111, 2311; *Angew. Chem Intl. Ed. Engl.* **1999**, 38, 2175

[6] H. Ohinishi, Y. Kondo, K. Takayanagi, *Nature* **1998**, 395, 780

[7] H. Hegger, K. Hecker, G. Reckziegel, A. Freimuth, B. Huckestein, M. Janssen, R. Tuzinski, *Phys. Rev. Lett.* **1996**, 77, 3885

[8] C. R. Martin, Acc. Chem. Res. **1995**, 28, 61

[9] J. Aizenberg, A. J. Black, G. M. Whitesides, *Nature*, **1999**, 398, 495

[10] M. Bartz, A. Terfort, W. Knoll, W. Tremel, Chem. Eur. J. **2000**, 6, 4149

[11] R. L. Whetten, J. T. Khoury, M. M. Alvarez, S. Murthy, I. Vezmar, Z. L. Wang, P. W. Stephens, C. L. Cleveland, W. D. Luedtke, U. Landmann, *Adv. Mater.* **1996**, 8, 428.

[12] M. Brust, J. Fink, D. Bethell, D. J. Shiffrin, C. Kiely, *J. Chem. Soc. Chem. Commun.* **1995**, 1655; M. Brust, M. Walker, D. Bethell, D. J. Shiffrin, R. Whyman, *J. Chem. Soc. Chem. Commun.* **1994**, 801

[13] M. Bartz, N. Weber, J. Küther, R. Seshadri, W. Tremel, *J. Chem. Soc. Chem. Commun.* **1999**, 2085

[14] M. Bartz, J. Küther, R. Seshadri, W. Tremel, *Angew. Chem.* **1998**, 110, 2646; *Angew. Chem. Intl. Ed. Engl.* **1998**, 37, 2466

[15] J. Küther, R. Seshadri, W. Knoll, W. Tremel, *J. Mater. Chem.* **1998**, 8, 641

[16] H. Nakamura, Y. Matsui, *J. Am. Chem. Soc.* **1995**, 117, 2651

[17] W. E. G. Müller, M. Wiens, R. Batel, R. Steffen, H. C. Schröder, R. Borojevic, M. Reis Custodio, *Mar. Ecol. Prog. Ser.* **1999**, 178, 205; M. Reis Custodio, I. Prokic, R. Steffen, C. Koziol, R. Borojevic, F. Brümmer, M. Nickel, W. E. G. Müller, *Mechanisms of Ageing and Development* **1998**, 105, 45

4. Conclusion

The present study displays new methods for the synthesis of structured inorganic materials with novel architecture in micrometer and nanometer range. The main role of the special design is based on template induced precipitation of inorganic materials on self - assembled monolayers. Suitable substrates are gold - coated glass slides and gold colloids, which show behavior like molecules, and at the same time they still display many properties of extended solids. On these substrates thiols can be adsorbed to form a monomolecular layer, which interferes with the physical properties of the obtained surface. The synthesis of special thiols, tuned for the special need in current applications, represents a main focus in the present study.

Gold coated glass as templates were used in the first part of this work. The precipitation of calcium carbonate was examined due to the film thickness of the adsorbed monolayer. Aragonite, one of the three important calcium carbonate phases, is formed on self assembled monolayers under ambient conditions using a polyaromatic amide surface with film thickness in ranges of 5 – 400 nm as nucleation template. The parameters that could be controlled were the polaramide chain length, the ω-substituent at the polymer, the connection to the gold surface using different amino thiols and the crystallization temperature. Here, the control of thickness of a polyaramide monolayer during its preparation using a step polymerization technique is presented the first time.

By using self - assembled monolayers (SAM) of alkane thiols gold-coated glass slides have been patterned. Through the use of a special thiol terminated with a styrene monomer, microstructures of 5 to 10 μm width and 70 Å height have been formed on the surface by graft polymerization of styrene. These patterned gold slides have then been used to template the precipitation of thin titania films from ethanolic solutions of titanium isopropoxide to create microstructured architectures in the film. Plasmon resonance spectra have established the presence of different steps in the

process and have been used to follow the kinetics of the precipitation of titania on the surface.

Tetraethylene glycol (HO-$(C_2H_4O)_4$-H) can be monofunctionalized by replacing one of the terminal hydroxyl groups with the thiol SH group. The resulting molecule can be self - assembled on gold (111) surfaces. More importantly, this molecule allows the simple one-step preparation of protected, water-soluble gold colloids within a single aqueous phase. Attempts are made to use such protected water-soluble colloids as nucleating "seeds" around which calcium carbonate can be crystallized.

Exposing bare gold colloids to long-chain dithiols results in their precipitation due cross-linking of the thiol groups with the gold surfaces. Here we demonstrate that through the use of a dithiol that has one of the thiol groups protected, we can, through attachment followed by deprotection, prepare gold colloids with exposed thiol. The use of such ´´sticky´´colloids in creating complex architectures is demonstrated by using them to template the growth of PbS particles.

Titania / Au/ Polystyrene composite tubes in the micrometer range have been obtained using a human hair as biogenic template, which can be dissolved after synthesis of the composite to set free the tubular structure.

Silica nanotubes can be obtained by using DL-tartaric acid during in a sol – gel method. These hollow tubes are used as templates for the synthesis of gold nanowires from gold colloid solutions. The structure of the gold wires results in 100 to 500 nm diameter range and 10 to 20 μm length and can be stabilized with dithiols after dissolving the template with hydrofluoric acid.

5. Table of Figures

In Zusammenhang mit dieser Arbeit verfasste Publikationen

1. **M. Bartz**, J. Küther, G. Nelles, N. Weber, R. Seshadri and W. Tremel
   Monothiols derived from glycols as agents for the stabilization of gold colloids in water: Preparation, self-assembly and use as crystallization templates
   J. Mater. Chem. **1999**, 9, 1121.

2. **M. Bartz**, N. Weber, J. Küther, R. Seshadri and W. Tremel
   "Sticky" gold colloids through protection-deprotection and their use in metal-organic-inorganic architectures
   J. Chem. Soc. Chem. Commun. **1999**, 2085.

3. **M. Bartz**, A. Terfort, W. Knoll and W. Tremel
   Stamping of Monomeric SAMs as a Route to Structured Crystallization Templates: Patterned Titania Films
   Chem. Eur. J. **2000**, 6, 4149

4. J. Küther, **M. Bartz,** R. Seshadri, G. Vaughan, W. Tremel
   Crystallization of SrCO3 on a Self-Assembled Monolayer Substrate: An In-Situ Synchrotron X-Ray Study
   J. Mater. Chem. **2001**, 11, 503.

5. M. Balz, **M. Bartz**, W. Tremel
   Activity Enhancement of a Hydrogenation Catalyst by Surface Binding
   J. Mater. Chem. **2001,** submitted

6. **M. Bartz**, M. Wenzel, H. König, W. Knoll, W. Tremel
   Synthesis of tubular titania composites: The use of human hair as template
   J. Chem. Soc. Chem. Commun. **2001**, submitted

7. **M. Bartz**, T. Julius, G. le Pennec, W. E. G. Müller, W. Tremel
   Preparation of Gold Nanowires Using Biogenic and Synthetic Silica nanotubes as Templates
   J. Amer. Chem. Soc. **2001**, submitted

8. **M. Bartz**, O. Lang, R. Kügler, Z. Ahmad, W. Knoll, W. Tremel
   Stabilization of Aragonite on Polyaromatic Amide – Surfaces obtained by Step-Polymerization: Effect of Thickness
   J. Mater. Chem. **2001,** submitted

Tagungsbeiträge

1. "Funktionalisierte Nanopartikel als Kristallisationstemplate von Calciumcarbonat und als Katalysatoren" (Poster), Dechema Workshop "Funktionalisierte Nanopartikel"
   23. – 24. April 1998, Frankfurt (Main)

2. "Inorganic Minerals on Structured Functionalized Surfaces" (Poster)
   9 th International Conference on Organized Molecular Films
   28. 08 – 01.09. 2000, Potsdam

Danksagung

Vielen Dank allen, die zum Gelingen dieser Arbeit beigetragen haben.